Effective Date: April 22, 2011
Revision -

GSFC JPSS CMO
December 5, 2011
Released

Joint Polar Satellite System (JPSS) Ground Project
Code 474
474-00041

Joint Polar Satellite System (JPSS) Cloud Top Algorithm Theoretical Basis Document (ATBD)

For Public Release

The information provided herein does not contain technical data as defined in the International Traffic in Arms Regulations (ITAR) 22 CFC 120.10. This document has been approved For Public Release.

National Aeronautics and Space Administration

Goddard Space Flight Center
Greenbelt, Maryland

Check the JPSS MIS Server at https://jpssmis.gsfc.nasa.gov/frontmenu_dsp.cfm to verify that this is the correct version prior to use.

This page intentionally left blank.

Joint Polar Satellite System (JPSS) Cloud Top Algorithm Theoretical Basis Document (ATBD)

JPSS Electronic Signature Page

Prepared By:

Neal Baker
JPSS Data Products and Algorithms, Senior Engineering Advisor
(Electronic Approvals available online at https://jpssmis.gsfc.nasa.gov/mainmenu_dsp.cfm)

Reviewed By:
Name(s) of Reviewers (Electronic Approvals available online at https://-------)
Name(s) of Reviewers (Original Signed By)

Approved By:

Heather Kilcoyne
DPA Manager
(Electronic Approvals available online at https://jpssmis.gsfc.nasa.gov/mainmenu_dsp.cfm)

Goddard Space Flight Center
Greenbelt, Maryland

This page intentionally left blank.

Preface

This document is under JPSS Ground AERB configuration control. Once this document is approved, JPSS approved changes are handled in accordance with Class I and Class II change control requirements as described in the JPSS Configuration Management Procedures, and changes to this document shall be made by complete revision.

Any questions should be addressed to:

JPSS Ground Project Configuration Management Office
NASA/GSFC
Code 474
Greenbelt, MD 20771

This page intentionally left blank.

Change History Log

Revision	Effective Date	Description of Changes (Reference the CCR & CCB/ERB Approve Date)
Original	04/22/2011	**474-CCR-11-0056:** This version baselines D43754, Cloud Top Algorithm Theoretical Basis Document ATDB, Rev B dated 03/01/2010 as a JPSS document, version Rev -. This is the version that was approved for NPP launch. Per NPOESS CDFCB - External, Volume V – Metadata, doc number D34862-05, this has been approved for Public Release into CLASS. This CCR was approved by the JPSS Algorithm ERB on April 22, 2011.

This page intentionally left blank.

NATIONAL POLAR-ORBITING OPERATIONAL ENVIRONMENTAL SATELLITE SYSTEM (NPOESS)

CLOUD TOP ALGORITHM THEORETICAL BASIS DOCUMENT (ATBD) (D43754 Rev B)

CDRL No. A032

Northrop Grumman Space & Mission Systems Corporation
One Space Park
Redondo Beach, California 90278

Copyright © 2004-2010
Northrop Grumman Corporation and Raytheon Company
Unpublished Work
ALL RIGHTS RESERVED

Portions of this work are the copyrighted work of Northrop Grumman and Raytheon. However, other entities may own copyrights in this work.

This documentation/technical data was developed pursuant to Contract Number F04701-02-C-0502 with the US Government. The US Government's rights in and to this copyrighted data are as specified in DFAR 252.227-7013, which was made part of the above contract.

This document has been identified per the NPOESS Common Data Format Control Book – External Volume 5 Metadata, D34862-05, Appendix B as a document to be provided to the NOAA Comprehensive Large Array-data Stewardship System (CLASS) via the delivery of NPOESS Document Release Packages to CLASS.

The information provided herein does not contain technical data as defined in the International Traffic in Arms Regulations (ITAR) 22 CFR 120.10.

This document has been approved by the Unites States Government for public release in accordance with NOAA NPOESS Integrated Program Office.

Distribution: Statement A: Approved for public release; distribution is unlimited.

NATIONAL POLAR-ORBITING OPERATIONAL ENVIRONMENTAL SATELLITE SYSTEM (NPOESS)

CLOUD TOP ALGORITHM THEORETICAL BASIS DOCUMENT (ATBD) (D43754 Rev B)

ELECTRONIC APPROVAL SIGNATURES:

_____

Roy Tsugawa Date
Algorithm & Data Processing IPT Lead &
Algorithm Change Control Board Chairperson

_____

Ben James Date
Operations & Support IPT Lead

The following individuals are recognized for their contributions to the current or previous versions of this document.

David Hogan
Hung-Lung Huang
Ted Kennelly
Richard Lynch
Jean-Luc Moncet
Szu-Cheng Ou
Craig Richard
Richard L. Slonaker
Gennadi Uymin
Eric Wong
Scott Zaccheo

Check the JPSS MIS Server at https://jpssmis.gsfc.nasa.gov/frontmenu_dsp.cfm to verify that this is the correct version prior to use.

Revision/Change Record

Document Number D43754

Revision	Document Date	Revision/Change Description	Pages Affected
---	1/24/2007	Initial PCIM Release to bring document into Matrix Accountability. Reference original document number: Y2395 delivered in 2003	All
A	11/28/2007	Initial PCIM Release to bring document into Matrix Accountability. Reference original document number AER Document #: P1187-TR-I-005 v6 rev 5 delivered in 2005. ECR A-057.	All
B	03/01/2010	In preparation for Public Release of this ATBD, the following administrative changes were made: all ITAR markings were removed, and Distribution Statement F added. Approved for Public Release per Contracts Letter 100610-02.	All

TABLE OF CONTENTS

Page

LIST OF FIGURES iii

LIST OF TABLES vi

DEFINITION OF SYMBOLS x

ABSTRACT xi

1 INTRODUCTION 1
- 1.1 PURPOSE 1
- 1.2 SCOPE 1
- 1.3 VIIRS DOCUMENTS 1
- 1.4 REVISION 1

2 EXPERIMENT OVERVIEW 3
- 2.1 OBJECTIVES OF CLOUD TOP PARAMETER RETRIEVALS 3
  - 2.1.1 Cloud Top Height 3
  - 2.1.2 Cloud Top Pressure 5
  - 2.1.3 Cloud Top Temperature 7
- 2.2 INSTRUMENT CHARACTERISTICS 7
- 2.3 RETRIEVAL STRATEGY 13

3 ALGORITHM DESCRIPTION 14
- 3.1 PROCESSING OUTLINE 15
  - 3.1.1 General Approach 15
  - 3.1.2 UCLA IR Algorithm for Retrieval of Ice Cloud and Night Water Cloud CTT 16
  - 3.1.3 Window IR Algorithm for Retrieval of Daytime Water Cloud CTT 17
  - 3.1.4 Cloud Top Parameter Interpolation 18
  - 3.1.5 Backup Cloud Top Parameter Algorithm 18
- 3.2 ALGORITHM INPUT 19
- 3.3 THEORETICAL DESCRIPTION OF THE CLOUD TOP PARAMETER RETRIEVAL ALGORITHMS 20
  - 3.3.1 Physics of the Problem 20
  - 3.3.2 Mathematical Description of the Algorithms 23

3.4 ALGORITHM TESTING AND ERROR ANALYSIS 39
3.4.1 Error Budget 39
3.4.2 Algorithm Testing 50
3.5 PRACTICAL CONSIDERATIONS 68
3.5.1 Numerical Computation Considerations 68
3.5.2 Configuration of Retrievals 68
3.5.3 Quality Assessment and Diagnostics 69
3.5.4 Exception Handling 70
3.6 ALGORITHM VALIDATION 70
4.0 ASSUMPTIONS AND LIMITATIONS 71
4.1 ASSUMPTIONS 71
4.2 LIMITATIONS 71
5.0 REFERENCES 73

LIST OF FIGURES

Page

Figure 1. Summary of VIIRS design concepts and heritage. 9

Figure 2. VIIRS detector footprint aggregation scheme for building "pixels." 9

Figure 3. Benefits of VIIRS aggregation scheme in reducing pixel growth at edge of scan. 10

Figure 4. VIIRS spectral bands, visible and near infrared. 11

Figure 5. VIIRS spectral bands, short wave infrared. 12

Figure 6. VIIRS spectral bands, medium wave infrared. 12

Figure 7. VIIRS spectral bands, long wave infrared. 13

Figure 8. High-level data flow for cloud top parameter retrieval. Processing path includes backup algorithms used when COP inputs are missing or degraded. 16

Figure 9. Window IR Daytime Water Cloud CTT Retrieval Algorithm. Two methods include the Newton-Raphson Iteration (left) and Search (right) algorithms. The search algorithm is used to address cases where convergence is a problem. 17

Figure 10. BackUp CTP retrieval based on precipitable-water correction 19

Figure 11. Vertical Optical Depth Profile of an Atmosphere Containing one Cloud Layer. T, p, z and τ represent temperature, pressure, height, and optical depth respectively. Subscripts ct, cb and sfc indicate cloud top, cloud base and surface respectively. 23

Figure 12. RMS Error for OSS Radiances compared to LBLRTM under clear conditions for a nadir viewing angle. Results based on the four-channel and single channel representations are shown. 27

Figure 13. Cloud Simulation schematic showing location of the surface, cloud top, and cloud base relative to a pressure grid with 8 levels. The components of top-of-atmosphere radiance from each level (attenuated to the TOA) are indicated. 28

Figure 14. Cloud top brightness temperature uncertainty resulting from the omission of scattering as a function of viewing angle, cloud particle size, and cloud optical thickness (defined for a nadir path). Maximum errors (identified in the plot) occur for partially transmissive clouds. Greyscale varies from 0 to 0.6 K. 29

Figure 15. Cloud top brightness temperature uncertainty representing errors in the MSC regression as a function of viewing angle, cloud particle size, and cloud optical thickness (defined for a nadir path). The largest errors (identified in the plot) occur for large view angles. The greyscale is the same as for Figure 14.....30

Figure 16. Multiple scattering model correction error as a function of scattering and non-scattering radiance emitted at top of cloud for four viewing angles.....31

Figure 17. The ratio of visible extinction efficiency to IR absorption efficiency used to convert 0.55 micron COT to COT at 10.763 microns. 32

Figure 18. Cloud Top Temperature as a function of Precipitable Water as determined by the Window IR algorithm. The 10.7625 μm brightness temperatures are indicated by the color scale. 36

Figure 19. Vertical Relationship of Cloud Top and Closest Atmospheric Profile Levels. 37

Figure 20. Radiometric Accuracy results for 0.1% (top) and 0.5% (bottom) perturbations in the 10.763 μm radiances using Scenario 4 and the Window IR algorithm. The measurement accuracy metric is plotted.....42

Figure 21. Radiometric Accuracy results for 1% (top) and 2% (bottom) perturbations in the 10.763 μm radiances using Scenario 4 and the Window IR algorithm. The measurement accuracy metric is plotted.....43

Figure 22. Radiometric Stability results for 0.1% (top) and 0.5% (bottom) perturbations of the 10.763 μm radiances using Scenario 4 and the Window IR algorithm. The long-term stability metric is plotted.....45

Figure 23. Instrument noise contour plot for measurement accuracy (Scenario 4, Model 3). 48

Figure 24. Instrument noise contour plot for measurement precision (Scenario 4, Model 3).....48

Figure 25. Instrument Noise Measurement Precision Results (Scenario 2). 49

Figure 26. M15 brightness temperature data for scene used in functional testing. 51

Figure 27. Retrieved cloud top temperature for the s10_DAY_MID_LAT_SPRING scene, including both water and ice cloud retrievals. A region with water clouds (shown in Figure 28) is identified by the green box in the lower right. 52

Figure 28. A portion of the s10_DAY_MID_LAT_SPRING scene showing cloud top temperature retrievals in a region identified with water clouds. Note how at the edges of the cloud where the cloud optical thickness IP reports low values, results in unrealistically low values of cloud temperature.....52

Figure 29. Retrieved cloud top pressure as a function of cloud optical thickness for all day water clouds. Red points indicate non-convergence. OSS pressure levels are indicated in green. 53

Figure 30. Number of iterations used in the Newton-Raphson solution for cloud top pressure. Red triangles represent retrievals using the observed M15 brightness temperature as the first guess. Black asterisks represent retrievals that use the solution from the previous retrieval as first guess. 53

Figure 31. M15 brightness temperatures for the VIIRS_2002190_1625 unit test scene. 54

Figure 32. Histogram of CTT retrieval errors as a function of COT for COT>1. Top left: Window IR algorithm. Top right: BackUp WindowIR algorithm. Bottom left: BackUp PW Regression algorithm. Bottom right: Brightness temperatures 61

Figure 33. Histogram of CTT retrieval errors as a function of COT for COT≤1. Top left: Window IR algorithm. Top right: BackUp WindowIR algorithm. Bottom left: BackUp PW Regression algorithm. Bottom right: Brightness temperatures 62

Figure 34. CTP accuracy, precision, uncertainty performance comparison for COT > 1 (left) and COT=1 (right). Shown are results for IR-Win: Window IR algorithm, BB-PR: Precipitable Water Regression BackUp Algorithm, BB-Reg: Window_IR BackUp algorithm, BB-UC: BackUp with no atmospheric correction, and Req: the requirements. 64

Figure 35. CTT accuracy, precision, uncertainty performance comparison for COT > 1 (left) and COT=1 (right). Shown are results for IR-Win: Window IR algorithm, BB-PR: Precipitable Water Regression BackUp Algorithm, BB-Reg: Window_IR BackUp algorithm, BB-UC: BackUp with no atmospheric correction, and Req: the requirements. 65

Figure 36. CTH accuracy, precision, uncertainty performance comparison for COT > 1 (left) and COT=1 (right). Shown are results for IR-Win: Window IR algorithm, BB-PR: Precipitable Water Regression BackUp Algorithm, BB-Reg: Window_IR BackUp algorithm, BB-UC: BackUp with no atmospheric correction, and Req: the requirements. 66

LIST OF TABLES

Table 1. System Specification Requirements for Cloud Top Height. 5

Table 2. System Specification Requirements for Cloud Top Pressure.....6

Table 3. System Specification Requirements for Cloud Top Temperature.....7

Table 4. VIIRS VNIR bands.....10

Table 5. VIIRS SWIR, MWIR, and LWIR bands. 10

Table 6. Bands Used for Cloud Retrievals. "x" denotes cloud algorithms that use the band.....13

Table 7. Description of the Input Data Required by the Cloud Top Parameters Retrieval Algorithms 20

Table 8. Inputs to OSS forward model. 25

Table 9. Outputs from OSS forward model.....25

Table 10. Bias values (in percent) above which threshold measurement accuracy is exceeded for water droplet clouds, with $r_e = 5$ and for $\tau = 1$ and 10. 44

Table 11. Bias values (in percent) above which threshold long-term stability is exceeded for water droplet clouds with re = 5 and for τ = 1 and 10. 46

Table 12. Precision Performance Estimates using Noise Model 3. Check mark indicates performance exceeds threshold. Question mark indicates performance marginally meets threshold.....50

Table 13. Errors applied to COT and EPS.....55

Table 14. Surface Emissivity and Errors 55

Table 15a. Cloud Top Pressure Performance for COT > 1 56

Table 15b. Cloud Top Temperature Performance for COT > 1 57

Table 15c. Cloud Top Height Performance for COT > 1 57

Table 16a. Cloud Top Pressure Performance for COT = 1 57

Table 16b. Cloud Top Temperature Performance for COT = 1 57

Table 16c. Cloud Top Height Performance for COT = 1 58

Table 17a. Performance for COT>1 based retrievals using black cloud Window IR algorithm. (Requirements are in parentheses.) 59

Table 17b. Performance for COT>1 based retrievals using black cloud PW regression..... 59

Table 17c. Performance for COT>1 based brightness temperatures 59

Table 17d. Performance for COT=1 based retrievals using black cloud physical retrieval 60

Table 17e. Performance for COT=1 based retrievals using black cloud PW regression..... 60

Table 17f. Performance for COT=1 based brightness temperatures..... 60

Table 18. Sumary of performance of non-day/ water algorithm against Cloud Top Parameter EDR performance requirements. Key: yes [green] = meets or exceed requriements; no [red] = does not meet; nearly [yellow] = within ~30% of meeting requirements; N/S = not specified. 67

Table 19. Data used by Retrieval Algorithms..... 70

GLOSSARY OF ACRONYMS

ARM	Atmospheric Radiation Measurement program
ATBD	Algorithm Theoretical Basis Document
AVHRR	Advanced Very High Resolution Radiometer
CDR	Critical Design Review
CHARTS	Code for High Resolution Accelerated Radiative Transfer with Scattering
CLW	Cloud Liquid Water
CMIS	Conical Scanning Microwave Imager/Sounder
CMIS	Conical Scanning Microwave Imager/Sounder
CMS	Cloud Multiple Scattering
COT	Cloud Optical Thickness
CrIS	Cross-track Infrared Sounder
CSSM	Cloud Scene Simulation Model
CTH	Cloud Top Height
CTP	Cloud Top Pressure
CTT	Cloud Top Temperature
DEM	Digital Elevation
DISORT	Discrete Ordinate Radiative Transfer
DoD	Department of Defense
ECMWF	European Center for Medium Range Weather Forecasting
EDR	Environmental Data Record
EOS	Earth Observing System
EPS	Effective Particle Size
FIRE	First ISCCP Regional Experiment
GIFOV	Ground Instantaneous Field of View
GSD	Ground Sampling Distance
HC	Horizontal Cell
HCS	Horizontal Cell Size
HIS	Horizontal Sampling Interval
HSR	Horizontal Spatial Resolution
IPO	Integrated Program Office
IPT	Integrated Product Team

IR	Infrared
ISCCP	International Satellite Cloud Climatology Program
IWC	Ice Water Content
LBLRTM	Line-by-line Radiative Transfer Model
LLLS	Low-level Light Sensor
LOS	Line-of-Sight
LUT	Look-Up Table
MAS	MODIS Airborne Simulator
MODIS	Moderate Resolution Imaging Spectroradiometer
MODTRAN	Moderate Resolution Atmospheric Radiance and Transmittance Model
MSC	Multiple Scattering Correction
MTF	Modulation Transfer Function
NASA	National Aeronautics and Space Administration
NOAA	National Oceanic and Atmospheric Administration
NPOESS	National Polar-orbiting Operational Environmental Satellite System
NWP	Numerical Weather Prediction
OLS	Operational Linescan System
OSS	Optimal Spectral Sampling
RSBR	Raytheon Santa Barbara Research
RSS	Root of the Sum of the Squares
RTM	Radiative Transfer Model
SBRS	Santa Barbara Remote Sensing
SDR	Sensor Data Record
SDSM	Solar Diffuser Stability Monitor
SNR	Sensor Signal-to-Noise Ratio
SRD	Sensor Requirements Document
TBD	To be Determined
TIROS	Television Infrared Observation Satellite
TOA	Top of the Atmosphere
UCLA	University of California at Los Angeles
VIIRS	Visible/Infrared Imager/Radiometer Suite
DW	Day Water
NDW	Non-Day-Water

DEFINITION OF SYMBOLS

z_{cb} (km - kilometers)	Cloud Base Height
r_e (μm or um (in figures) – micrometers)	Cloud Mean Effective Particle Radius
D_e (μm - micrometers)	Cloud Mean Effective Particle Diameter
H(p)	Geopotential height as function of pressure
τ (unitless)	Cloud Optical Depth
z (km - kilometers)	Height
z_{cb} (km - kilometers)	Cloud Base Height
z_{ct} (km - kilometers)	Cloud Top Height
p (mb - millibars)	Pressure
p_{ct} (mb - millibars)	Cloud Top Pressure
Q(p) (g/kg)	Water vapor mixing ratio as function of pressure
T_{cb}(K - degrees Kelvin)	Cloud Base Temperature
T_{ct} (K - degrees Kelvin)	Cloud Top Temperature
T(p) (Kelvins)	Atmospheric temperature as function of pressure
T_s (Kelvins)	Surface tempreature
ε (unitless)	Surface emissivity
μ_0	Cosine of Solar Zenith Angle
μ	Cosine of Sensor Zenith Angle
I	Radiance
Δϕ (angular degrees)	Sun-Sensor Relative Azimuth Angle
ϕ (angular degrees)	Sensor Azimuth Angle
θ (angular degrees)	Sensor Zenith Angle
ϕ_0 (angular degrees)	Solar Azimuth Angle
θ_0 (angular degrees)	Solar Zenith Angle
λ	Wavelength
$mW/(m^2\ sr\ cm^{-1})$	Radiance units in milli-Watts per meter squared per steradian per wave-number
$mW/(m^2\ sr\ cm^{-1})$ / mb	Derivative of radiance in milli-Watts per meter squared per steradian per wave-number per mill-bar
μm	length units micrometers, used for wavelength

ABSTRACT

The Visible/Infrared Imager/Radiometer Suite (VIIRS) Cloud Top Parameters Algorithm estimates Cloud Top Temperature (CTT), Cloud Top Pressure (CTP) and Cloud Top Height (CTH) using VIIRS radiances, other VIIRS Cloud Intermediate Products (IPs), derived quantities (e.g., cloud mask and phase) and an ancillary profile of atmospheric temperature and moisture. Pixels identified as clouds by the VIIRS Cloud Mask (VCM) (and for which the required intermediate products and ancillary data are present) are processed with one of two methods depending on the cloud phase and the solar conditions. One method applies to water phase clouds in daytime, referred to day-water (DW) conditions. The other method applies to all other conditions (these conditions are water phase clouds in nighttime and ice phase clouds both day and night), referred to as non-day-water (NDW) conditions.

NDW conditions use the CTT derived from the Cloud Optical Properties (COP) unit (i.e., UCLA algorithm (Ou *et al.*, 2004)). CTH is then determined using a linear interpolation and an input ancillary temperature sounding (Rossow *et al.*, 1991). CTP is computed using the hypsometric equation. This is referred to as the CTP Interpolation Algorithm.

DW conditions employ the Window Infrared (IR) algorithm to first derive CTP for water clouds during the day. The approach employs an iterative physical retrieval that determines the cloud Top Pressure (CTP) that minimizes the difference between the observed 10.763 μm band radiance and a radiance estimate produce by a fast radiative transfer model that uses as inputs atmospheric profiles of temperature and moisture, cloud optical thickness/ particle size, and surface temperature/ emissivity. CTT and CTH are then derived from CTP by interpolation methods based on the same physical principles as with the NDW Algorithm.

This document describes the generation of the CTP Intermediate Product, a product produced at M-band pixel resolution (~ 0.8 km at nadir). A separate algorithm, called Grid Cloud EDRs (GCE), aggregates the pixel level products to the horizontal cells required by the System Specification for the delivered EDR. The GCE algorithm is not discussed here.

The Window IR Algorithm and the Cloud Top Parameter Interpolation Algorithms are described in detail in this report. In addition, this report provides a description of data flow, the retrieval algorithms and their physical basis, flowdown and sensitivity studies and algorithm implementation considerations. Measurement requirements for cloud top parameters are specified in the VIIRS System Specification Document and the VIIRS System Requirements Document (SRD) and are repeated in this report. Window IR algorithm cloud top parameters retrieval performance analysis has been conducted. Current simulation results demonstrate specification requirements will be met.

1 INTRODUCTION

1.1 PURPOSE

This document describes algorithms that will be used to retrieve cloud top parameters using data from the Visible/Infrared Imager/Radiometer Suite (VIIRS) instrument. A description is provided of data flow, the retrieval algorithms and their physical basis, flowdown, EDR performance and sensitivity studies and implementation considerations. Measurement requirements for cloud top parameters, including CTT, CTP and CTH, are identified in the VIIRS System Specification Document.

1.2 SCOPE

This document focuses on the theoretical basis for retrieval of CTT, CTP and CTH using VIIRS data. Because multiple algorithms are used for cloud parameter retrieval (i.e., retrieval of cloud optical depth, effective particle size, base height, and amount/layers) and because these parameters are related to the cloud top parameters, frequent reference is made to the other cloud parameter Algorithm Theoretical Basis Documents (ATBDs). In addition, some algorithms estimate multiple parameters, including CTT. The details of these algorithms are not repeated here; instead, the appropriate ATBD is referenced.

The document is organized into five major sections. The first section is an introduction. The next section provides an overview of the retrieval algorithms, including objectives, instrument characteristics and retrieval strategy. Section 3 describes the retrieval algorithms and their physical basis, data requirements and issues, algorithm sensitivities to input and flowdown, error budget, practical considerations and validation. Section 4 provides a brief description of major algorithm assumptions and limitations, and Section 5 is a list of references cited.

1.3 VIIRS DOCUMENTS

[V-1] VIIRS System Specification (SS154640).

1.4 REVISION

Y2395, Version 5, Revision 1, Cloud Top Parameters ATBD, March 2002.

Y2395, Version 5, Revision 2, Cloud Top Parameters ATBD, January 2004.

> Remove ambiguity regarding use of LUT. Add algorithm for precipitable water correction for Window IR technique. Correct hypsometric equation to show use of virtual temperature instead of temperature.

P1131-TR-005, Version 6, Initial Release, Cloud Top Parameters ATBD, September 2004. (AER Internal Version 1), modified from Raytheon document Y2395, Version 5, Release 2

> Atmospheric and Environmental Research (AER), Inc. selected in May 2004 by the Northrop Grumman Space Technology NPOESS Program Office to revise and upgrade the Cloud Top Parameters (CTP) Intermediate Product Version 5, Release 2 ATBD and

corresponding algorithm science grade code. The original algorithm through Version 5 (ATBD and code) was developed by Raytheon Technical Services Company LLC, Information Technology and Scientific Services.

Version 5, Release 2 of the ATBD and corresponding software for the Cloud Top Parameter algorithm assumed daytime water phase clouds applied an empirically derived water vapor correction to the observed window infrared brightness temperature. This method has two implicit assumptions:

(1) the clouds are optically thick so that emission from the cloud occurs within a thin layer very near the physical cloud top and emission/ absorption below the cloud can be ignored, and

(2) scattering effects are negligible

Versions of the ATBD prior to Version 5, Release 2 (including the original Version 5 release defining VIIRS CDR baseline) describe a method that uses cloud optical thickness and particle size to account for optically thin clouds where the absorption and emission occurs over a finite vertical extent and the clouds may be partially transparent (so that radiative effects from below the cloud need to be considered).

Version 6 of this ATBD (and the corresponding science grade algorithm code) address the two limitations of the Version 5, Release 2 algorithm listed above. The approach employs a fast radiative transfer model for VIIRS band M15 (10.763 μm) that accounts for emission, absorption and scattering from a complete range of cloud optical thicknesses. The model was integrated into the algorithm as part of an iterative physical retrieval that solves directly for cloud top pressure (and indirectly for temperature and height) for DW clouds. The fast RT model is an extension of the same fast RT model employed by the CrIS algorithm: the Optimal Spectral Sampling (OSS) model. A version optimized for moderate resolution channels (order 1 μm) was developed and tested against more exact line by line codes. A parametric correction for multiple scattering in the cloud is used.

We note daytime water-phase algorithm approach follows the same general scientific approach as the method described in Version 5, Release 0 of the CTP ATBD (as delivered at the VIIRS CDR), but is globally applicable.

The method for processing clouds other than water-phase daytime clouds (referred to here as non-day/ water or NDW clouds) was not changed in any significant way.

To maintain maximum consistency with the overall architecture of the VIIRS Cloud Module, the basic interfaces to the other cloud algorithm units was not changed. Thus, the Version 6 Algorithm described in this version of the ATBD is based on the same basic scientific approach that was developed and accepted as part the VIIRS CDR algorithm delivery.

P1131-TR-005, Version 6, Revision 1, Cloud Top Parameters ATBD, October 2004

Update to DayWater Performance and minor formatting corrections.

P1131-TR-005, Version 6, Revision 2, Cloud Top Parameters ATBD, October 2004

Made consistent references to band M15 wavelength as 10.763 μm (consistent with . SPCR ALG Oct 2004)

P1131-TR-005, Version 6, Revision 3, Cloud Top Parameters ATBD, October 2004

Additional corrections based on comments from IDPS (R. Slonaker 20OCT2004)

P1131-TR-005, Version 6, Revision 4, Cloud Top Parameters ATBD, May 2005

Added back-up algorithms that do not require inputs from Cloud Optical Properties unit to be run in cases when the COP products are bad or unavailable; modified code for new cloud mask (the new mask includes a designation of cases with multi-level clouds); modified code for new quality control flags

P1131-TR-005, Version 6, Revision 5, Cloud Top Parameters ATBD, 16 Jun 2004

Resolved any discrepancies between revisions

2 EXPERIMENT OVERVIEW

This section contains three major subsections. Subsection 2.1 describes the objectives of the cloud top parameter retrievals. Subsection 2.2 describes the characteristics of the VIIRS instrument. Subsection 2.3 addresses the cloud top parameter retrieval strategy.

2.1 OBJECTIVES OF CLOUD TOP PARAMETER RETRIEVALS

The cloud top parameter retrieval algorithms, together with the prospective VIIRS sensor, will be developed to meet System Specification requirements for CTT, CTP and CTH. For reference, these requirements are provided in Sections 2.1.1 through 2.1.3. Under the VIIRS sensor/algorithm development concept, these requirements are "flowed down" to the design of the most cost-effective sensor/algorithm solution that meets the Specification requirements. This is accomplished through a series of flowdown tests and error budget analyses, which effectively simulate sensor and algorithm performance over a range of environmental and operational scenarios. The error budgets are briefly described in Section 3.4.1 and described in much more detail in the Raytheon VIIRS Error Budget, Version 3 (Y3249).

2.1.1 Cloud Top Height

The SRD provides the following definition for CTH:

> *"Cloud Top Height (CTH) is defined for each cloud-covered Earth location as the set of heights of the tops of the cloud layers overlying the location. The reported heights are horizontal spatial averages over a cell, i.e., a square region of the Earth's surface. If a cloud layer does not extend over an entire cell, the spatial average is limited to the portion of the cell that is covered by the layer. CTH is not defined or reported for cells that are clear. As a threshold, only the height at the top of the highest altitude cloud*

layer is required. The objective is to report the CTH for all distinct cloud layers. This EDR must be generated as a dual product at two spatial scales, one meeting the moderate HCS requirements and the other meeting the fine HCS requirements. The moderate HCS product is the operational requirement, and the fine HCS product is for augmented applications only."

Table 1 summarizes the System Specification requirements for this parameter.

Table 1. System Specification Requirements for Cloud Top Height.

Requirement Number	Parameter	Requirement
SSV0251	EDR CLTPHT Moderate HCS worst case:	25 km
SSV0252	EDR CLTPHT Fine HCS at nadir:	5 km
SSV0253	EDR CLTPHT HRI:	HCS
SSV0254	EDR CLTPHT Horizontal Coverage:	Global
SSV0255	EDR CLTPHT Vertical Reporting Interval:	Up to 4 layers
SSV0256	EDR CLTPHT Measurement Range:	0 to 20 km
SSV0257	EDR CLTPHT Moderate Measurement Accuracy, Cloud layer optical thickness > 1.0 day water cloud:	0.5 km
SSV0806	EDR CLTPHT Moderate Measurement Accuracy, Cloud layer optical thickness > 1.0 night water cloud:	1.0 km
SSV0807	EDR CLTPHT Moderate Measurement Accuracy, Cloud layer optical thickness > 1.0 ice cloud (day and night):	1.0 km
SSV0258	EDR CLTPHT Moderate Measurement Accuracy, Cloud layer optical thickness ≤ 1.0:	2.0 km
SSV0259	EDR CLTPHT Moderate Measurement Precision:	0.3 km
SSV0261	EDR CLTPHT Fine Measurement Uncertainty, Cloud layer optical thickness > 1.0, day water cloud:	0.5 km
SSV0899	EDR CLTPHT Fine Measurement Uncertainty, Cloud layer optical thickness > 1.0, night water cloud:	1.0 km
SSV0900	EDR CLTPHT Fine Measurement Uncertainty, Cloud layer optical thickness <= 1.0, day water cloud:	2.0 km
SSV0901	EDR CLTPHT Fine Measurement Uncertainty, Cloud layer optical thickness <= 1.0, night water cloud:	2.0 km
SSV0262	EDR CLTPHT Fine Measurement Uncertainty, ice cloud (day and night):	1 km
SSV0263	EDR CLTPHT Measurement Long Term Stability:	0.2 km
SSV0265	EDR CLTPHT Swath Width:	3000 km

2.1.2 Cloud Top Pressure

The SRD provides the following definition for CTP:

> *"Cloud Top Pressure (CTP) is defined for each cloud-covered Earth location as the set of atmospheric pressures at the tops of the cloud layers overlying the location. The reported pressures are horizontal spatial averages over a cell, i.e., a square region of the Earth's surface. If a cloud layer does not extend over an entire cell, the spatial average is limited to the portion of the cell that is covered by the layer. CTP is not defined or reported for cells that are clear. As a threshold, only the pressure at the top of the highest altitude cloud layer is required. The objective is to report the CTP for all distinct cloud layers. This EDR must be generated as a dual product at two spatial scales, one meeting the moderate HCS requirements and the other meeting the fine HCS requirements. The moderate HCS product is the operational requirement, and the fine HCS product is for augmented applications only."*

Table 2 summarizes the System Specification requirements for this parameter.

Table 2. System Specification Requirements for Cloud Top Pressure.

Requirement Number	Parameter	Requirement
SSV0267	EDR CLTPPR Moderate HCS worst case:	25 km
SSV0268	EDR CLTPPR Fine HCS at nadir:	5 km
SSV0269	EDR CLTPPR HRI:	HCS
SSV0270	EDR CLTPPR Horizontal Coverage:	Global
SSV0271	EDR CLTPPR Measurement Range:	50 to 1050 mb
SSV0272	EDR CLTPPR Moderate Measurement Accuracy, 0 to 3 km altitude, optical thickness <= 1.0, day water cloud:	100 mb
SSV0902	EDR CLTPPR Moderate Measurement Accuracy, 0 to 3 km altitude, optical thickness <= 1.0, night water cloud:	100 mb
SSV0903	EDR CLTPPR Moderate Measurement Accuracy, 0 to 3 km altitude, optical thickness > 1.0, day water cloud:	40 mb
SSV0904	EDR CLTPPR Moderate Measurement Accuracy, 0 to 3 km altitude, optical thickness > 1.0, night water cloud:	70 mb
SSV0273	EDR CLTPPR Moderate Measurement Accuracy, 3 to 7 km altitude, optical thickness <= 1.0:	65 mb
SSV0905	EDR CLTPPR Moderate Measurement Accuracy, 3 to 7 km altitude, optical thickness > 1.0:	40 mb
SSV0274	EDR CLTPPR Moderate Measurement Accuracy, > 7 km altitude:	30 mb
SSV0275	EDR CLTPPR Moderate Measurement Precision, 0 to 3 km altitude:	25 mb
SSV0276	EDR CLTPPR Moderate Measurement Precision, 3 to 7 km altitude:	20 mb
SSV0277	EDR CLTPPR Moderate Measurement Precision, > 7 km altitude:	13 mb
SSV0278	EDR CLTPPR Fine Measurement Uncertainty, 0 to 3 km altitude, optical thickness <= 1.0, day water cloud:	130 mb
SSV0906	EDR CLTPPR Fine Measurement Uncertainty, 0 to 3 km altitude, optical thickness <= 1.0, night water cloud:	100 mb
SSV0907	EDR CLTPPR Fine Measurement Uncertainty, 0 to 3 km altitude, optical thickness > 1.0, day water cloud:	40 mb
SSV0908	EDR CLTPPR Fine Measurement Uncertainty, 0 to 3 km altitude, optical thickness > 1.0, night water cloud:	80 mb
SSV0810	EDR CLTPPR Fine Measurement Uncertainty, 3 to 7 km altitude, optical thickness <= 1.0:	70 mb
SSV0909	EDR CLTPPR Fine Measurement Uncertainty, 3 to 7 km altitude, optical thickness > 1.0:	45 mb
SSV0811	EDR CLTPPR Fine Measurement Uncertainty, > 7 km altitude:	30 mb
SSV0279	EDR CLTPPR Measurement Long Term Stability, 3 km altitude:	10 mb
SSV0280	EDR CLTPPR Measurement Long Term Stability, 3 to 7 km altitude:	7 mb
SSV0281	EDR CLTPPR Measurement Long Term Stability, > 7 km altitude:	5 mb
SSV0283	EDR CLTPPR Swath Width:	3000 km

2.1.3 Cloud Top Temperature

The SRD provides the following definition for CTT:

> *"Cloud Top Temperature (CTT) is defined for each cloud-covered Earth location as the set of atmospheric temperatures at the tops of the cloud layers overlying the location. The reported temperatures are horizontal spatial averages over a cell, i.e., a square region of the Earth's surface. If a cloud layer does not extend over an entire cell, the spatial average is limited to the portion of the cell that is covered by the layer. CTT is not defined or reported for cells that are clear. As a threshold, only the temperature at the top of the highest altitude cloud layer is required. The objective is to report the CTT for all distinct cloud layers. This EDR must be generated as a dual product at two spatial scales, one meeting the moderate HCS requirements and the other meeting the fine HCS requirements. The moderate HCS product is the operational requirement, and the fine HCS product is for augmented applications only."*

Table 3 summarizes the System Specification requirements for this parameter.

Table 3. System Specification Requirements for Cloud Top Temperature.

Requirement Number	Parameter	Requirement
SSV0285	EDR CLTPTM Moderate HCS worst case:	25 km
SSV0286	EDR CLTPTM Fine HCS at nadir:	5 km
SSV0287	EDR CLTPTM HRI:	HCS
SSV0288	EDR CLTPTM Horizontal Coverage:	Global
SSV0289	EDR CLTPTM Measurement Range:	180 K to 310 K
SSV0290	EDR CLTPTM Moderate Measurement Accuracy, Cloud layer optical thickness > 1.0, water cloud day:	2 K
SSV0812	EDR CLTPTM Moderate Measurement Accuracy, Cloud layer optical thickness > 1.0, water cloud night:	3 K
SSV0813	EDR CLTPTM Moderate Measurement Accuracy, Cloud layer optical thickness > 1.0, ice cloud (day and night):	3 K
SSV0291	EDR CLTPTM Moderate Measurement Accuracy, Cloud layer optical thickness ≤ 1.0	6 K
SSV0292	EDR CLTPTM Moderate Measurement Precision	1.5 K
SSV0295	EDR CLTPTM Fine Measurement Uncertainty, water cloud:	3 K
SSV0816	EDR CLTPTM Fine Measurement Uncertainty, ice cloud:	5 K
SSV0893	EDR CLTPTM Long-term Stability	1 K
SSV0298	EDR CLTPTM Swath Width	3000 km

2.2 INSTRUMENT CHARACTERISTICS

The VIIRS instrument will now be briefly described to clarify the context of the descriptions of the Cloud Top Parameter EDR presented in this document. VIIRS can be pictured as a convergence of three existing sensors, two of which have seen extensive operational use at this

writing.

The Operational Linescan System (OLS) is the operational visible/infrared scanner for the Department of Defense (DoD). Its unique strengths are controlled growth in spatial resolution through rotation of the ground instantaneous field of view (GIFOV) and the existence of a low-level light sensor (LLLS) capable of detecting visible radiation at night. OLS has primarily served as a data source for manual analysis of imagery. The Advanced Very High Resolution Radiometer (AVHRR) is the operational visible/infrared sensor flown on the National Oceanic and Atmospheric Administration (NOAA) Television Infrared Observation Satellite (TIROS-N) series of satellites (Planet, 1988). Its unique strengths are low operational and production cost and the presence of five spectral channels that can be used in a wide number of combinations to produce operational and research products. In December 1999, the National Aeronautics and Space Administration (NASA) launched the Earth Observing System (EOS) morning satellite, *Terra*, which includes the Moderate Resolution Imaging Spectroradiometer (MODIS). This sensor possesses an unprecedented array of thirty-two spectral bands at resolutions ranging from 250 m to 1 km at nadir, allowing for unparalleled accuracy in a wide range of satellite-based environmental measurements.

VIIRS will reside on a platform of the National Polar-orbiting Operational Environmental Satellite System (NPOESS) series of satellites. It is intended to be the product of a convergence between DoD, NOAA and NASA in the form of a single visible/infrared sensor capable of satisfying the needs of all three communities, as well as the research community beyond. As such, VIIRS will require three key attributes: high spatial resolution with controlled growth off nadir, minimal production and operational cost, and a large number of spectral bands to satisfy the requirements for generating accurate operational and scientific products.

Figure 1 illustrates the design concept for VIIRS, designed and built by Raytheon Santa Barbara Remote Sensing (SBRS). At its heart is a rotating telescope scanning mechanism that minimizes the effects of solar impingement and scattered light. Calibration is performed onboard using a solar diffuser for short wavelengths and a V-groove blackbody source and deep space view for thermal wavelengths. A solar diffuser stability monitor (SDSM) is also included to track the performance of the solar diffuser. The nominal altitude for NPOESS will be 833 km. The VIIRS scan will extend to 56 degrees on either side of nadir.

The VIIRS SRD places explicit requirements on spatial resolution for the Imagery EDR. Specifically, the horizontal spatial resolution (HSR) of bands used to meet threshold Imagery EDR requirements must be no greater than 400 m at nadir and 800 m at the edge of the scan. This led to the development of a unique scanning approach which optimizes both spatial resolution and signal to noise ratio (SNR) across the scan. The concept is summarized in Figure 2 for the imagery bands; the nested lower resolution radiometric bands follow the same paradigm at exactly twice the size. The VIIRS detectors are rectangular, with the smaller dimension projecting along the scan. At nadir, three detector footprints are aggregated to form a single VIIRS "pixel." Moving along the scan away from nadir, the detector footprints become larger both along track and along scan, due to geometric effects and the curvature of the Earth. The effects are much larger along scan. At around 32 degrees in scan angle, the aggregation scheme is changed from 3x1 to 2x1. A similar switch from 2x1 to 1x1 aggregation occurs at 48 degrees. The VIIRS scan consequently exhibits a pixel growth factor of only 2 both along track and along

scan, compared with a growth factor of 6 along scan which would be realized without the use of the aggregation scheme. Figure 3 illustrates the benefits of the aggregation scheme for spatial resolution.

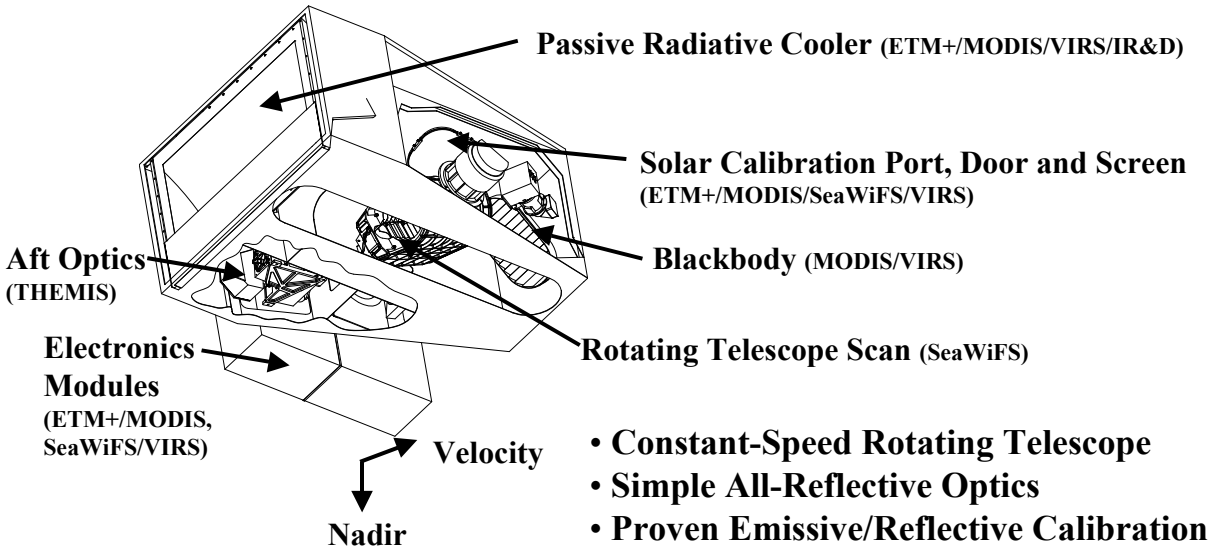

Figure 1. Summary of VIIRS design concepts and heritage.

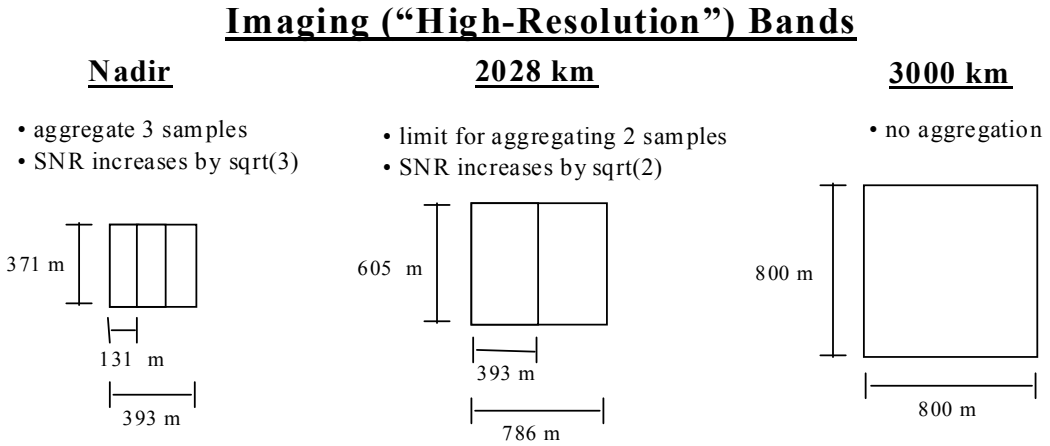

Figure 2. VIIRS detector footprint aggregation scheme for building "pixels."

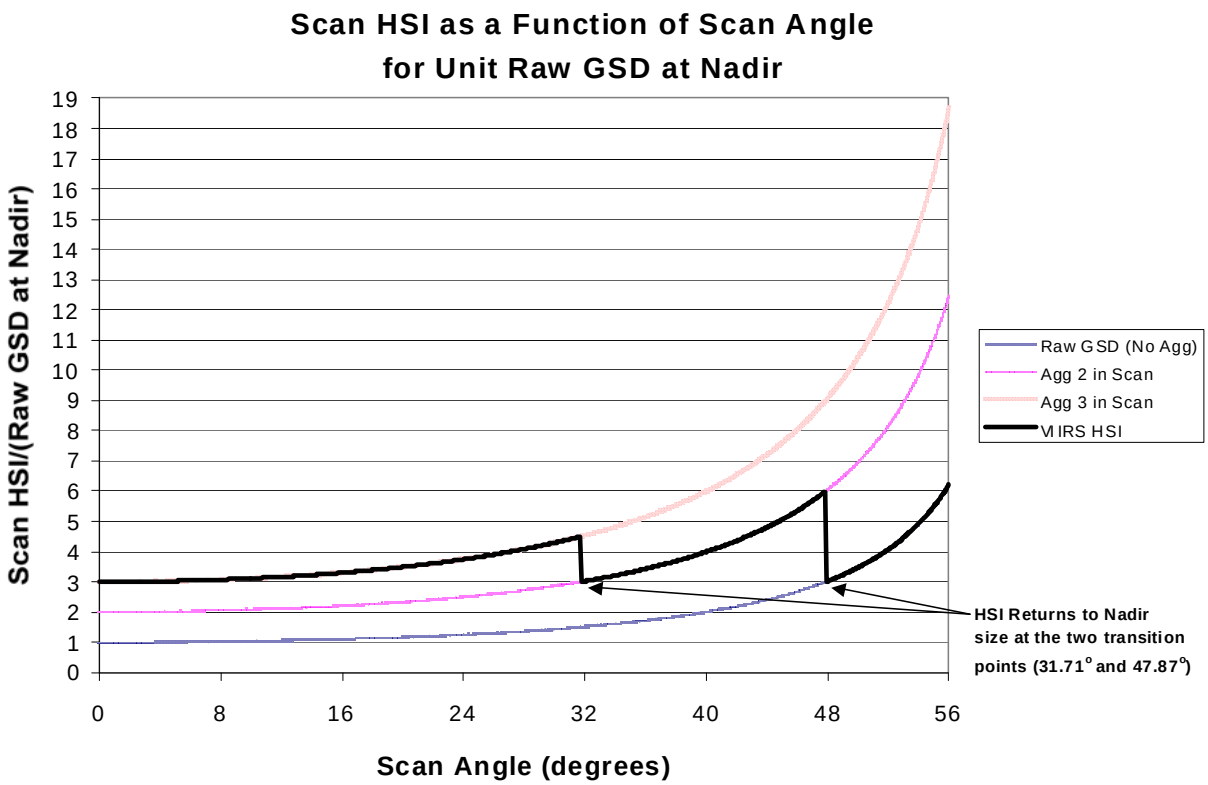

Figure 3. Benefits of VIIRS aggregation scheme in reducing pixel growth at edge of scan.

The VIIRS bands are summarized in Table 4 and Table 5. The positioning of the VIIRS spectral bands is summarized in Figure 4 through Figure 7.

Table 4. VIIRS VNIR bands.

Band Name	Wavelength (μm)	Bandwidth (μm)
Day Night Band	0.700	0.400
M1	0.412	0.020
M2	0.445	0.018
M3	0.488	0.020
M4	0.555	0.020
I1	0.640	0.080
M5	0.672	0.020
M6	0.746	0.015
I2	0.865	0.039
M7	0.865	0.039

Table 5. VIIRS SWIR, MWIR, and LWIR bands.

Band Name	Wavelength (μm)	Bandwidth (μm)
M8	1.240	0.020
M9	1.378	0.015

I3	1.610	0.060
M10	1.610	0.060
M11	2.250	0.050
I4	3.740	0.380
M12	3.700	0.180
M13	4.050	0.155
M14	8.550	0.300
M15	10.763	1.000
I5	11.450	1.900
M16	12.0125	0.950

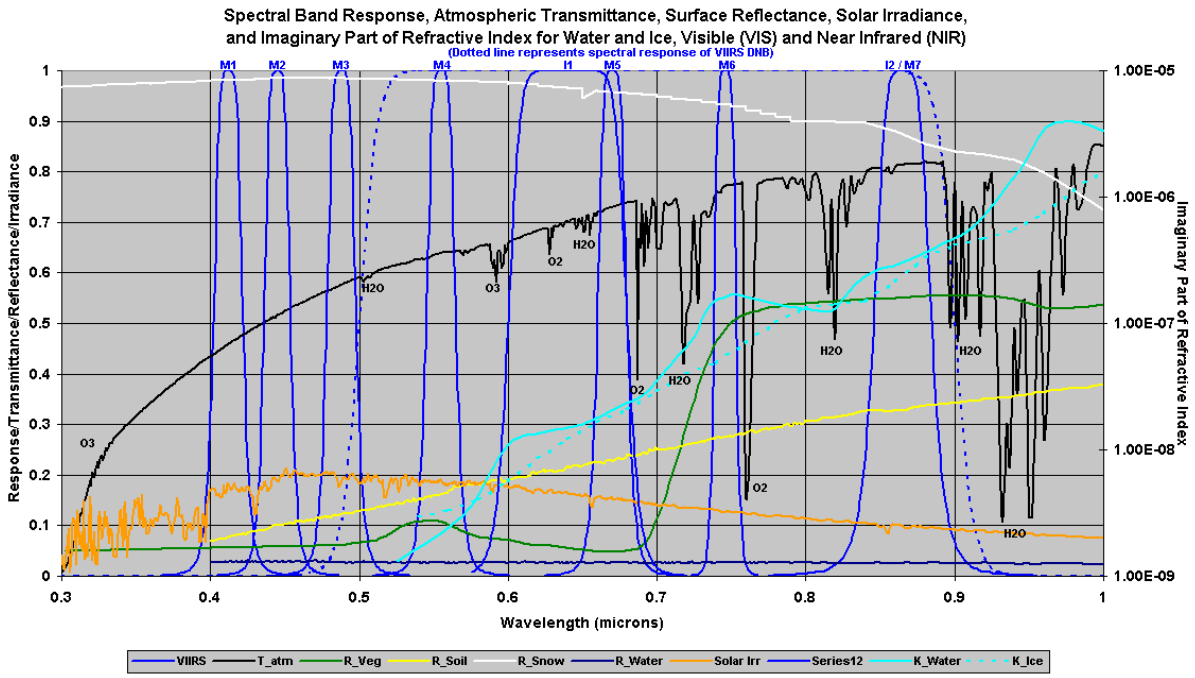

Figure 4. VIIRS spectral bands, visible and near infrared.

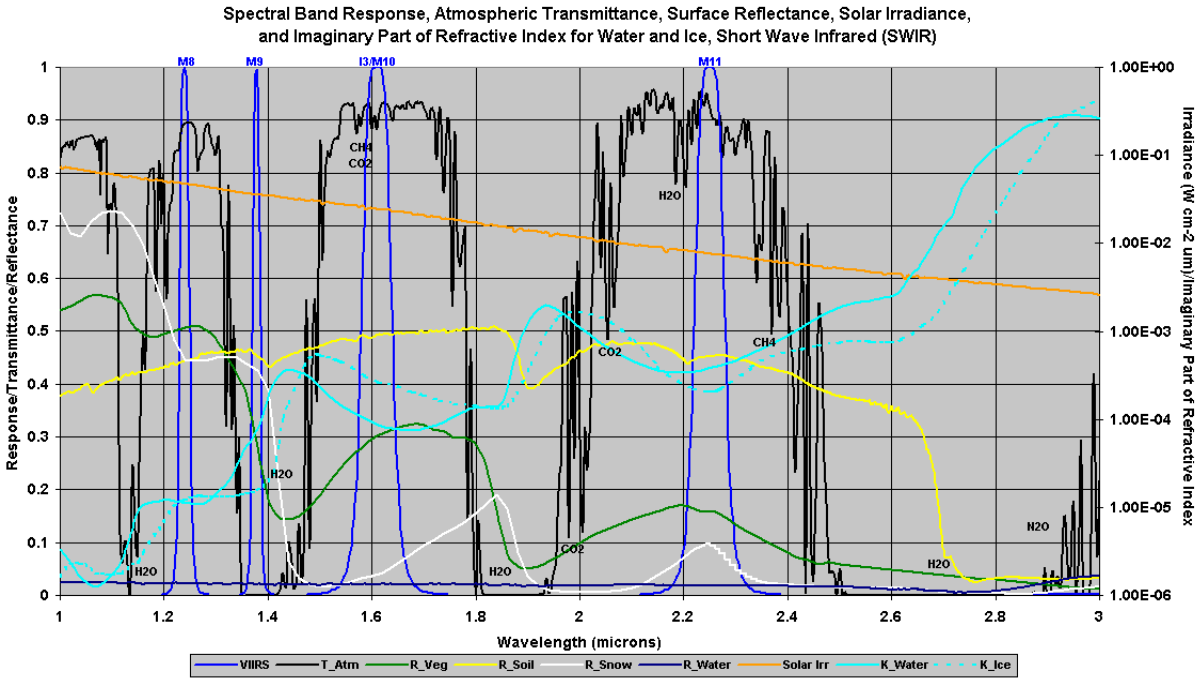

Figure 5. VIIRS spectral bands, short wave infrared.

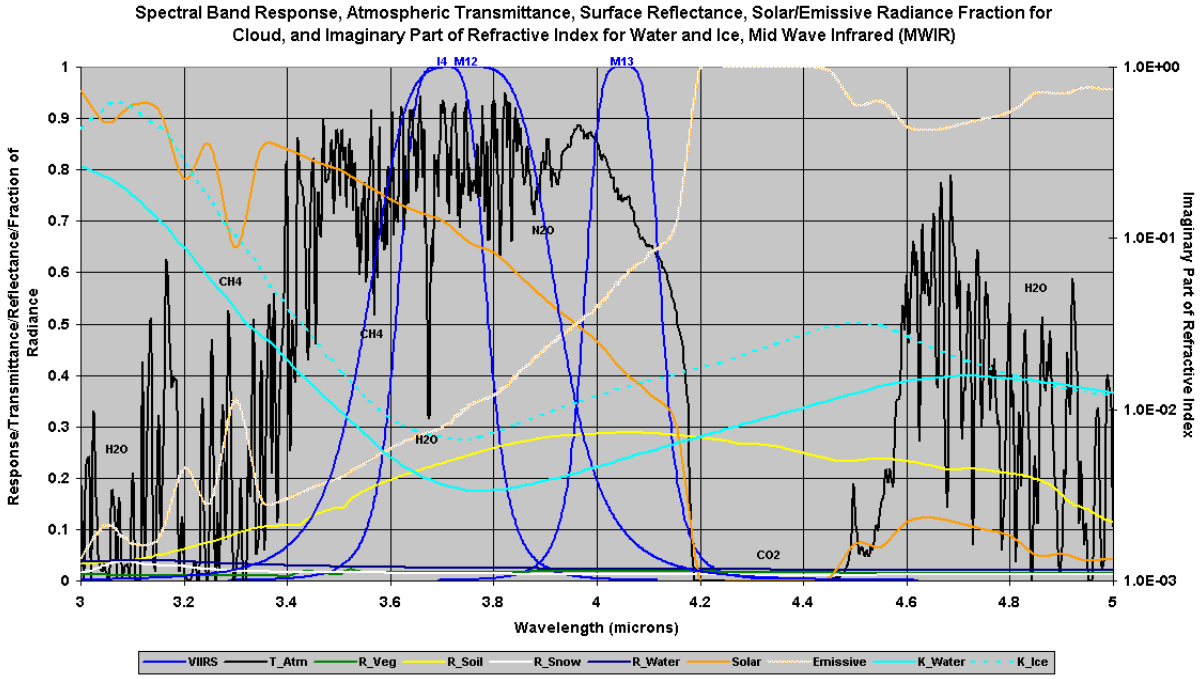

Figure 6. VIIRS spectral bands, medium wave infrared.

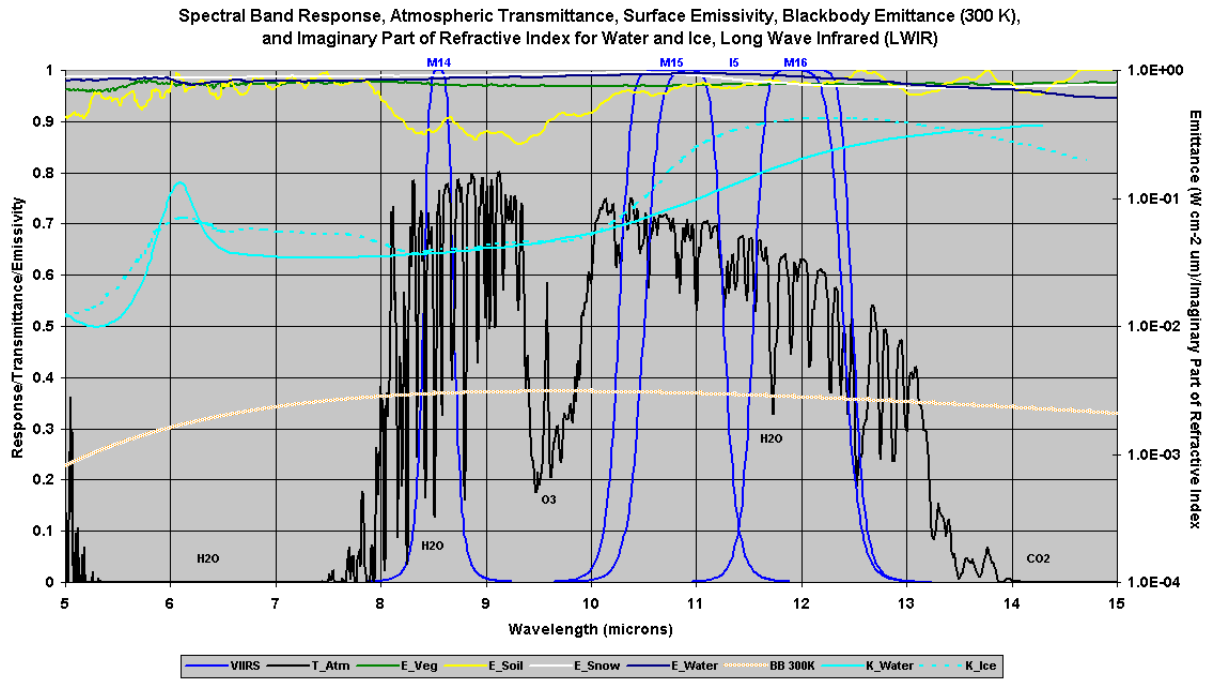

Figure 7. VIIRS spectral bands, long wave infrared.

Table 6 indicates the wavelength bands being used for VIIRS Cloud Top Temperature (CTT), cloud Effective Particle Size (EPS) and Cloud Optical Thickness (COT) retrievals. Five different bands can be used, depending on conditions, by the Cloud Optical Properties (COP) module to generate EPS and COT (Ou *et al.*, 2004). The band centered at 10.763 µm is used for the Window Infrared (IR) retrieval of the cloud top parameters unit for daytime water clouds. Not all bands are used in all conditions. The CT Properties Algorithm directly uses only band M15 radiances/ brightness temperatures.

Table 6. Bands Used for Cloud Retrievals. "x" denotes cloud algorithms that use the band.

VIIRS Band Number	Bandcenter λ (µm)	Bandwidth (µm)	Cloud Top Temperature	Cloud Effective Particle Size	Cloud Optical Depth
M5	0.672	0.020		x	x
M8	1.240	0.020		x	x
M10	1.610	0.060		x	x
M12	3.700	0.180	x	x	x
M15	10.763	1.000	x	x	x

2.3 RETRIEVAL STRATEGY

The cloud top parameter retrieval algorithms will use 10.763 µm brightness temperature data, CTT as generated by the COP unit, internal cloud IP (VIIRS cloud mask and phase) and an ancillary profile of atmospheric temperature and moisture. The VIIRS cloud mask will identify

whether each VIIRS pixel is clear or cloudy. The phase will identify the cloud as one of 6 possible phases (partly cloudy, water, mixed phase, opaque ice, cirrus, or cloud overlap). The Cloud Optical Properties algorithm operates next in the cloud module processing chain. Depending on the conditions/ cloud properties the COP algorithm simultaneous derives either two parameters (cloud optical thickness and cloud effective particle size for daytime water phase clouds) or three parameters (cloud optical thickness, cloud particle size and cloud top temperature for all other conditions). See the COP ATBD for a discussion of the rationale and techniques employed. The Cloud Top Parameter Algorithm works in concert with the COP algorithm with different processing paths for each of the two sets of conditions.

For daytime water phase clouds, an iterative physical retrieval is used to determine the cloud top pressure that best matches the observed VIIRS Channel M15 (10.763 μm) to that predicted from the atmospheric/ surface state as specified by numerical weather prediction model inputs and other data. The iterative retrieval uses a fast radiative transfer model and includes parameterization of cloud multiple scattering. The cloud optical thickness and effective particle size are used as explicit inputs and so it can account for both optically thick and thin clouds. This iterative retrieval is referred to as the Window IR Algorithm. Next it is assumed that the atmosphere is hydrostatically consistent and the cloud Top Temperature and Height corresponding to estimated cloud top pressure are determined. This approach vertically interpolates the ancillary data input profiles of atmospheric temperature and height. This latter step is referred to as the Interpolation Algorithm.

For nighttime water phase clouds and ice phase clouds in both day and night, the COP Algorithm has already determined the cloud top temperature. In this case, a slightly different form of the Interpolation Algorithm is used: First vertical interpolation is used to determine the cloud top height corresponding to the input CTT. Then the hypsometric equation is used to determine the corresponding the cloud top pressure.

In some instances, the inputs required from the COP module may be missing or degraded. For this reason, a BackUp algorithm has been introduced that is based on the assumption that the cloud is optically thick (i.e. black cloud approximation). Two methods have been added to support this mode of operation. Both include a means to address atmospheric water vapor. The first method derived the cloud top parameters using the Window IR physical retrieval algorithm with default values set to represent optically thick clouds. The second method performs a correction on the observed M15 brightness temperature based on a regression on an estimate of the above-cloud precipitable water derived from the NWP inputs. The BackUp algorithms may also be invoked if the normal Window IR (using COP inputs) fails to converge.

3 ALGORITHM DESCRIPTION

This section contains six major subsections addressing the cloud top parameter processing: outline; algorithm input; the algorithm theoretical basis and mathematical description; algorithm sensitivity to calibration and instrument noise; practical implementation considerations; and validation.

3.1 PROCESSING OUTLINE

3.1.1 General Approach

A high-level flow diagram of the general approach to determining cloud top parameters appears in Figure 8. Input parameters required by the algorithms include pixel-level, VIIRS internal products (e.g., cloud mask and phase), VIIRS radiances/brightness temperatures, and ancillary atmospheric profile data. The cloud phase along with the day/night flag are used to determine which of two processing paths is taken.

Water phase clouds in the daytime are processed using the sequence on the left side of the diagram. The Cloud Optical Properties Algorithm derives the Cloud Optical Thickness (COT) and Cloud Effective Particle Size (EPS). An iterative physical retrieval algorithm then determines the Cloud Top Pressure that minimizes the difference between the observed 10.763 μm channel radiances and those which are predicted from the cloud optical parameters and ancillary data (atmospheric profiles and surface properties). The next step for the Day/ water path is then to determine the Cloud Top Temperature and Height from CTP using interpolation methods that assume hydrostatic consistency of the atmosphere.

The second path, taken for all ice clouds and nighttime water-phase clouds, is shown on the right side of the diagram. CTT is derived in the COP Algorithm using the UCLA IR algorithm that also simultaneously solves for COT and EPS. CTT is input to the Interpolation Algorithm that solves for CTP and CTH using the same physical principles as the interpolation algorithm.

If the COP inputs required for the daytime water or non-daytime water processing paths are missing, then the backup algorithms are used to derive CTT, CTP, and CTH based on the opaque cloud assumption. Two methods are available and can be run in series. The first backup algorithm derives the cloud top parameters using the Window IR physical retrieval using default values for the COT and EPS. The second method applies a correction to the observed brightness temperature based on an estimate of the water vapor above the cloud to determine CTT. An interpolation algorithm then solves for CTP and CTH. The backup algorithms may also be used to derive a solution if the Window IR algorithm for daytime water clouds fails.

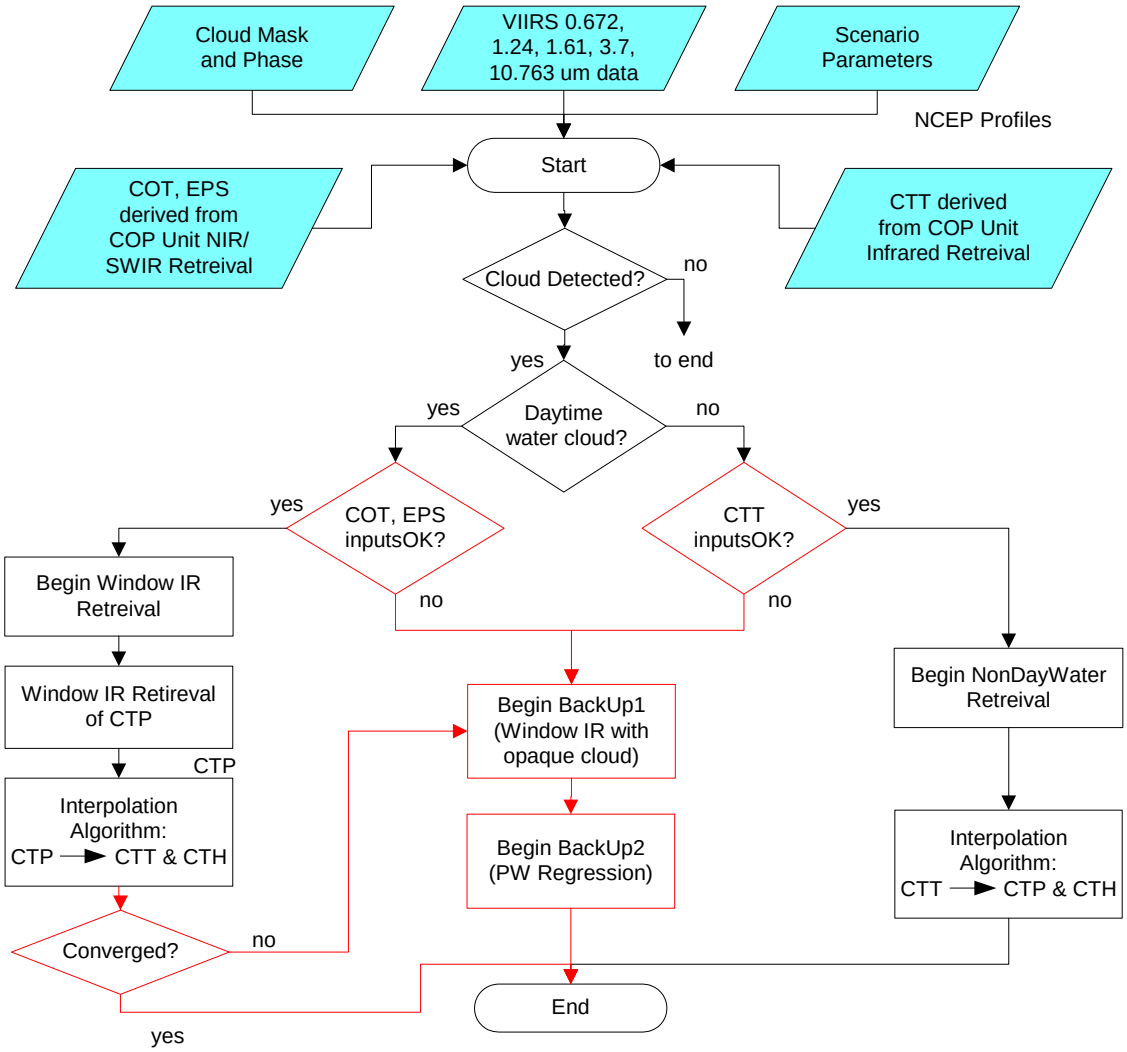

Figure 8. High-level data flow for cloud top parameter retrieval. Processing path includes backup algorithms used when COP inputs are missing or degraded.

3.1.2 UCLA IR Algorithm for Retrieval of Ice Cloud and Night Water Cloud CTT

The UCLA IR Cirrus Parameter Retrieval Algorithm calculates CTT using a 2-band IR approach during nighttime. During daytime, a solar retrieval using 2 reflectance bands is combined with the 2-band IR retrieval. The algorithm also retrieves cirrus cloud effective particle size and emissivity/optical depth. CTH and CTP are obtained by interpolation using an atmospheric sounding and the Cloud Top Parameter Interpolation Algorithm. The IR Water Cloud Parameter Retrieval Algorithm is similar utilizing the same two IR bands. Details are available in Ou *et al.* (2004).

3.1.3 Window IR Algorithm for Retrieval of Daytime Water Cloud CTT

The retrieval of cloud top parameters for daytime water clouds is based on an algorithm that matches radiative transfer model (RTM) calculations to observations in the IR window channel at 10.763 µm. The RTM calculation includes temperature and water vapor profile information from NWP data so that any absorption owing to water vapor is accounted for. The cloud optical thickness (COT) and effective particle size (EPS) obtained from other VIIRS algorithms are also used in the calculations. In addition to the top-of-atmosphere radiance, the radiance derivative with respect to the cloud top is computed analytically by the RTM calculations. The RTM radiance calculations include a correction for multiple scattering within the cloud. Two methods are availalble to solve for the cloud top pressure. The Newton-Raphson iteration method derives CTPgiven an initial first guess based on the observed brightness temperature and based on results from neighboring pixels.This process is shown in Figure 9. The search method identifies the CTP by comparing model radiances to the observations for clouds located at each pressure level. The iterative approach is usually much faster than the search algorithm. However, the iterative routine can encounter difficulties that lead to nonconvergence (e.g., if a temperature inversion is present). The ProcessDayWater module defaults to the search algorithm if the solution begins to diverge for any reason.

The Window IR algorithm is used as backup when inputs required from the COP module are missing or degraded. In that case, the COT and EPS are set to default (optically thick) values. Also the correction for multiple scattering is turned off.

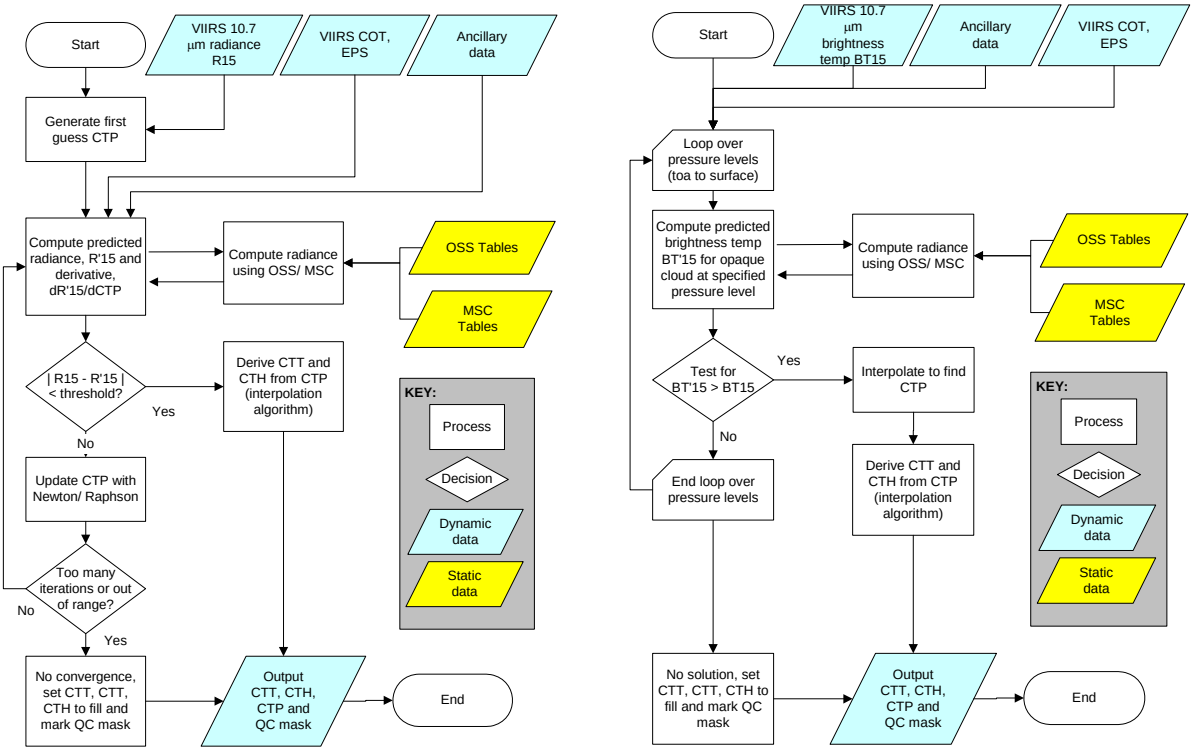

Figure 9. Window IR Daytime Water Cloud CTT Retrieval Algorithm. Two methods include the Newton-Raphson Iteration (left) and Search (right) algorithms. The search

algorithm is used to address cases where convergence is a problem.

3.1.4 Cloud Top Parameter Interpolation

The CTP Interpolation algorithm assumes that atmosphere is in hydrostatic equilibrium. This assumption is a good one for the spatial scales of interest, the vast majority of the time, the principal exception being for severe convection.

The Interpolation Algorithm is run in two forms. These are summarized next.

For daytime conditions with water phase clouds (DW), the previous algorithm step derives the cloud top pressure. Interpolation is used to derive cloud top temperature and cloud top height, consistent with the hydrostatic assumptions. The EDRs are derived in the following order CTP → CTT → CTH.

For non-day/water conditions (NDW), the CTP algorithm has already been supplied an estimate of cloud top temperature from the Cloud Optical Properties Algorithm. A slightly different interpolation process is used. The order in this case is CTT → CTH → CTP. Since, there is possibility of more than one pressure corresponding to a given temperature, a set of tests are applied to determine the most likely correct correspondence. See Section 3.3.2.5.3 for a description.

3.1.5 Backup Cloud Top Parameter Algorithm

The backup cloud top algorithm is run when required inputs from the COP module are missing or degraded. It may also be used when daywater retrieval fails to find a solution. The back up algorithm assumes that the cloud is optically thick, and can therefore be approximated by the observed brightness temperature. This estimate is refined by introducing a correction for the absorption due to water vapor above the cloud. In this case, the correction takes the form of a regression as a function of integrated precipitable water along the path from the cloud top to the top of atmosphere. The regression coefficients are computed in advance based on RT simulations. The procedure is illustrated in Figure 10. By iterating only a few times, the precipitable water estimate can be refined based on the derived CTT. The CTP and CTH are computed using an interpolation algorithm.

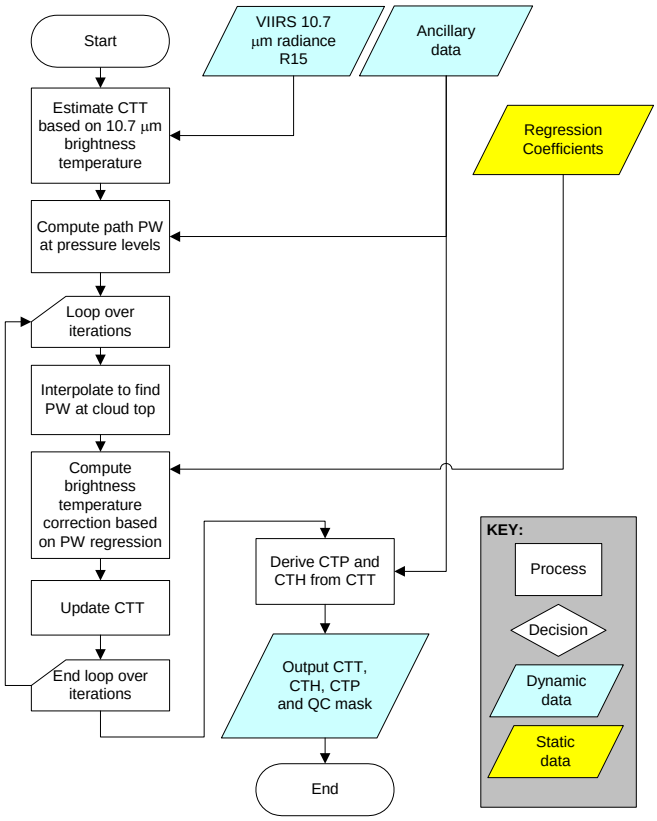

Figure 10. BackUp CTP retrieval based on precipitable-water correction

3.2 ALGORITHM INPUT

Table 7 provides VIIRS and non-VIIRS input data required by the Cloud Top Parameter Algorithms.

Table 7. Description of the Input Data Required by the Cloud Top Parameters Retrieval Algorithms

Data Type	Description	Use	Potential Source
Cloud Top Temperature	Previously determined using the UCLA IR algorithms within the COP Unit	Needed for all cloud cases except daytime water clouds	VIIRS Cloud Optical Properties Unit
INWCTT Quality Flag	A bit mask describing the quality of the CTT retreivasl from the COP module	Used to flag degraded CTT inputs resulting from non-convergence	VIIRS Cloud Optical Properties Unit
Cloud Optical Thickness IP	The M-band pixel level cloud optical thickness for day/ water clouds	Used for window IR algorithm for day/ water clouds to model cloud transmission and scattering	COP Algorithm (near-IR, shortwave-IR algorithm)
Cloud Particle Size IP	The M-band pixel level cloud effective particle size for day/ water clouds	Used for window IR algorithm for day/ water clouds to model cloud transmission and scattering	COP Algorithm (near-IR, shortwave-IR algorithm)
COP Quality Flag	A bit mask describing the quality of the COP retrievals	Used to flag degraded COT and EPS inputs resulting from non-convergence	COP Algorithm (near-IR, shortwave-IR algorithm)
VIIRS Data	10.763μm Brightness Temperature and Radiances	Needed to determine CTT for daytime water clouds	VIIRS
Cloud Mask	Cloud/no cloud for each pixel	Determine if cloud top parameter should be processed	VIIRS Cloud Mask algorithm
Cloud Phase	Ice or water cloud flag	Choose cloud top parameter retrieval algorithm	VIIRS Cloud Mask algorithm
Atmospheric Sounding	Atmospheric temperature and moisture as functions of pressure and/or height	Used to interpolate CTH and CTP once CTT is established	NCEP forecast , CrIS sounding data, CMIS sounding data

3.3 THEORETICAL DESCRIPTION OF THE CLOUD TOP PARAMETER RETRIEVAL ALGORITHMS

3.3.1 Physics of the Problem

The physics of the UCLA IR Cirrus and Water Cloud Parameter Retrieval algorithms, which determine EPS, COT and CTT, is described in Ou *et al.* (2004). The discussion here will focus on the Window IR Algorithm and on the determination of CTH and CTP given CTT.

The physical basis of the Window IR Algorithm relies on the following characteristics of the Earth-atmosphere system:

- The radiation reaching the top of the atmosphere in the 10.3 to 11.3 μm region (referred to as the LWIR window below) is due primarily to thermal emission by the ground, the atmosphere, and clouds.

- Although radiances for cloudy pixels in the LWIR window are dominated by absorption/ emission properties, scattering (including multiple order scattering) can result in differences

of a few K compared with calculations considering absorption/emission only.

- Although water clouds tend to be optically thick (COT >> 1), the algorithm must work with cases where COT ≤ 1.

- The atmosphere is nearly transparent in the 10.3 to 11.3 μm region, although some attenuation does occur. Atmospheric attenuation is primarily due to absorption by H_2O, CO_2 and aerosols.

- To a reasonable approximation, atmospheric pressure decreases exponentially with height following the hydrostatic equation. Atmospheric temperature decreases monotonically with height in most cases (exceptions being surface inversions in the troposphere and above the tropopause in the stratosphere).

As a result of these characteristics of the Earth-atmosphere system in the 10.3 to 11.3 μm region, the radiation reaching the top of the atmosphere (TOA) is strongly affected by cloud layers, when they are present, permitting retrieval of cloud top parameters. Optically thick water droplet clouds are nearly blackbodies, and most of the upwelling radiation at cloud top is from the cloud itself when a VIIRS pixel is completely covered by cloud. Little radiation from below the cloud layer reaches the cloud top because it is absorbed by the cloud. When cloud layers are not present, most of the upwelling radiance at the TOA is from the ground. Both the clouds and the ground contribute to the TOA radiance when the clouds are not optically thick; the relative contribution depends on the cloud thickness and effective particle size. The relationship between atmospheric pressure, temperature and height enables one to determine CTP and CTH, if CTT is known and an atmospheric temperature profile is available.

In describing IR radiative transfer mathematically, we use the plane parallel atmospheric approximation as depicted in Figure 11 for a single layer cloud. In that approximation, it is assumed that variations in atmospheric parameters occur only in the vertical direction. Following Liou (1992), the equation defining monochromatic thermal upwelling intensity at TOA in a plane parallel atmosphere is:

$$I_\lambda(\tau^*) = \varepsilon_\lambda B_\lambda(T_{sfc}) t_\lambda(\tau^*/\mu) + \int_0^{\tau^*} B_\lambda(\tau') t_\lambda(\tau'/\mu) d\tau'/\mu + < scattering\ contribution > \quad (1)$$

where:

I_λ = monochromatic radiance

τ = vertical optical depth

τ^* = total vertical optical depth

ε_λ = surface emissivity

λ = monochromatic wavelength

B_λ = Planck function

$B_\lambda(\tau') = B_\lambda(T(\tau')$

T = atmospheric temperature at specified level

T_{sfc} = skin temperature at Earth's surface

t_λ = monochromatic transmittance = $e^{-(\tau/\mu)}$

μ = cosine of sensor viewing angle

<scattering contribution> = the contribution to the final radiance from scattering of all orders

Figure 11 provides a notional characterization of the vertical optical depth profile. As depicted here and as frequently occurs in the atmosphere, the largest contribution to optical depth is from the cloud layer. If the cloud is optically thin, the contribution from the surface (first term of Eq. 1) will also be significant. The contribution from the atmosphere above and below the cloud will depend on (primarily) the water vapor content. Figure 11 also indicates another aspect of the problem: the emission from a cloud will emanate from a finite physical depth of the cloud. Thus, even under conditions where only absorption/ emission are significant, the average brightness temperature of an optically thick cloud will correspond approximately to the temperature of the cloud where the cloud optical thickness reaches ~0.7.

We will restrict our consideration to cases where the cloud occupies the entire pixel (cloud fraction equals one). Our approach in these cases is to solve (i.e. invert) Eq. 1. Since the scattering correction is much smaller than the total observed radiance, a parameterization is used that estimates the scattering term from other observable or estimated quantities. The parameterization is derived from exact multiple scattering calculations performed with an adding/ doubling type model. This type of solution will implicitly account for the difference between the actual cloud top temperature and the effective cloud emitting temperature.

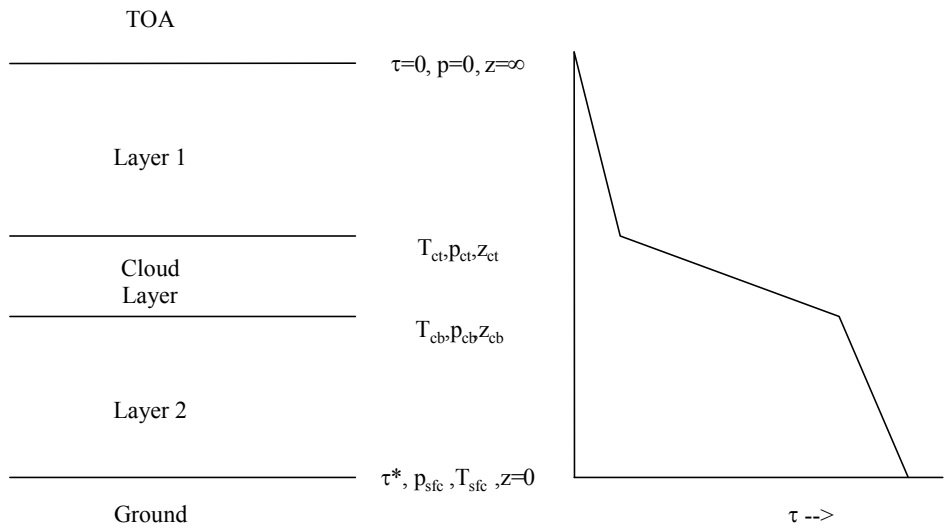

Figure 11. Vertical Optical Depth Profile of an Atmosphere Containing one Cloud Layer. T, p, z and τ represent temperature, pressure, height, and optical depth respectively. Subscripts ct, cb and sfc indicate cloud top, cloud base and surface respectively.

3.3.2 Mathematical Description of the Algorithms

3.3.2.1 UCLA IR Algorithm

The UCLA IR cirrus and water cloud parameter retrieval algorithms are used for CTT retrieval for all ice clouds and water clouds at night. These algorithms are part of the COP unit and a complete description is available in Ou *et al.* (2004).

3.3.2.2 Window IR Algorithm Overview

The Window IR Algorithm derives the cloud top pressure by solving a form of Eq. 1, given as Eq. 2 below.

$$I_\lambda(\tau^*) = \varepsilon_\lambda B_\lambda(T_{sfc}) t_\lambda(\tau^*/\mu) + \int_0^{\tau^*} B_\lambda(\tau') t_\lambda(\tau'/\mu) d\tau'/\mu + \Delta I_{s/c}\tau_{c0}/\mu \qquad (2)$$

where:

$\Delta I_{s/c}$ = is difference between the total radiance emitted at the top of the cloud (from aborption/ emission/ scattering) and the radiance due only to absorption/ emission (i.e. the scattering effect)

τ_{c0} = transmission along a vertical line of sight from the top of the cloud to the top of the atmosphere

The transmission is based on contributions from atmospheric gases and clouds. The atmospheric

absorption is dominated by water vapor with secondary contributions from carbon dioxide and ozone. The atmospheric calculation must consider line-emission as well as that from the continuum. Since we are dealing with water clouds in this portion of the algorithm, the transmission properties of the clouds are determined by Mie Theory and can be easily calculated given the cloud optical depth profile and particle size distribution.

The algorithm strategy is given below:

1. Get the (non-cloudy) atmospheric state including atmospheric temperature and moisture profiles, surface pressure and column ozone

2. Get the surface properties: surface temperature from the numerical weather prediction ancillary data input; surface emissivity is estimated from the surface type

3. Get the cloud properties: cloud topical thickness (assume visible ~0.55 µm wavelength) and effective particle size.

4. Derive a first guess of the cloud top pressure (see below)

5. Compute the radiance for band M15 using a fast radiative transfer model including all relevant physical effects (gaseous absorption and emission) and cloud water particle absorption/ emission and scattering.

6. Compare the calculated and observed M15 radiance. If less than a threshold Go To Step 8. Otherwise Go To Step 7.

7. Determine an adjustment to the predicted cloud top pressure based on the Newton method. This requires an estimate of the derivative of the radiance with respect to the derived quantity (cloud top pressure) which for convenience, is usually calculated in Step 5. Go To Step 5.

8. Assuming vertical hydrostatic consistency of the atmosphere, determine the cloud top temperature and height corresponding to the derived cloud top pressure.

For the Fast Radiative Transfer Model we begin with the Optimal Spectral Sampling (OSS) Model that is used for the CrIS EDR algorithm.

The fast RT model is described in detail in the next section.

3.3.2.3 Fast Radiative Transfer Model

A fast, accurate radiative transfer model (or forward model) is central to the Cloud Top Properties (CTP) daytime water-cloud retrieval algorithm. The forward model computes line-of-sight, top-of-atmosphere (TOA) radiances for a given atmospheric and geophysical state (temperature, water vapor profiles, surface properties, and cloud properties) as well as the derivatives (Jacobians) of radiance with respect to the atmospheric, surface, and cloud parameters, for use in the inversion routine. To meet the requirements for fast, accurate calculations, the AER-developed Optimal Spectral Sampling (OSS) technique has been adopted

as the forward model for the VIIRS CTP Daytime Water-Cloud retrieval.

3.3.2.3.1 Overview of the OSS Technique

Optimal Spectral Sampling (OSS) is a general approach to radiative transfer that is applicable from the microwave through ultraviolet spectral regions and can be applied to any instrument line shape or spectral response function. In this approach, the TOA radiance for each channel is represented by a linear combination of radiances computed at selected monochromatic locations within the instrument response function. The optimal selection of frequencies is determined off-line by comparing radiances derived from the OSS formulation with those obtained using a reference line-by-line model. The optimization procedure minimizes the root mean square error of the radiance differences for an ensemble of globally representative atmospheric profiles and over the full range of satellite viewing angles. For additional details, see AER (2004) and Moncet, Uymin and Snell (2004).

3.3.2.3.2 Forward Model Inputs/ Outputs

The forward model calculations require as input a description of the geophysical state including atmosphere and surface data (from NWP), viewing geometry, and a cloud description based on latest guess for the cloud top pressure and cloud base pressure plus information about the cloud optical properties as determined from the VIIRS cloud optical thickness (COT) and effective particle size (EPS) EDRs. The inputs to the forward model are summarized in **Table 8**.

The outputs from the forward model calculation include the TOA radiance at 10.763 μm plus the derivatives of radiance with respect to the cloud top pressure. These quantities are used to compare against the observations and to update the cloud pressure if the retrieval has not yet converged. In addition, the upwelling top-of-cloud radiance, the upwelling bottom-of-cloud radiance, and the downwelling top-of-cloud radiance are produced and used as input in the multiple scattering correction routine. The complete list of outputs from the forward model are summarized in **Table 9**.

Table 8. Inputs to OSS forward model.

Inputs	Units
Temperature profile (24 lev)	K
Water vapor profile (24 lev)	g/kg
Surface skin temperature	K
Surface pressure	Mbar
Surface emissivity	
View angle	Degrees
Cloud top pressure	Mbar
Cloud bottom pressure	Mbar
Cloud Optical Thickness at 10.763 microns	
Effective Particle Size	μm

Table 9. Outputs from OSS forward model.

Outputs	Units
TOA radiance	mw/(m^2 sr cm^{-1})
Upwelling top-of-cloud radiance	mw/(m^2 sr cm^{-1})
Upwelling bottom-of-cloud radiance	mw/(m^2 sr cm^{-1})
Downwelling top-of-cloud radiance	mw/(m^2 sr cm^{-1})
Temperature at cloud top	K
Transmittance to TOA	
Derivatives of radiances wrt cloud top pressure	mw/(m^2 sr cm^{-1})/mbar
Upwelling radiance from all layers	mw/(m^2 sr cm^{-1})
Downwelling radiance from all layers	mw/(m^2 sr cm^{-1})

3.3.2.3.3 OSS Implementation and Performance

The increase in computational efficiency of the OSS model is afforded through the optimized selection of a small number of representative frequencies. A training set of 52 ECMWF atmospheric profiles has been used to select the OSS spectral locations and weights. The CTP algorithm has adopted a set of 24 pressure levels that represents a compromise between computational speed and accuracy. To evaluate the impact on accuracy, OSS was trained on profiles interpolated to both 24 and 101 levels. OSS has been trained assuming a square response for the VIIRS 10.7 micron band. An update to the training will be necessary once the shape of the response is determined. Two independent trainings were performed, one dividing the band into 4 channels, the other treating the band as a single channel.

The performance of the OSS model meets the objective to keep the errors in the RTM calculation to a negligible level. When compared to LBLRTM, the OSS radiances match to better than 0.05 mw/(m^2 sr cm^{-1}) at all angles. The additional interpolation error is less than 0.02 mw/(m^2 sr cm^{-1}) at all angles. Furthermore, errors associated with limited vertical resolution provided by 24 pressure levels are less than 0.05 mw/(m^2 sr cm^{-1}) at all angles. Finally, no significant improvement in performance is obtained by dividing the VIIRS IR band into 4 channels instead of treating it as a single channel. Results are shown in Figure 12.

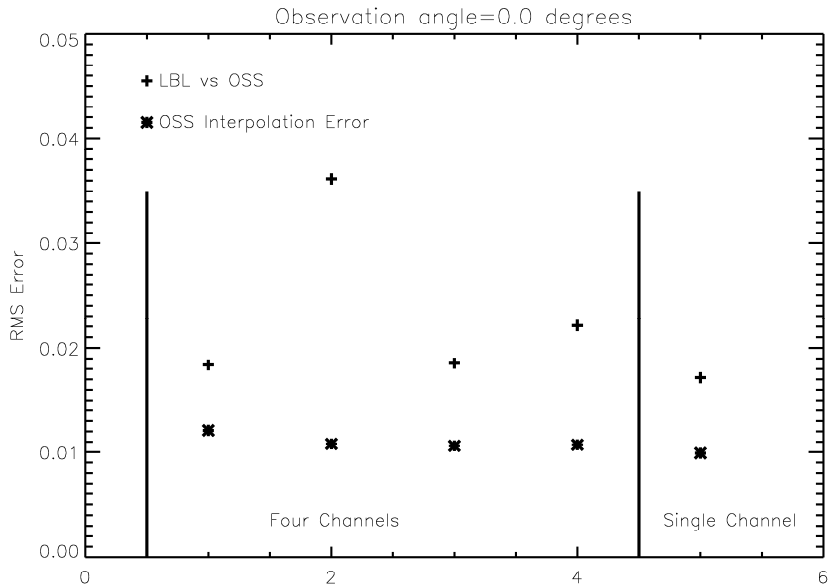

Figure 12. RMS Error for OSS Radiances compared to LBLRTM under clear conditions for a nadir viewing angle. Results based on the four-channel and single channel representations are shown.

Clouds were included in the OSS RTM calculations as an additional component of absorption and emission. The cloud top pressure specification identifies the cloud top within a given layer of the OSS model. This layer is then treated as two components. Above the cloud, the radiative properties are determined by an effective temperature and transmittance for the portion of the atmospheric layer above the cloud. Within the cloud the radiative properties are determined by an effective temperature and transmittance for the cloud. The contributions from the cloud are included both in the calculation of the downward component of the radiance that is reflected by the surface and in the upward-directed component.. Figure 13 illustrates the model assumptions.

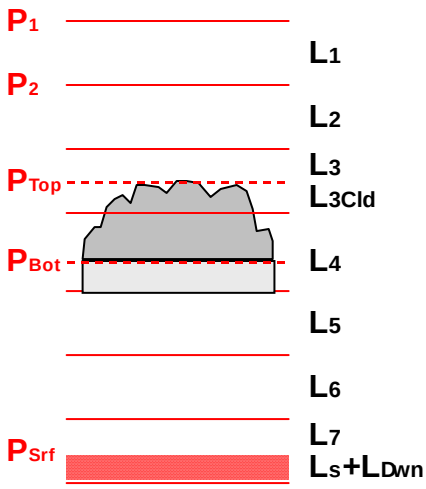

Figure 13. Cloud Simulation schematic showing location of the surface, cloud top, and cloud base relative to a pressure grid with 8 levels. The components of top-of-atmosphere radiance from each level (attenuated to the TOA) are indicated.

The derivatives of top-of-atmosphere radiance with respect to cloud top pressure are computed analytically by the OSS model and used to converge to the solution for the cloud pressure based on the Newton-Raphson iteration approach. This calculation includes two components to describe the change in radiance between cloudy and non-cloudy layers and to described the change in radiance within a layer that is partially filled with cloud.

Clear sky radiance for N layers is computed by first calculating the downward directed radiance for each layer down to the surface, adding the contribution from the surface, then calculating the total contribution for all layers back up to the top-of-atmosphere. For the MSC routine, the downward-directed radiance at the nearest level above the cloud top is used to approximate the radiance incident on the cloud from above while the upward-directed radiance at the nearest level below the cloud base is used to approximate the radiance incident on the cloud from below.

3.3.2.3.4 Multiple Scattering Correction

The OSS forward model omits the effect of scattering within the cloud. The following models were used to estimate errors owing to scattering and to determine a correction.

- ***Mie Code*** - Used to determine cloud absorption and scattering properties for a range of particle sizes.
- ***Line-By-Line Radiative Transfer Model (LBLRTM)*** – Used to compute layer absorption optical depths for a given atmospheric profile.
- ***Code for High-resolution Accelerated Radiative Transfer with Scattering (CHARTS)*** – Used to generate monochromatic TOA radiance as a function of view angle for a range of atmospheric profiles, cloud particle sizes, cloud optical thickness, cloud physical

thickness, and cloud top heights.

A correction to the OSS radiances for multiple scattering was derived based on LBLRTM/Charts simulations for a subset of the 52 ECMWF profiles. Clouds were simulated for 6 particle sizes, 11 optical thickness, and 6 heights. Runs were conducted with and without multiple scattering included. The output from charts consisted of monochromatic radiances from 884 to 973 cm^{-1} produced at 5 angles (0.0, 21.4, 47.9, 70.7, and 86.0 degrees) and representing the up-welling/down-welling radiance above and below the cloud layer. LBLRTM was then used to compute band-integrated radiances (and brightness temperatures) assuming a square response function for the 10.7 micron band. In Figure 14, the difference in brightness temperature at the cloud top with and without multiple scattering is represented as an uncertainty as a function of view angle, cloud particle size, and cloud optical depth. For partially transmissive clouds, the uncertainty is as large as 0.55 K.

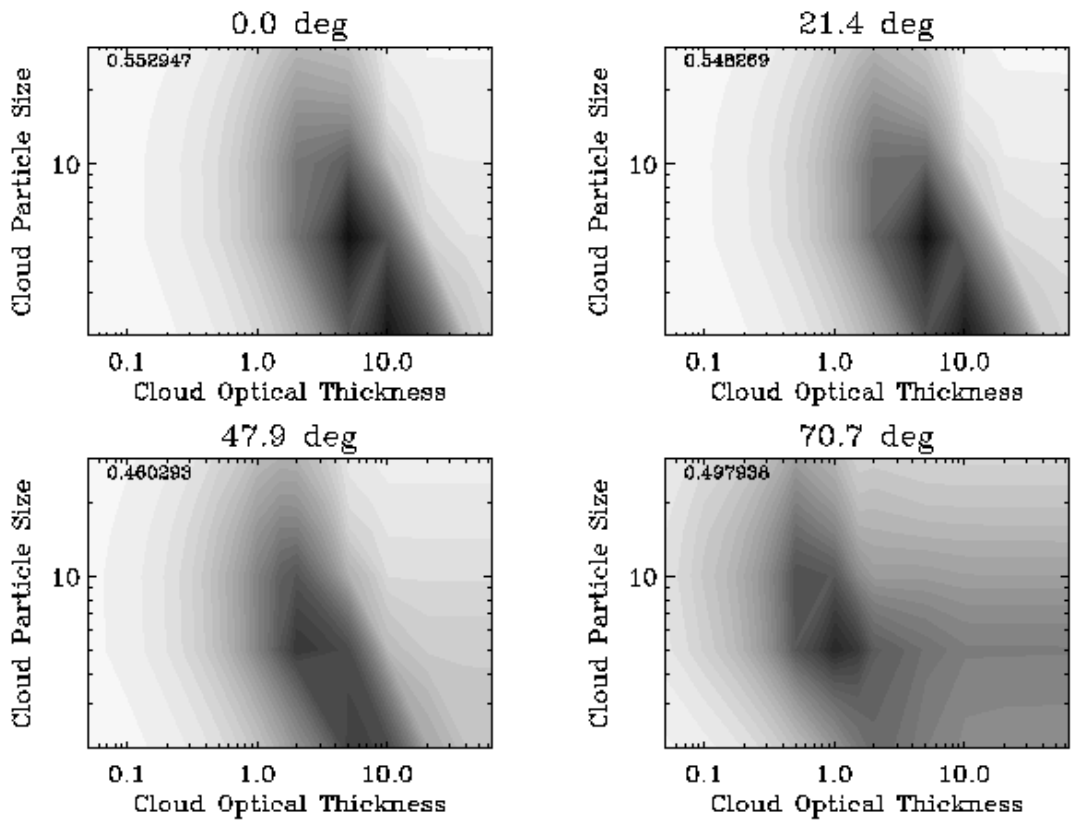

Figure 14. Cloud top brightness temperature uncertainty resulting from the omission of scattering as a function of viewing angle, cloud particle size, and cloud optical thickness (defined for a nadir path). Maximum errors (identified in the plot) occur for partially transmissive clouds. Greyscale varies from 0 to 0.6 K.

The regression analysis was conducted for fixed EPS, COT, and view angle but included clouds simulated at difference heights. Three quantities determined by the non-scattering calculations were found to be good predictors of the multiple scattering correction term. These were

- the up-welling line-of-sight radiance leaving the cloud top $L_{\uparrow top}$,
- the up-welling line-of-sight radiance incident on the cloud from below $L_{\uparrow bot}$, and
- the down-welling line-of-sight radiance incident on the cloud from above $L_{\downarrow top}$.

With these terms computed by the OSS forward model, the multiple scattering correction equation for top-of-cloud radiance is written as

$$L_{MS} = c_0 + c_1 L_{\uparrow top} + c_2 L_{\uparrow bot} + c_3 L_{\downarrow top} \tag{3}$$

Figure 15 shows the remaining top-of-cloud brightness temperature errors after applying the MSC regression. Clearly the errors associated with scattering are greatly reduced.

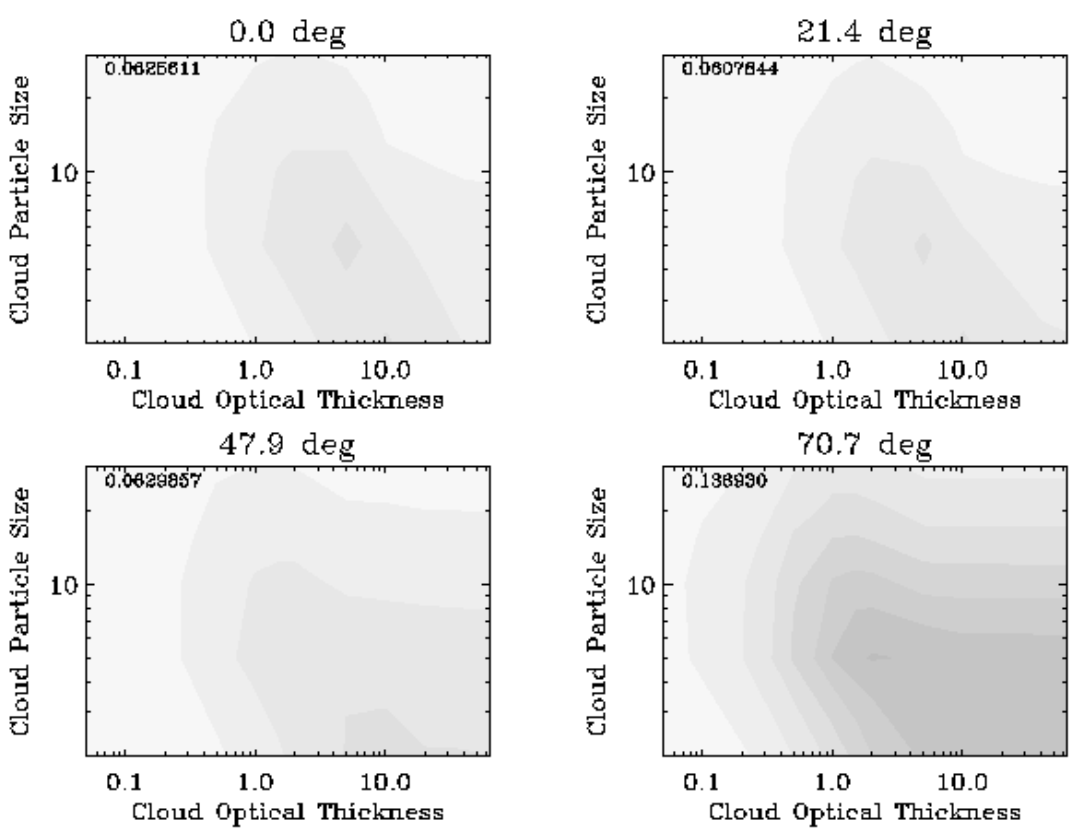

Figure 15. Cloud top brightness temperature uncertainty representing errors in the MSC regression as a function of viewing angle, cloud particle size, and cloud optical thickness (defined for a nadir path). The largest errors (identified in the plot) occur for large view angles. The greyscale is the same as for Figure 14.

Figure 16 shows the individual results for our test data set for four angles: 0, 21.4, 47.9 and 70.7 degrees. The x-axis is the difference between scattering and non-scattering radiance at the top of the cloud (at the specified angle). The y-axis is the difference between the value calculated with the MSC look-up table and an "exact" value computed with the CHARTS multiple scattering model – that is, the model error. All values are brightness temperatures for Band M15 (10.763 μm). The total scattering correction can be up to ~3 K or greater increasing with increasing view angle. Except for the 70.7° view angle the vast majority of errors are less than 0.2 K. Although the performance begins to degrade somewhat at 70.7°, the performance is still quite good, with RMS errors less than 0.14 K. While some improvements might ultimately be developed for the high angle cases (likely including radiances at more than one angle in the regression), the current model performance is adequate for current purposes.

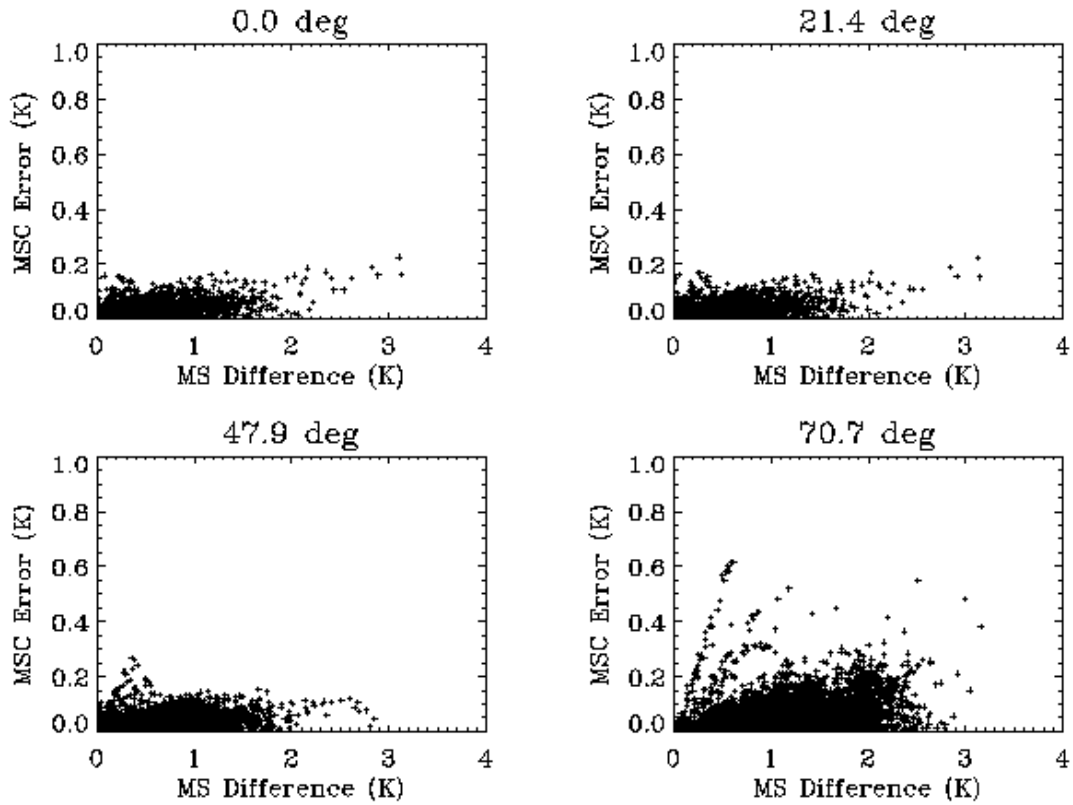

Figure 16. Multiple scattering model correction error as a function of scattering and non-scattering radiance emitted at top of cloud for four viewing angles.

3.3.2.3.5 MSC Implementation

The correction for multiple scattering is applied each time the RTM models is accessed based on the outputs from the OSS calculations. A look-up table LUT of regression coefficients (i.e., c_0,

c_1, c_2, and c_3) from Eqn 3 was constructed as a function of cloud effective particle size (EPS), cloud optical thickness (COT), and viewing angle. A general algorithm for linear interpolation within a multi-dimensional look-up table forms the basis for the MSC algorithm. The LUT is fairly small with 6 values of EPS, 11 values of COT, and 4 viewing angles (from 0 to 70 degrees) so that the calculation of the correction has negligible effect on the CPU time.

Currently the algorithm introduces no correction for multiple scattering to the derivatives computed by the OSS model.

3.3.2.3.6 Cloud Optical Thickness

The inputs to the OSS forward model include the cloud optical thickness at 10.7 microns. This quantity is computed from the VIIRS Cloud Optical Thickness EDR defined at 0.55 microns based on LUT containing the ratio of visible extinction efficiency to infrared absorption efficiency as a function of effective particle size. The relationship is illustrated in Figure 17.

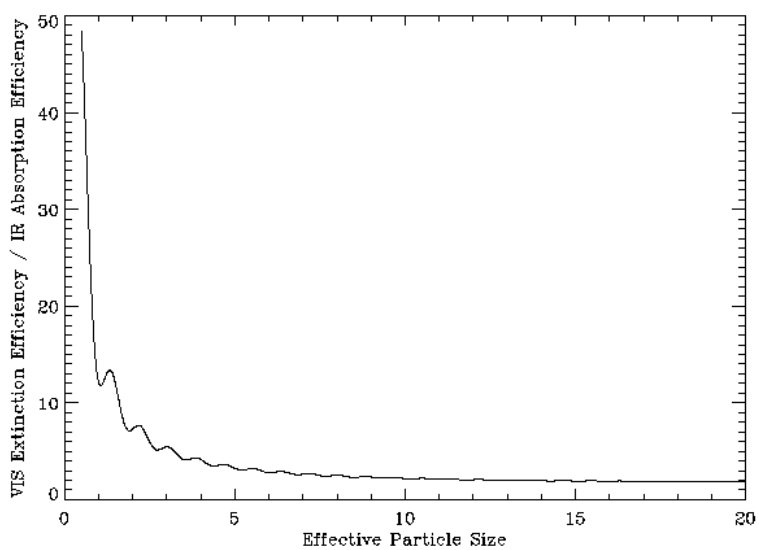

Figure 17. The ratio of visible extinction efficiency to IR absorption efficiency used to convert 0.55 micron COT to COT at 10.763 microns.

3.3.2.4 Window IR Algorithm Detailed Description

The solution to the cloud top retrievals is based on the detailed RT model described above that combines the OSS model for calculating absorption/ emission in a plane parallel atmosphere with the parametric multiple scattering corrections. The steps below are applied to all day/ water cloud pixels.

1. Obtain required inputs:
    a. M15 Radiance L_{M15} and brightness temperature B_{M15}

   b. Cloud optical properties: COT and EPS IPs
   c. Temperature T(p), Moisture Q(p), and geopotential height H(p) profiles from a numerical weather prediction model
   d. Tropopause pressure (or height) P_{tr}, from a NWP model
   e. the local satellite view angle at the surface θ
   f. the surface temperature from the NWP model T_s
   g. surface emissivity at the band M15 wavelength ε
   h. the effective noise of band M15 including sensor noise, RT model error and algorithm approximations: radNoise
   i. parameters related to termination of the iterations: maxIter, maximum number of iterations; chisqFac, the minimum chi-square "goodness of fit" parameter to terminate the iterations; minDeltaCtp, the minimum change in CTP to continue the iterations
   j. Digital elevation map (DEM) terrain height from the SDR input file
2. Get the surface pressure, P_s: either computed from DEM and H(p) or preferably directly input from a NWP model
3. Compute a first-guess CTP for the pixel (see below for details), assign to CTP_0
4. The algorithm then proceeds to derive CTP using the Newton-Raphson Iterative method
   a. Loop over iterations
      i. Calculate R_i and $R_i' = dR_i / dCTP_i$ as a function of the following: R_{M15} , COT, EPS, T(p), Q(p), H(p), θ, T_s , ε using the combined OSS and Multiple scattering correction models described in the above section
      ii. Set chisq =abs(R_{M15} - R_i) / radNoise
      iii. If (chisq <= chisqFit) then break out of loop (go to step 5)
      iv. Calculate $CTP_{i+1} = CTP_i - (R_{M15} - R_i) / R_i'$ (Newton-Raphson Method)
      v. Set $CTP_{i+1} = \min(CPT_{i+1}, P_s)$, make sure pressure isn't greater than surface pressure
      vi. Set $CTP_{i+1} = \max(CTP_{i+1}, P_{tr})$, make sure pressure isn't lower than tropopause pressure

   However if the algorithm fails to converge (i.e., chisq increases from one iteration to the next) then the method for retrieving CTP switches to the Search algorithm
   b. Loop over all pressure levels from tropopause to the surface
      i. Compute Ri for cloud top at current level
      ii. Set chisq =abs(R_{M15} - R_i) / radNoise
      iii. If (Ri >RM15 and Ri-1 < RM15) then interpolote to find CTP and break out of loop
      iv. If no solution is found then identify the level with the smallest chisq and adopt this pressure as the CTP if the chisq meets a specified threshold.
5. Compute CTT and CTH from last CTP
6. Set quality flags
7. Return with final CTP, CTT, CTH values

For optically thick clouds, the observed M15 brightness temperature is a good first guess at the cloud top temperature. Thus convergence to a solution can be expected to occur fairly rapidly if this is the case. For thin clouds, an initial guess at the cloud temperature is not as easily determined. Near its edge, clouds may become more transmissive while the temperature of the

cloud generally remains locally uniform. Thus the cloud top pressure for a neighboring cloud pixel represents a good first guess for the current pixel. This property is used by the algorithm to reduce the number of iterations and to solve the problem of providing a first guess for transmissive clouds. Each data buffer input into the algorithm is processed as a series of blocks. The data within these blocks are sorted by brightness temperature and processed. The brightness temperature of the first pixel in the list is used as the first guess for the retrieval. Afterwards, the most recent solution (provided the retrieval converged) is used as the initial guess for all subsequent retrievals. Once all pixels in the block are processed, the procedure is repeated on the next block. In this way, several iterations may be required for the first retrieval but many fewer should be needed for the subsequent calculations.

In the case of an inversion, multiple solutions maybe possible. The Iterative algorithm will settle on which ever solution is closest to the initial guess. On the other hand, the search algorithm described above will terminate on the first solutions that is found (i.e., higher altitude). This may tend to bias certain clouds (e.g., marine strat) towards higher values.

3.3.2.5 Window IR Algorithm with Opaque Cloud Approximation

When inputs from COP module are not available, the Window-IR algorithm is used to perform the CTP retrievals under the assumption that the cloud is opaque. In this mode of operation, the COT and EPS inputs are set to nominal values that represent optically thick clouds. Also the option to include a correction for multiple scattering is turned off. This is necessary since the coefficients for the correction have been derived for water clouds only, whereas the WindowIR BackUp algorithm may be used for both water and ice clouds. However since the contribution due to multiple scattering is less important for opaque clouds (see Figure 14) the omission of this correction has little imapct on the retrievals. With these minor changes, the algorithm operates normally as described above to derive the CTP.

3.3.2.6 Window IR Precipitable Water Correction Algorithm

Section 3.3.2.5 describes a back-up algorithm when the outputs from the COP module are not available or are maked as poor quality.To add further robustness to the processing, an additional back-up algorithm is added to cover the case when the approach in Section 3.3.2.5 failures to converge. This secondary back-up is described in this section.

The CTT is computed based on the VIIRS 10.7625 μm brightness temperature (BTM15) after correcting for intervening water vapor above the cloud. This water vapor absorbs some of the emitted radiation from the cloud and simultaneously emits at its own temperature, generally lower than the underlying cloud due to the tropospheric lapse rate. The correction for this effect involves the following steps:

1. Compute total column precipitable water from the Top Of Atmosphere (TOA) down to each pressure level for the input NWP field
2. Set CTT = M15 brightness temperature
3. Loop over iterations
    a. Loop over levels from the tropopase to the surface to identify levels

correpsonding to CTT

b. Interpolate between levels to find PW

c. Compute regression correction using estimate of precipitable water

d. Update CTT and continue to next iteration

The Precipitable Water (PW) for a layer is estimated based on the pressure and mixing ratio of the bordering levels:

$$PW_{1,2} = | (MR_1 + MR_2) * (pres_2 - pres_1) | / F \quad (4)$$

where F = 1961.33. This functionalization expects pressure in hPa and mixing ratio in g/kg and produces PW in cm. PW from each layer must be summed from TOA down to cloud top. Since cloud top is currently unknown, it is initially estimated from the sounding profile assuming no water vapor absorption (i.e., CTT is set equal to BTM15). This integrated PW amount is then used to estimate CTT as follows:

$$CTT = BTM15 + a_0 + a_1PW + a_2PW^2 + a_3(T_{max} - T_{surf}) \quad (5)$$

where BTM15 is the 10.7625 μm brightness temperature, T_{max} is the maximum profile temperature (K), T_{surf} is the surface temperature (K) and the a_n coefficients are defined as (a_0, a_1, a_2, a_3) =(0.067, -0.002, 0.220, 0.105). The value of CTT is refined by updating PW for the last CTT estimate. Only a few iterations are needed to converge to a solution.

Figure 18 illustrates the amount of correction applied to the brightness temperature as a function of PW. Most atmospheric situations result in less than 2K correction to the brightness temperature. Low clouds in a tropical environment could require correction up to 6K.

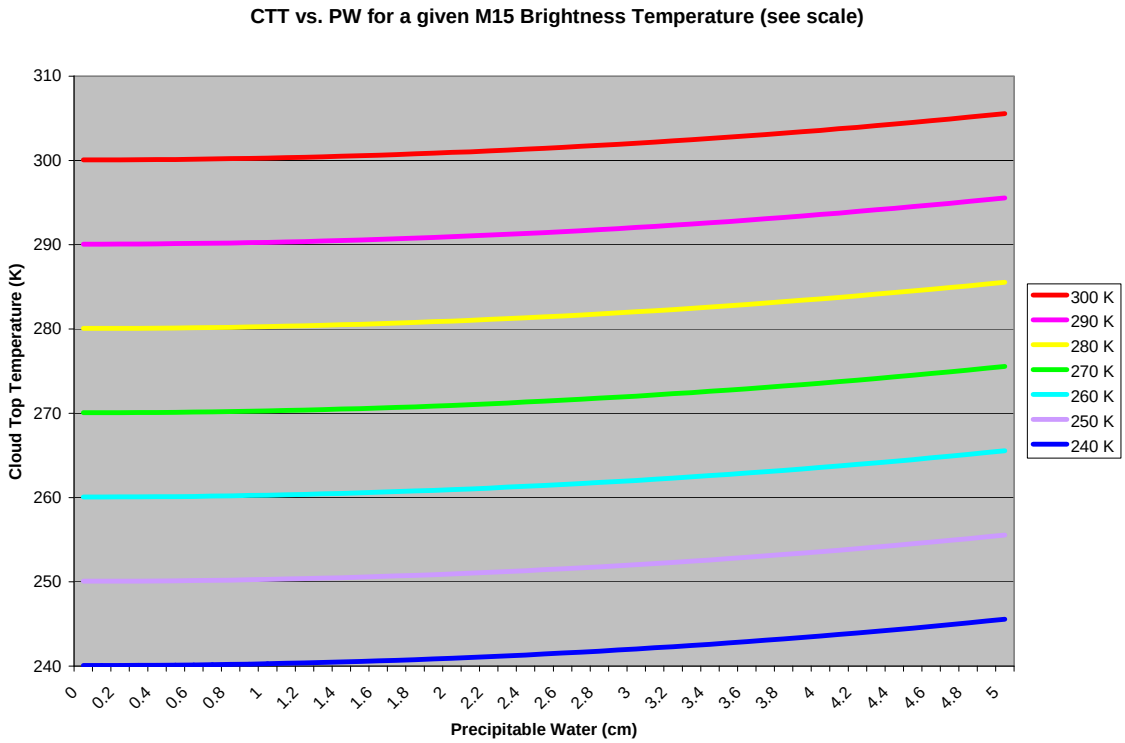

Figure 18. Cloud Top Temperature as a function of Precipitable Water as determined by the Window IR algorithm. The 10.7625 μm brightness temperatures are indicated by the color scale.

3.3.2.7 Interpolation Algorithm

The interpolation algorithm operates differently with day/ water clouds and non-day/ water clouds, although the physical principles are the same. For non-day/ water clouds the processing order is: CTT → CTH → CTP. The steps are described in Section 3.3.2.7.1-3. For day/water clouds the processing sequence is: CTP → CTT → CTH. This is described Section 3.3.2.7.4.

3.3.2.7.1 Cloud Top Height Interpolation

Based on the input CTT for non-day/water clouds, CTH is determined via linear interpolation of the surrounding temperature/height points from the input ancillary temperature profile. Figure 19 illustrates the relative positions of cloud top and the closest levels from the temperature profile where:

T_n = temperature at level n

p_n = pressure at level n

z_n = height at level n

$T_{V\,n}$ = virtual temperature at level n

T_{ct} = cloud top temperature

p_{ct} = cloud top pressure

z_{ct} = cloud top height

$T_{V\,ct}$ = cloud top virtual temperature

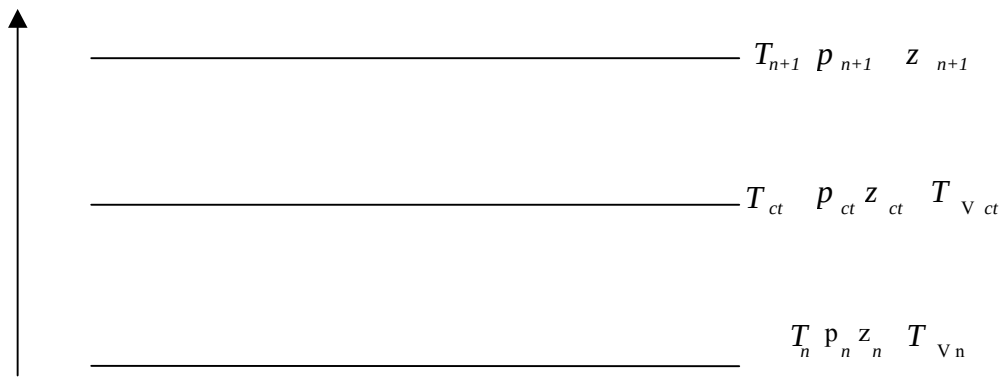

Figure 19. Vertical Relationship of Cloud Top and Closest Atmospheric Profile Levels.

3.3.2.7.2 Cloud Top Pressure Interpolation

For non-day/water clouds, CTT is also used to determine CTP from the input atmospheric profile. Linear interpolation is not used however. The hypsometric equation is best used to interpolate CTP from CTT and CTH as follows:

$$p_{ct} = p_n \bullet \exp\left(\frac{g(z_n - z_{ct})}{R\overline{T}_V}\right) \tag{4}$$

where g = 9.80665 m s^{-2}, R = 287.05 J kg^{-1} K^{-1}, and $\overline{T}_V = (T_{V\,n} + T_{V\,ct})/2$.

R is the dry air gas constant and can only be used if the atmosphere contains no water vapor. Virtual temperature, T_V, accounts for the moisture in the air thus allowing the dry air gas constant to be used. The derivation of the hypsometric equation can be found in Section 2.2.2 of Wallace and Hobbs (1977). Virtual temperature is calculated as follows:

$$T_V = T / [1 - ((0.379 * e) / pres)] \tag{5}$$

where T_V is virtual temperature (K), T is temperature (K), e is water vapor pressure (hPa) and pres is total atmospheric pressure (hPa). Water vapor pressure is computed as follows:

$$e = 6.1078 * 10\text{^}[(T_d * A)/(T_d + B)] \tag{6}$$

where T_d is dewpoint (°C) and A and B are constants. A and B vary depending upon whether the vapor pressure is computed with respect to ice or water. The water (ice) values are used for

dewpoints above (below) 0°C as follows:

A = 7.5 } for use in vapor pressure
B = 237.3 } with respect to WATER

A = 9.5 } for use in vapor pressure
B = 265.5 } with respect to ICE

For most situations $T_V \cong T$. Using virtual temperature will affect the CTP answer for very humid cases.

3.3.2.7.3 Atmospheric Temperature Inversion/Isothermal

In most cases the tropospheric temperature decreases with increasing height. Inversions do form occasionally in which the temperature increases with increasing height. These are prevalent at the surface during polar winter. The algorithm ensures proper linear interpolation for CTH and correct use of the hypsometric equation for CTP regardless of inversions.

One problem associated with inversions is solution non-uniqueness. If CTT is within the temperature profile at multiple locations, the algorithm must decide which level is correct. The retrieval code initially checks the profile to determine which possible levels have a dewpoint depression less than 3°C since clouds are generally close to saturation. If only one level passes this test, then this level is selected. If no level passes the dewpoint depression criterion, then the highest altitude is chosen as CTH from all original possibilities. If multiple levels pass the dewpoint depression test, then the highest altitude is chosen as CTH from all passing levels. In all cases where the dewpoint depression criterion fails to provide a unique solution, the highest possible altitude is selected as CTH due to the higher probability associated there considering the observations are from a downward viewing satellite sensor.

The algorithm determines the minimum and maximum of the input temperature profile. Each profile temperature value has some error in addition to discretization due to the finite number of reported levels. An accurate CTT could be discarded as out-of-range due to errors in the input ancillary temperature profile. To allow for profile error, CTT values greater than the maximum temperature contained within the profile are allowed provided they do not exceed the maximum by more than 5°C. In these cases, CTH and CTP are set to the profile height and pressure associated with the profile maximum temperature. The same allowance is given for CTT values below the minimum profile temperature. CTT values beyond the 5°C additional envelope are assumed in error, and no CTH/CTP values are returned.

3.3.2.7.4 Derivation of Cloud Top Height and Cloud Top Pressure for Day/ Water Clouds

For day/ water clouds, the window IR algorithm directly derives the cloud top pressure. Then, cloud top temperature and height are derived assuming temperature and height vary linearly with log of pressure. This is consistent with the assumption of hydrostatic equillibrium.

Since cloud top pressure is a single valued quantity (unlike cloud top temperature), this form of

the interpolation algorithm has a single unique solution. Thus, the considerations of Section 3.3.2.7.3 do not apply.

3.4 ALGORITHM TESTING AND ERROR ANALYSIS

3.4.1 Error Budget

The Error Budgets for Cloud Top Parameters are provided in the Raytheon VIIRS Error Budget, Version 3 (Y3249). For non-day/ water clouds, the portion of the algorithm not changed with the ATBD release, the budget in Y3249 document still applies. This analysis follows standard error propagation analysis methodologies. The verification of the Cloud Top Temperature for these cases is described in the COP ATBD. The impact to Cloud Top Height and Pressure is summarized in Sections 3.4.1.1 and 3.4.1.2.

The error budget for daytime water phase clouds in Y3249 is no longer applicable as the algorithm has substantially changed. A comprehensive analysis with joint variation of all inputs consistent with expected error levels was performed as part of the Algorithm Testing. See Section 3.4.2.

3.4.1.1 Error Budget – Daytime/Nighttime Ice Clouds

Pixel-level CTT is estimated using the UCLA IR Cirrus Algorithm during day and night. The algorithm uses the 0.672 (during daytime), 3.70, and 10.763 μm channels. The remaining two cloud top parameters are determined using atmospheric vertical profile information. For optical depth < 1, nadir and off-nadir performance is better than objective, while edge-of-scan performance exceeds threshold. For optical depths > 1, nadir and off-nadir performances are generally better than threshold and edge-of-scan performance exceeds threshold. Precision performance is generally better than objective for many optical depth bins and view geometries. It exceeds threshold only in the CTH 5–10 optical depth bin. Fine resolution (nadir) performances for optical depths < 1 are better than threshold for all three parameters. Fine resolution performances for the 1–5 optical depth bin are again better than threshold for all three parameters.

3.4.1.2 Error Budget – Nighttime Water Clouds

The UCLA IR water cloud retrieval algorithm uses the 3.70 and 10.763 μm bands to determine CTT. The remaining two cloud top parameters are determined using atmospheric vertical profile information. Error budget analysis shows accuracy results for nadir view and several optical depth bins. These results show that measurement accuracy is better than threshold for optical depth less than 10 and are better than objective for optical depths greater than 10. The budget shows that measurement precision is better than objective for most cases and is between threshold and objective for CTH in the 5–10 optical depth bin and for CTT in the 1–5 and 5–10 optical depth bins. Fine resolution product performance for optical depth less than 1 is better than threshold for CTT, at threshold for CTH, and exceeds threshold for CTP. Note that, in general, these requirements are more stressful than would be obtained by computing the RSS of the corresponding measurement accuracy and precision requirements. In particular, the CTP

threshold uncertainty requirement is 50 mb, while the threshold accuracy requirement for low clouds is 100 mb. The performance of the nighttime water cloud algorithm is impressive. It is anticipated that off-nadir performance should be similar and edge-of-scan performance somewhat degraded relative to nadir. Therefore, overall performance at night is expected to exceed specification.

3.4.1.3 Algorithm Sensitivity To Sensor Errors

Algorithm sensitivity studies were conducted in earlier stages of the project to determine the impact of individual sensor error contributions on algorithm performance. A number of standard scenes were used to support these studies. These studies led to the initial estimates of sensor performance required to meet or exceed the requirements.

The studies were divided into two categories: calibration and instrument noise.

3.4.1.3.1 Calibration Errors

Calibration errors refer to errors in EDR parameter retrievals due to uncompensated biases in radiance measurements. These particular studies address biases that would cause all thermal, and separately, all solar channels to be biased in the same direction. These types of biases occur when the emissivity of the on-board blackbody or the reflectivity of the on-board solar diffuser drifts over time. In these studies, the impact of biases on long-term stability and absolute radiometric accuracy are examined. To examine absolute radiometric accuracy, we use the measurement accuracy metric defined in the SRD:

$$\beta = \left| \mu(\gamma\%) - x_{\mathrm{T}} \right| \tag{7}$$

where $\mu(\gamma\%)$ is the average parameter retrieval for the same truth value with a $\gamma\%$ radiance perturbation

where

$$\mu = \sum_{\mathrm{N}} x_i \,/\, \mathrm{N} \tag{8}$$

x_{T} is the truth value of the parameter

N is the number of values included in the average.

To examine long-term stability, we define a metric similar to the long-term stability metric defined in the SRD. [*Note*: the SRD definition of long-term stability treats time series data. The approximate formula that follows treats perturbations as though they were short-term biases in radiance measurements.]

$$\rho = \sum_{N} \left| \left(x_i(\gamma\%) - x_i(-\gamma\%) \right) \right| / N \tag{9}$$

3.4.1.3.2 Radiometric Accuracy Results

Figure 20 and Figure 21 show the results for Scenario 4: a US Standard Atmosphere case, nadir satellite view, and with a water cloud inserted between 3 and 4 km. These results demonstrate the effect on retrieved CTT of biases of 0.1, 0.5, 1 and 2 percent in the 10.763 μm radiance, for a range of cloud effective particle sizes and optical depths. The light grey shading indicates where errors exceed the Measurement Accuracy objective values and the dark grey shading shows where errors exceed the threshold values contained in the requirements for clouds of optical depth greater than 0.1. The size of the bias that can be tolerated tends to increase with effective particle size and optical depth; this is typical of the results for other scenarios. For $r_e = 5$ (a typical size for an altocumulus cloud) and $\tau = 1$, we see that the threshold is met at a perturbation of 1 percent and for optical depths greater than 2, perturbations exceeding 2 percent meet threshold.

It is interesting to examine results for typical effective particle sizes for water droplet clouds, which generally occur in the range 4.0 to 5.0 μm (see Liou, 1992, p. 187). Table 10 shows the bias above which threshold measurement accuracy is exceeded, for $r_e = 5$ and for $\tau = 1$ and 10 for CTH, temperature and pressure. Biases range from about 1 to 5 percent, in general.

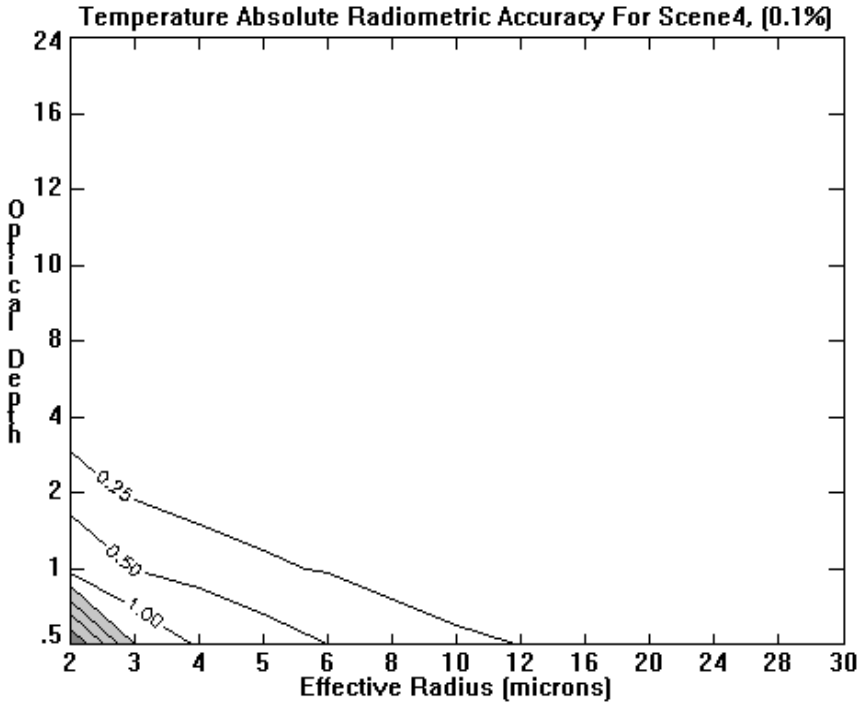

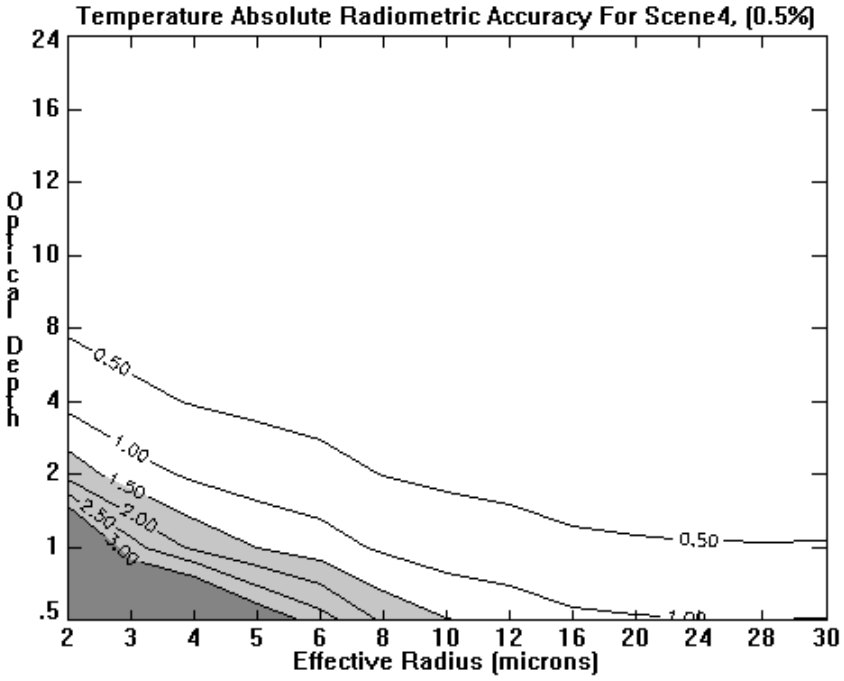

Figure 20. Radiometric Accuracy results for 0.1% (top) and 0.5% (bottom) perturbations in the 10.763 μm radiances using Scenario 4 and the Window IR algorithm. The measurement accuracy metric is plotted.

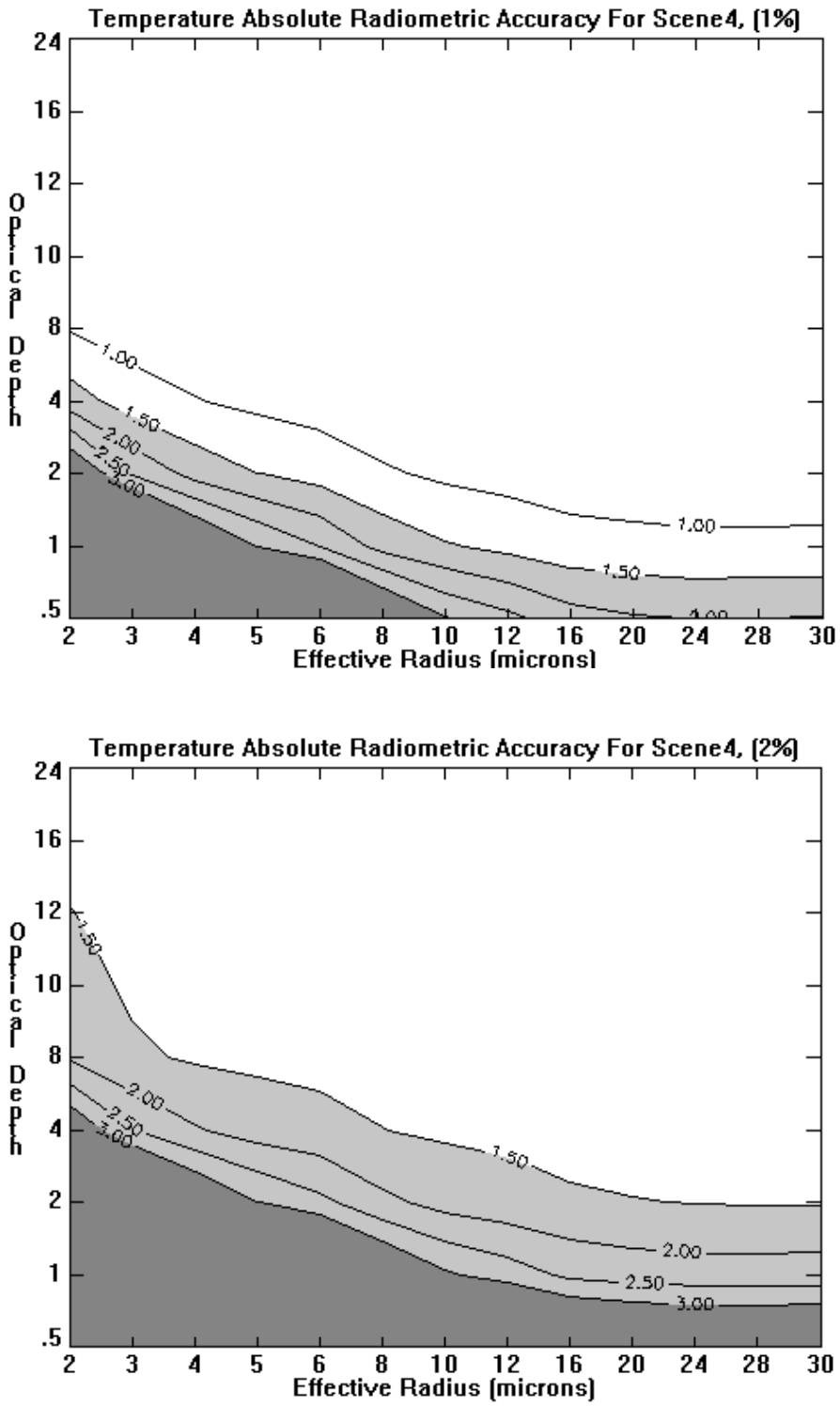

Figure 21. Radiometric Accuracy results for 1% (top) and 2% (bottom) perturbations in the 10.763 μm radiances using Scenario 4 and the Window IR algorithm. The measurement accuracy metric is plotted.

Table 10. Bias values (in percent) above which threshold measurement accuracy is exceeded for water droplet clouds, with $r_e = 5$ and for $\tau = 1$ and 10.

EDR Parameter: CTH, Temperature, and Pressure
Sensor Parameter: Radiometric Accuracy
Algorithm: Window IR
Effective Radius: Effective Radius = 5 μm

		Height		Temperature		Pressure	
Scene	Scene Description	τ = 10	τ = 1	τ = 10	τ = 1	τ = 10	τ = 1
4	Water Cloud (4/1km), US Standard Veg., θ= 0, θ_0 = Night	5%	5%	1%	4%	1.5%	5%
7	Water Cloud (4/1km), US Standard Veg., θ= 40, θ_0 = Night	5%	5%	1.1%	4%	2%	5%
8	Water Cloud (7/1km), Tropical Veg., θ= 0, θ_0 = Night	5%	5%	0.4%	2.5%	5%	5%
17	Water Cloud (4/1km), US Standard Veg., θ= 55, θ_0 = Night	5%	5%	2%	4%	5%	5%
18	Water Cloud (7/1km), Tropical Veg., θ= 40, θ_0 = Night	5%	5%	0.75%	4%	5%	5%
19	Water Cloud (7/1km), Tropical Veg., θ= 55, θ_0 = Night	5%	5%	2%	4.5%	5 %	5%

3.4.1.3.3 Radiometric Stability Results

Figure 22 provides results of the computation of the long-term stability metric, as a function of optical depth and effective particle size for scenario 4. The size of the bias that can be tolerated tends to increase with effective particle size and optical depth; this is typical of the results for other scenarios. Biases between 0.1 and 0.5 percent will meet threshold requirements for most optical depths and effective particle sizes. For r_e = 5 (typical altocumulus cloud), biases exceeding 0.5 percent can be tolerated for optical depths exceeding 4.

It is interesting to examine results for typical effective particle sizes for water droplet clouds which generally occur in the range 4.0 to 5.0 μm (see Liou, 1992, pg. 187). Table 11 shows the bias above which threshold long-term stability is exceeded for $r_e = 5$ and for $\tau = 1$ and 10 for CTH, temperature and pressure. Biases range from about 0.1 to 0.7 percent, in general. The analysis includes mid-latitude and tropical scenarios for nadir and edge-of-scan cases.

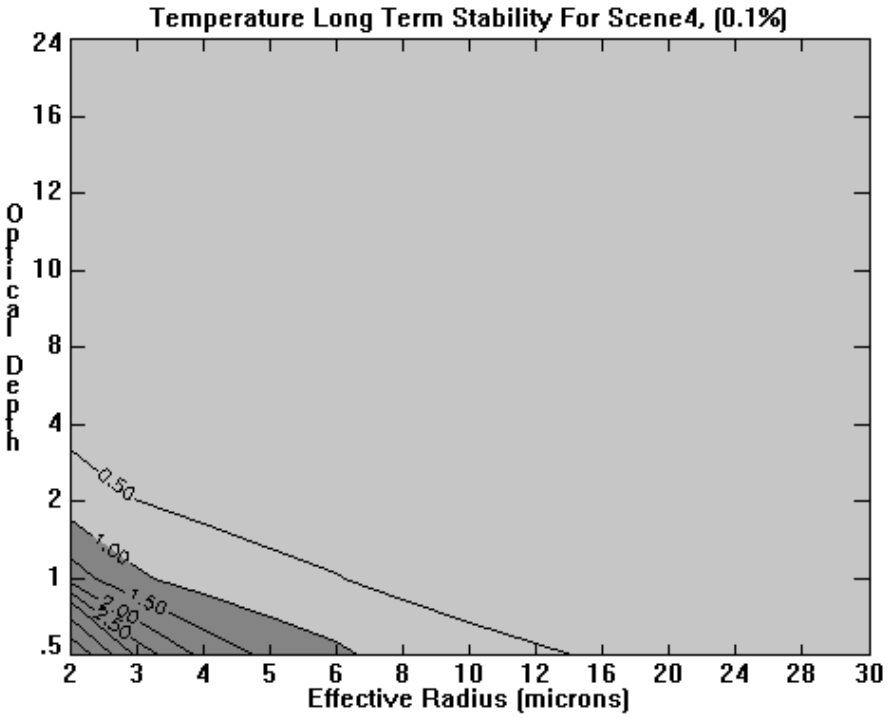

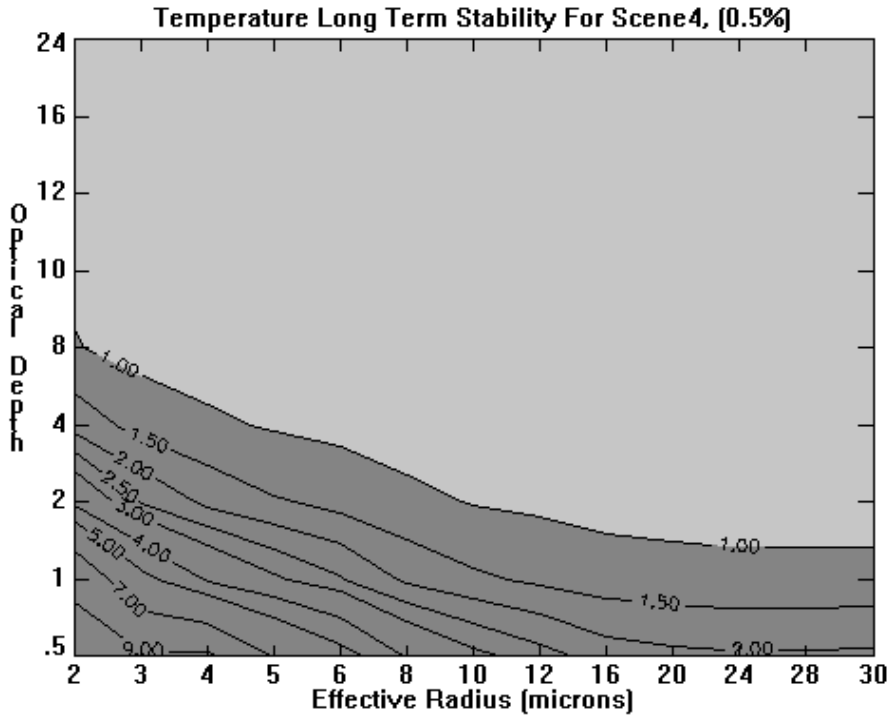

Figure 22. Radiometric Stability results for 0.1% (top) and 0.5% (bottom) perturbations of the 10.763 μm radiances using Scenario 4 and the Window IR algorithm. The long-term stability metric is plotted.

Table 11. Bias values (in percent) above which threshold long-term stability is exceeded for water droplet clouds with re = 5 and for τ = 1 and 10.

EDR Parameter: Cloud Top Height, Temperature and Pressure
Sensor Parameter: Radiometric Stability
Algorithm: Window IR
Effective Radius: Effective Radius = 5 μm

		Height		Temperature		Pressure	
Scene	Scene Description	τ = 10	τ = 1	τ = 10	τ = 1	τ = 10	τ = 1
4	Water Cloud (4/1km), US Standard Veg., θ = 0, θ_0 = Night	0.2%	0.7%	0.1%	0.5%	< 0.1%	0.3%
7	Water Cloud (4/1km), US Standard Veg., θ = 40, θ_0 = Night	0.3%	0.75%	0.2%	0.6%	< 0.1%	0.3%
8	Water Cloud (7/1km), Tropical Veg., θ = 0, θ_0 = Night	0.1%	0.6%	< 0.1%	0.3%	< 0.1%	0.3%
17	Water Cloud (4/1km), US Standard Veg., θ = 55, θ_0 = Night	0.4%	0.75%	0.3%	0.7%	0.15%	0.4%
18	Water Cloud (7/1km), Tropical Veg., θ = 40, θ_0 = Night	0.2%	0.7%	0.15%	0.6%	< 0.1%	0.3%
19	Water Cloud (7/1km), Tropical Veg., θ = 55, θ_0 = Night	0.4%	0.7%	0.3%	0.7%	0.15%	0.3%

3.4.1.3.4 Instrument Noise

Instrument noise refers to random noise introduced into the measured radiances by the VIIRS instrument. It is assumed that the noise is uncorrelated in time, from pixel-to-pixel, and across bands. Instrument noise is being investigated through application of seven noise models provided by RSBR (Raytheon Santa Barbara Research). Noise model 3 is believed to be the best current estimates of instrument specification performance and therefore the detail EDR performance shown below is using this noise model. The noise is modeled using a Gaussian distribution, with mean and standard deviation dependent on the waveband and magnitude of radiance. The noise models are numbered 1 through 7, with noise increasing with model number.

Two metrics were applied to investigate the effect of instrument noise on EDR retrieval accuracy: measurement accuracy and measurement precision. For these experiments, the measurement accuracy metric was applied as follows:

$$\beta = \left|\mu - x_{\mathrm{T}}\right| \tag{10}$$

where symbols are defined as in Section 3.4.1.3.1 For these tests, the mean was developed by randomly adding noise 32 times to the unperturbed radiance value(s) used by the retrieval algorithms. The perturbed radiances were then processed through the retrieval algorithm and the measurement accuracy metric computed. This process was repeated for each noise model.

The measurement precision metric is the standard deviation of the retrieved values, relative to

the mean of the retrieval values, with the same truth-value for all retrievals.

$$\sigma = \sqrt{\sum_N (x_i - \mu)^2 / (N-1)} \tag{11}$$

If we assume that the response of the EDR retrieval algorithm is linear for small radiance perturbations, we can see that the measurement accuracy metric should be insensitive to noise and that the precision metric should be sensitive to noise. This was found to be the case for all but the largest noise models (i.e., noise models 6 and 7).

Figure 23 and Figure 24 show contour plots of measurement accuracy and precision results, respectively, for a range of optical depths and effective particle sizes for baseline noise model 3. The results are for Scenario 4, which is a U.S. Standard Atmosphere case, nadir satellite view, with a water cloud inserted between 3 and 4 km in altitude. In these plots, the light gray shaded regions are regions where the objective is exceeded and the dark gray shaded regions are regions where the threshold is exceeded. It is obvious that measurement accuracy meets both threshold and objective. Measurement accuracy results for other scenarios are consistent with these findings; therefore, no further instrument noise measurement accuracy results will be shown. On the other hand, measurement precision is affected by instrument noise. Figure 24 indicates that the threshold measurement precision is met for virtually all r_e and $\tau > 1$, and the objective is met for $r_e > 4$ and $\tau > 1$. Only in the small region where $r_e < 4$ and $\tau < 1$ is the threshold measurement precision requirement not met.

Figure 25 shows measurement precision results for Scenario 2, a cirrus case. Again, this case is for the U.S. Standard atmosphere, nadir view, and the cirrus cloud is between 9 and 10 km in altitude. For these plots, the results for all effective particle sizes were aggregated and the precision is depicted as a function of optical depth. Note that the measurement precision meets threshold for most noise models for optical depths greater than about 0.5; the threshold is met for baseline noise model 3 for $\tau > 0.125$.

It is interesting to examine results for typical effective particle sizes for water droplet clouds which generally occur in the range 4.0 to 5.0 μm (see Liou, 1992, pg. 187). Table 12 shows the use of specification noise model (model 3) for which threshold measurement precision can be met (with a check mark) or marginally met (question mark) for $r_e = 5$ and for $\tau = 1$ and 10 for CTH, temperature, and pressure. In general, specification noise model is acceptable for all except scene 8 (tropical water cloud with optical thickness=1) temperature EDR.

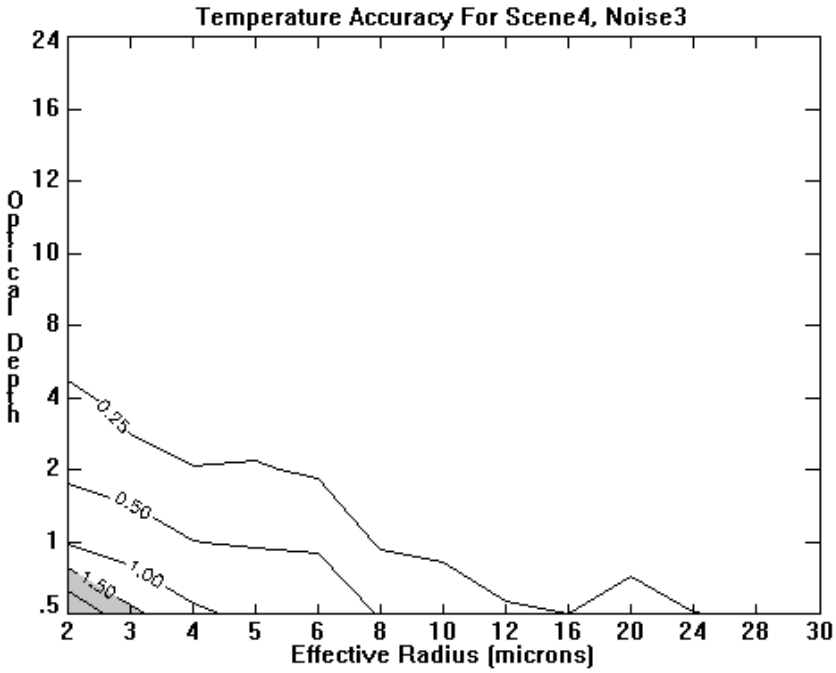

Figure 23. Instrument noise contour plot for measurement accuracy (Scenario 4, Model 3).

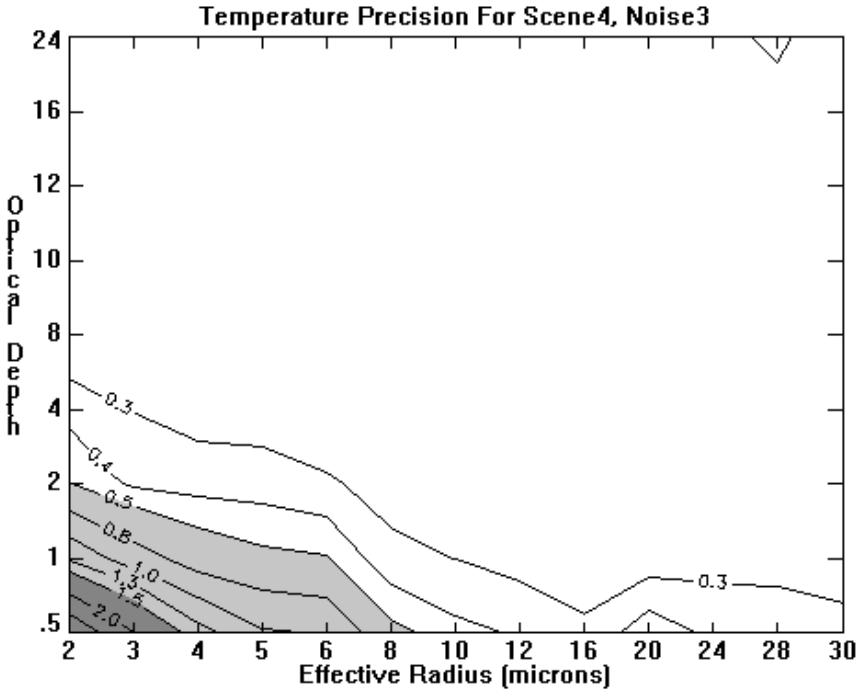

Figure 24. Instrument noise contour plot for measurement precision (Scenario 4, Model 3).

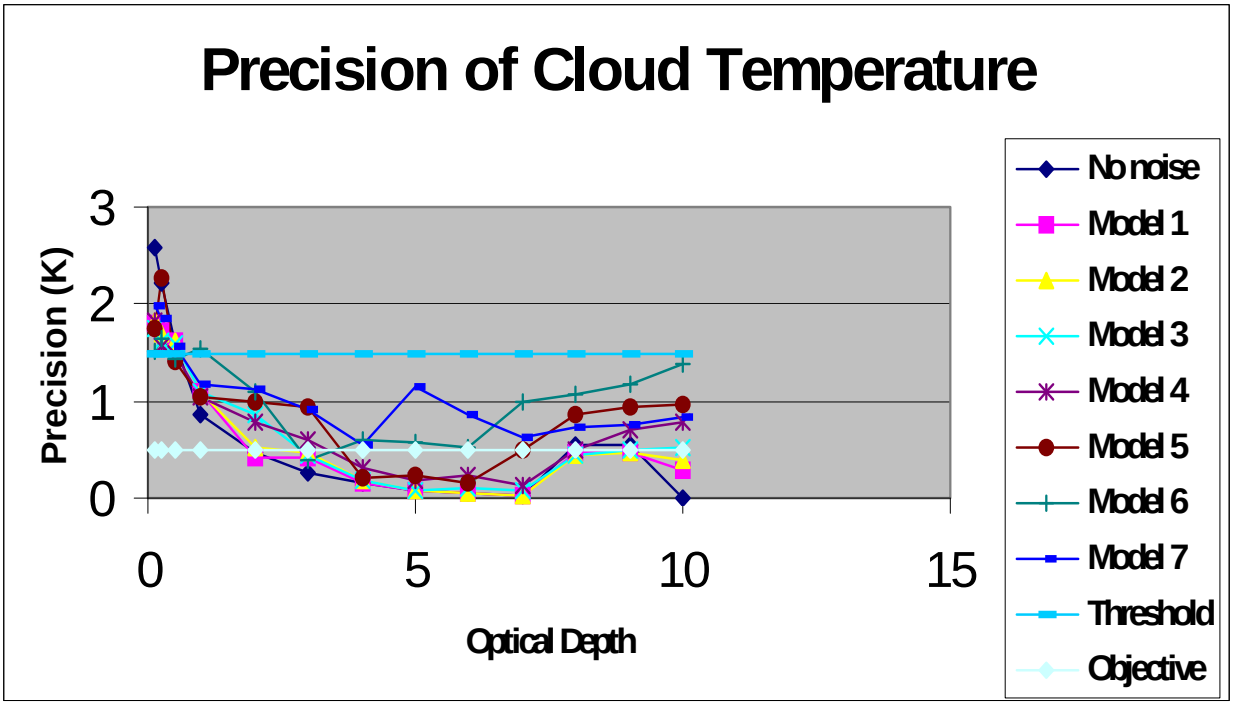

Figure 25. Instrument Noise Measurement Precision Results (Scenario 2).

Table 12. Precision Performance Estimates using Noise Model 3. Check mark indicates performance exceeds threshold. Question mark indicates performance marginally meets threshold.

EDR Parameter: CTH, Temperature, and Pressure
Sensor Parameter: Radiometric Noise
Algorithm: Window IR
Effective Radius: Effective Radius = 5 μm

		Height		Temperature		Pressure	
Scene	Scene Description	τ = 1	τ = 10	τ = 1	τ = 10	τ = 1	τ = 10
4	Water Cloud (4/1km), US Standard Veg., θ = 0, θ_0 = Night	x	x	x	x	x	x
7	Water Cloud (4/1km), US Standard Veg., θ = 40, θ_0 = Night	x	x	x	x	x	x
8	Water Cloud (7/1km), Tropical Veg., θ = 0, θ_0 = Night	x	x	?	x	x	x
17	Water Cloud (4/1km), US Standard Veg., θ = 55, θ_0 = Night	x	x	x	x	x	x
18	Water Cloud (7/1km), Tropical Veg., θ = 40, θ_0 = Night	x	x	x	x	x	x
19	Water Cloud (7/1km), Tropical Veg., θ = 55, θ_0 = Night	x	x	x	x	x	x

3.4.2 Algorithm Testing

The testing described in this Section was performed with the delivered versions of the Science Code. It is primarily focussed on testing of the daytime water phase clouds.

3.4.2.1 Functional Testing

Functional testing of the daytime water cloud retrieval algorithm is based on the "s10_DAY_MID_LAT_SPRING" scene data. The M15 brightness temperatures from this data are illustrated in Figure 26. Figure **27** shows the retrievals of cloud top temperature for both water and ice clouds. Figure **28** shows the retrieved cloud top temperature for a portion of the scene, derived using the day water algorithm. Note in this example, retrievals of COP in the sunglint region were excluded. (At the time of testing, the backup algorithms which would normally be exercised in this situation had not been included as part of the CTP algorithm development). Therefore CTP retrievals were made only for those pixels where all inputs are available. For example if the COT or EPS IPs don't exist for a pixel then the results are set to FILL values. Note also that the retrieval depends on the accuracy of the inputs. In this case, the radiances and optical properties associated with optically thin clouds near the cloud edges result in what appears to be non-physical results, i.e., T < 250 K.

Figure 29 is a diagnostic plot showing the retrieved cloud top pressure as a function of cloud optical depth. Cases that failed to converge are indicated by the red points. The low values of CTP for optically thin clouds indicates an inconsistency between the COT and EPS EDRs and the SDRs. Some cases with optical thick clouds also failed to converge. Figure 30 shows a histogram of the number of iterations used for all day water retrievals. By processing the data in cells, sorted by radiance, the number of iterations required to arrive at the solution is much improved.

While the functional testing was primarliy focused on testing the day/ water clouds, it also served to demonstrate that no signifcant changes were introduced to the algorithm for non-day/ water clouds (the portion that was not changed in the latest algorithm version).

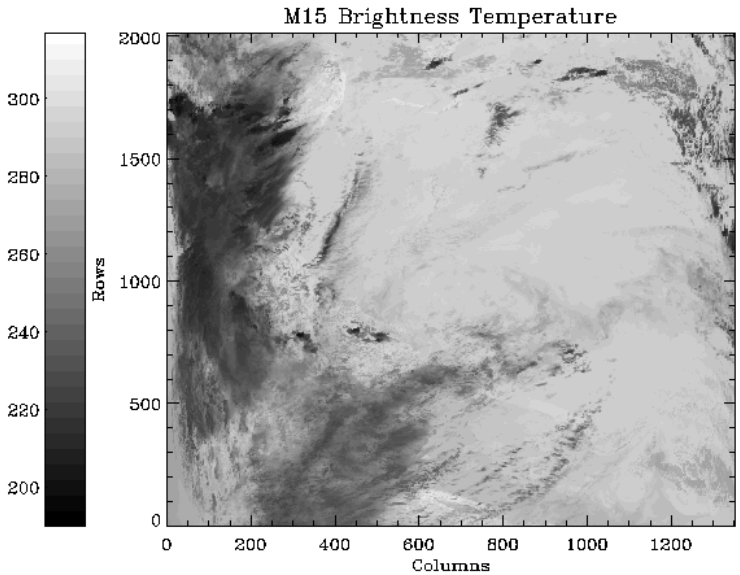

Figure 26. M15 brightness temperature data for scene used in functional testing.

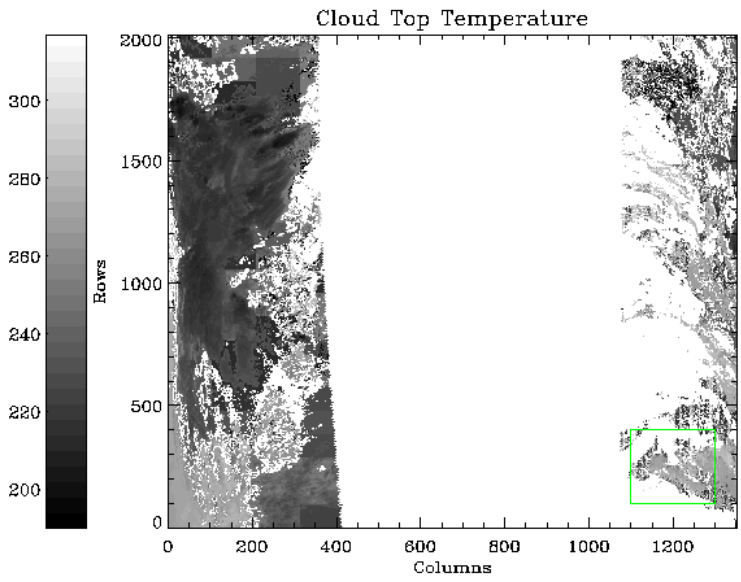

Figure 27. Retrieved cloud top temperature for the s10_DAY_MID_LAT_SPRING scene, including both water and ice cloud retrievals. A region with water clouds (shown in Figure 28) is identified by the green box in the lower right.

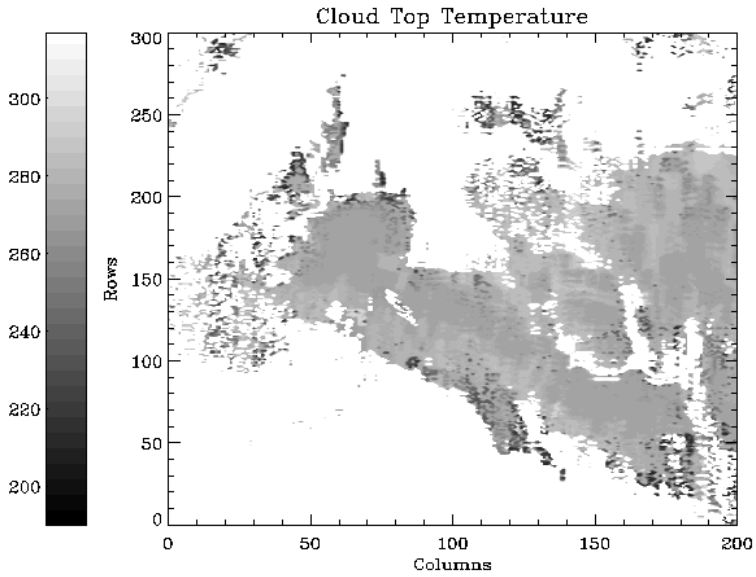

Figure 28. A portion of the s10_DAY_MID_LAT_SPRING scene showing cloud top temperature retrievals in a region identified with water clouds. Note how at the edges of the cloud where the cloud optical thickness IP reports low values, results in unrealistically low values of cloud temperature.

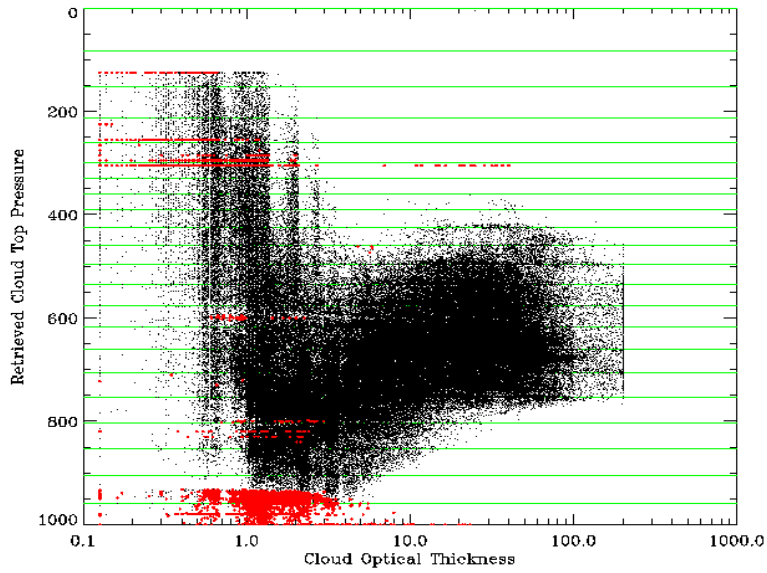

Figure 29. Retrieved cloud top pressure as a function of cloud optical thickness for all day water clouds. Red points indicate non-convergence. OSS pressure levels are indicated in green.

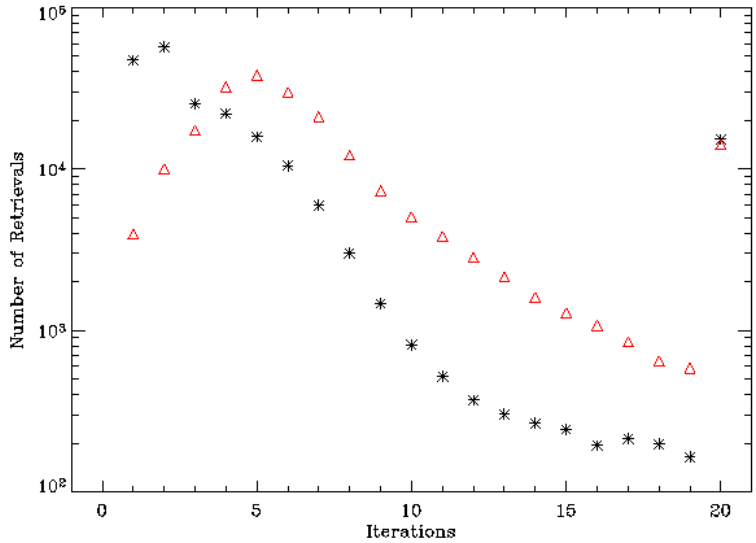

Figure 30. Number of iterations used in the Newton-Raphson solution for cloud top pressure. Red triangles represent retrievals using the observed M15 brightness temperature as the first guess. Black asterisks represent retrievals that use the solution from the previous retrieval as first guess.

Testing of the opaque cloud BackUp algorithms was performed based on the VIIRS_2002190_1625 unit test scene shown in Figure 31. This scene contains a mix of pixels

identified with all the cloud phases (i.e., clear, partly cloudy, water, mixed, opaque ice, cirrus, and overlap cloud). A portion of the scene is also identified with sun glint. The unit test scene thus serves as a good case with which to test the workings of the CTP algorithm.

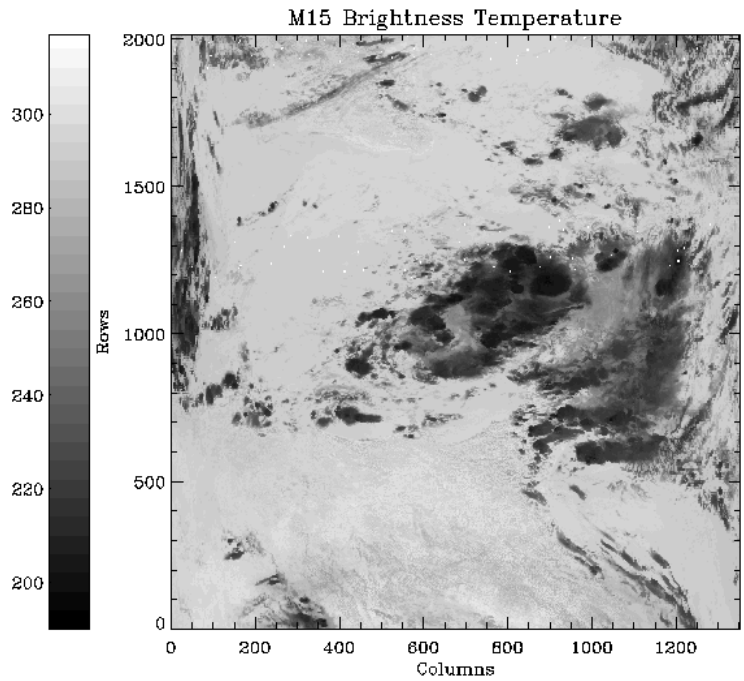

Figure 31. M15 brightness temperatures for the VIIRS_2002190_1625 unit test scene.

The following features of the CTP algorithm were exercised using VIIRS_2002190_1625 unit test data.

- BackUp DaytimeIce retrievals for pixels with missing CTT inputs.
- BackUp DaytimeWater retrievals for pixels with missing COT and EPS inputs.
- BackUp DaytimeIce retrievals for pixels with degraded CTT inputs as identified by the convergence bits in the INWCTT Quality Flag.
- BackUp DaytimeWater retrievals for pixels with degraded COT and EPS inputs as identified by the convergence bits in the COP Quality Flag.
- Retrievals under potentially degraded conditions (e.g., sunglint, partly cloud, mixed phase, cloud overlap, and probably clear)
- BackUp to DaytimeWater retrievals for cases that failed to converge using the input COT and EPS IPs.

- Two different BackUp algorithms: i.e., Window IR BackUp algorithm and Precipitable Water Correction BackUp algorithm.

- Window IR (DayWater) retrievals performed with the Newton Raphson Iterative method using the Search method for pixels with convergence problems.

3.4.2.2 Performance Testing

Simulations were constructed to evaluate the performance of the CTP day water cloud retrieval algorithm. The simulations were divided into two sets to represent high-optical depth and low-optical depth clouds. For the optically thin clouds, COT= 0.85, 0.90, 0.95, and 1.0. For the optically thick clouds, COT = 5, 10, 30 and 64. Other parameterizations included cloud particle size (5, 10, and 20 microns), view zenith angle (0, 30, 45, 60, and 68 degrees), and cloud top pressure (400, 500, 700, 850, 900 mbar) for a total of 300 combinations for each simulation. Atmospheric profiles were selected at random from the ECMWF database, and for each parameter combination, 400 realizations with different profiles was included.

For each combination of parameters, a 10 by 10 cell of pixels was constructed. Within this cell, the inputs to the forward model were perturbed before generating radiances, then random noise with a standard deviation of 0.4 K was added to represent sensor/model errors. In each case, the origin of each cell was simulated with unperturbed values to serve as a reference. The perturbations to each parameter were introduced as a bias, held fixed over all pixels in the cell, or as a random component that varied between pixels. Both biases and the random perturbations were computed as normally distributed variables with a given standard deviation.

Table 13 summarizes the errors applied to COT and EPS. Both bias and random perturbations were included.

Table 13. Errors applied to COT and EPS

COT Range	COT Errors		EPS Errors (μm)	
	Bias	Random	Bias	Random
COT < 1	0.28	0.1	5.5	1
COT > 1	0.16	4%	2.0	1

The ECMWF profile dataset identified profiles as either land or water. This assignment has been further expanded to water, land, snow, ice, and desert based on surface air temperature values. Table 14 summarizes the emissivities and the corresponding errors used in the simulation for each surface class. The emissivity errors were added as a random perturbation within the 10 by 10 cell.

Table 14. Surface Emissivity and Errors

Type	Selection	Emissivity	Error
Water	ECMWF water, T > 0 C	0.98	0.002
Land	ECMWF land T > 0 C	0.96	0.008

Snow	ECMWF land, T < 0 C	0.98	0.005
Ice	ECMWF water T < 0 C	0.98	0.005
Desert	ECMWF land, T > 30 C	0.95	0.015

The errors in the NWP profiles were represented by a bias over all pixels in the 10 by 10 cell. The perturbed temperature and water vapor profiles were constructed from EOFs based on a forecast covariance matrix.

The CTP retrievals were based on the simulated (perturbed) SDR radiances plus the unperturbed inputs for COT, EPS, surface emissivity, and the NWP profiles. The resulting errors in the retrievals reflects the sensitivity to errors in the inputs and to noise. The performance of the retrievals were evaluated based on measurements of accuracy, precision, and uncertainty for the cloud top pressure, temperature, and height EDRs. The results were binned into three altitude regimes, 0 to 3 km, 3 to 7 km, and above 7 km, and into two COT categories, COT < =1 and COT > 1.

The accuracy of the retrievals was evaluated on a cell-by-cell basis by computing the difference between the retrieved quantity and the truth, averaged over all pixels in the cell. The origin of the cell, which was reserved as a reference was not included in the calculation. Also, retrievals that did not converge were excluded from the statistics. The final reported bias was represented by the average from all cells.

The precision was also evaluated on a cell-by-cell basis by computing the standard deviation of the measure quantity relative to the mean value for the cell. Again the reference pixel and non-converged results were excluded. The final precision represents the average over all cells.

The uncertainty was computed from the accuracy and precision using the standard formula U=sqrt(A^2 + P^2).

Table 15a, 15b, and 15c summarize the performance of the CTP day water algorithm for optically thick clouds. In all cases, the performance meet the requirements for accuracy, precision, and uncertainty for cloud top pressure, temperature, and height.

Table 15a. Cloud Top Pressure Performance for COT > 1

Altitude (km)	Accuracy (mb)		Precision (mb)		Uncertainty (mb)		N Points
	Calc.	Req.	Calc.	Req.	Calc.	Req.	
0	10.9	40	15.2	25	18.7	40	5238
3	12.4	40	10.0	20	15.9	45	4360
7	11.2	30	10.1	13	15.1	30	2398
All	11.5	N/A	12.3	N/A	16.8	N/A	11996

Table 15b. Cloud Top Temperature Performance for COT > 1

Altitude (km)	Accuracy (K)		Precision (K)		Uncertainty (K)		N Points
	Calc.	Req.	Calc.	Req.	Calc.	Req.	
0	0.28	N/A	0.50	N/A	0.57	N/A	5238
3	0.89	N/A	0.73	N/A	1.15	N/A	4360
7	1.14	N/A	1.01	N/A	1.52	N/A	2398
All	0.67	2.0	0.68	1.5	0.96	3.0	11996

Table 15c. Cloud Top Height Performance for COT > 1

Altitude (km)	Accuracy (km)		Precision (km)		Uncertainty (km)		N Points
	Calc.	Req.	Calc.	Req.	Calc.	Req.	
0	0.12	N/A	0.17	N/A	0.21	N/A	5238
3	0.17	N/A	0.14	N/A	0.22	N/A	4360
7	0.19	N/A	0.17	N/A	0.25	N/A	2398
All	0.16	0.5	0.16	0.3	0.22	0.5	11996

Tables 16a, 16b, and 16c summarize the performance of the CTP day water algorithm for cloud with COT = 1.

Table 16a. Cloud Top Pressure Performance for COT = 1

Altitude (km)	Accuracy (mb)		Precision (mb)		Uncertainty (mb)		N Points
	Calc.	Req.	Calc.	Req.	Calc.	Req.	
0	59.	100	29.	25	65.	130	1261
3	96.	65	36.	20	103.	70	1007
7	121.	30	44.	13	129.	30	561
All	84.	N/A	34.	N/A	91.	N/A	2829

Table 16b. Cloud Top Temperature Performance for COT = 1

Altitude (km)	Accuracy (K)		Precision (K)		Uncertainty (K)		N Points
	Calc.	Req.	Calc.	Req.	Calc.	Req.	
0	2.8	N/A	1.4	N/A	3.1	N/A	1261
3	7.3	N/A	2.6	N/A	7.8	N/A	1007
7	11.3	N/A	4.1	N/A	12.0	N/A	561
All	6.1	6.0	2.4	1.5	6.6	3.0	2829

Table 16c. Cloud Top Height Performance for COT = 1

Altitude (km)	Accuracy (km)		Precision (km)		Uncertainty (km)		N Points
	Calc.	Req.	Calc.	Req.	Calc.	Req.	
0	0.6	N/A	0.48	N/A	0.75	N/A	1261
3	1.2	N/A	0.52	N/A	1.3	N/A	1007
7	1.9	N/A	0.71	N/A	2.0	N/A	561
All	1.0	2.0	0.54	0.3	1.2	2.0	2829

The performance of the BackUp algorithms for retrieving CTP, CTT, and CTH was evaluated by running these algorithms on all pixels in the simulated scenes. The results for COT > 1, presented in Table 17a,b,c show a degradation in performance relative to the main Window IR physical retrieval. The errors implicit in these algorithm impact the accuracy, while the precision error may be reduced due to the fact that the random errors associated with the COP do not contribute to the retrieval error. The PW regression algorithm does not perform as well as the Window IR backup algorithm (and may require further optimization). In fact, the performance for the backup algorithm with no atmospheric correction (i.e., using the observed brightness temperature as the cloud top temperature) is superior to that of the PW regression algorithm and comparible to that of the window IR backup algorithm. The errors in CTT are shown as histograms as a function of COT in Figure 32. A comparison of the performance is presented in Figure 34, Figure 35, and Figure 36.

Note the CTP, CTH, and CTT products are recorded as scaled bytes. This limitation significantly contributes to the precision performance reported for the COT>1 case in this study. For example the quantization associated with CTT is 0.75 K. We recommend that the quantization be increased to 16 bits for all the CTP products and intermediate products.

For COT ≤ 1, the BackUp algorithms will be unreliable because the the opaque cloud assumption

is invalid. The performance of the BackUp algorithms for COT ≤ 1 is presented in Tables 17d,e,f and the plot of CTT errors is shown in Figure 33. Clearly the error can be large, especially when the cloud is not located near the surface.

Table 17a. Performance for COT>1 based retrievals using black cloud Window IR algorithm. (Requirements are in parentheses.)

		Accuracy	Precision	Uncertainty	Number
CTP (mbar):					
	0-3 km	19.9 (**40**)	14.0 (**25**)	24.4 (**40**)	5215
	3-7 km	25.3 (**40**)	9.8 (**20**)	27.2 (**45**)	4358
	> 7 km	27.4 (**30**)	9.5 (**13**)	29.0 (**30**)	2400
	All	23.4 (NA)	11.6 (NA)	26.1 (NA)	11973
CTT (K):					
	0-3 km	0.69 (NA)	0.48 (NA)	0.84 (NA)	5215
	3-7 km	1.83 (NA)	0.67 (NA)	1.95 (NA)	4358
	> 7 km	2.78 (NA)	0.87 (NA)	2.91 (NA)	2400
	All	1.52 (**2.0**)	0.63 (**1.5**)	1.65 (**3.0**)	11973
CTH (km):					
	0-3 km	0.19 (NA)	0.17 (NA)	0.25 (NA)	5215
	3-7 km	0.34 (NA)	0.13 (NA)	0.36 (NA)	4358
	> 7 km	0.47 (NA)	0.15 (NA)	0.50 (NA)	2400
	All	0.30 (**0.5**)	0.15 (**0.3**)	0.34 (**0.5**)	11973

Table 17b. Performance for COT>1 based retrievals using black cloud PW regression

		Accuracy	Precision	Uncertainty	Number
CTP (mbar):					
	0-3 km	49.1 (**40**)	11.9 (**25**)	50.5 (**40**)	3592
	3-7 km	31.9 (**40**)	10.3 (**20**)	33.5 (**45**)	4347
	> 7 km	28.7 (**30**)	9.6 (**13**)	30.3 (**30**)	2393
	All	37.2 (NA)	10.7 (NA)	38.7 (NA)	10322
CTT (K):					
	0-3 km	2.20 (NA)	0.55 (NA)	2.27 (NA)	3592
	3-7 km	2.27 (NA)	0.71 (NA)	2.37 (NA)	4347
	> 7 km	2.93 (NA)	0.88 (NA)	3.05 (NA)	2393
	All	2.40 (**2.0**)	0.69 (**1.5**)	2.49 (**3.0**)	10322
CTH (km):					
	0-3 km	0.47 (NA)	0.12 (NA)	0.48 (NA)	3592
	3-7 km	0.42 (NA)	0.13 (NA)	0.44 (NA)	4347
	> 7 km	0.40 (NA)	0.15 (NA)	0.52 (NA)	2393
	All	0.45 (**0.5**)	0.13 (**0.3**)	0.47 (**0.5**)	10322

Table 17c. Performance for COT>1 based brightness temperatures

		Accuracy	Precision	Uncertainty	Number
CTP (mbar):					
	0-3 km	22.6 (**40**)	12.0 (**25**)	25.6 (**40**)	5196
	3-7 km	25.5 (**40**)	9.5 (**20**)	27.2 (**45**)	4358
	> 7 km	26.7 (**30**)	9.5 (**13**)	28.3 (**30**)	2385
	All	24.5 (NA)	10.6 (NA)	26.7 (NA)	11939
CTT (K):					
	0-3 km	0.76 (NA)	0.49 (NA)	0.90 (NA)	5196

	3-7 km	1.86 (NA)	0.68 (NA)	1.98 (NA)	4358
	> 7 km	2.71 (NA)	0.87 (NA)	2.85 (NA)	2385
	All	1.55 (**2.0**)	0.63 (**1.5**)	1.67 (**3.0**)	11939
CTH (km):					
	0-3 km	0.22 (NA)	0.12 (NA)	0.25 (NA)	5196
	3-7 km	0.34 (NA)	0.13 (NA)	0.36 (NA)	4358
	> 7 km	0.46 (NA)	0.15 (NA)	0.49 (NA)	2385
	All	0.31 (**0.5**)	0.13 (**0.3**)	0.34 (**0.5**)	11939

Table 17d. Performance for COT=1 based retrievals using black cloud physical retrieval

		Accuracy	**Precision**	**Uncertainty**	**Number**
CTP (mbar):					
	0-3 km	86.3 (**100**)	13.2 (**25**)	87.3 (**130**)	1270
	3-7 km	223.5 (**65**)	19.0 (**20**)	224.3 (**70**)	1019
	> 7 km	320.7 (**30**)	23.9 (**13**)	321.5 (**30**)	599
	All	183.3 (NA)	17.5 (NA)	184.2 (NA)	2888
CTT (K):					
	0-3 km	4.2 (NA)	0.55 (NA)	4.2 (NA)	1270
	3-7 km	14.8 (NA)	0.96 (NA)	14.8 (NA)	1019
	> 7 km	26.1 (NA)	1.51 (NA)	26.1 (NA)	599
	All	12.5 (**6.0**)	0.90 (**1.5**)	12.5 (**3.0**)	2888
CTH (km):					
	0-3 km	0.90 (NA)	0.43 (NA)	1.00 (NA)	1270
	3-7 km	2.59 (NA)	0.31 (NA)	2.61 (NA)	1019
	> 7 km	4.50 (NA)	0.34 (NA)	4.52 (NA)	599
	All	2.24 (**2.0**)	0.37 (**0.3**)	2.27 (**2.0**)	2888

Table 17e. Performance for COT=1 based retrievals using black cloud PW regression

		Accuracy	**Precision**	**Uncertainty**	**Number**
CTP (mbar):					
	0-3 km	108.8 (**100**)	11.3 (**25**)	109.4 (**130**)	492
	3-7 km	233.9 (**65**)	19.8 (**20**)	234.8 (**70**)	840
	> 7 km	318.6 (**30**)	25.7 (**13**)	319.6 (**30**)	561
	All	226.5 (NA)	19.3 (NA)	227.3 (NA)	1893
CTT (K):					
	0-3 km	5.4 (NA)	0.60 (NA)	5.4 (NA)	492
	3-7 km	16.1 (NA)	1.21 (NA)	16.1 (NA)	840
	> 7 km	26.1 (NA)	1.66 (NA)	26.2 (NA)	561
	All	16.3 (**6.0**)	1.18 (**1.5**)	16.3 (**3.0**)	1893
CTH (km):					
	0-3 km	1.03 (NA)	0.11 (NA)	1.04 (NA)	492
	3-7 km	2.82 (NA)	0.21 (NA)	2.83 (NA)	840
	> 7 km	4.54 (NA)	0.30 (NA)	4.55 (NA)	561
	All	2.87 (**2.0**)	0.21 (**0.3**)	2.87 (**2.0**)	1893

Table 17f. Performance for COT=1 based brightness temperatures

		Accuracy	**Precision**	**Uncertainty**	**Number**
CTP (mbar):					
	0-3 km	83.6 (**100**)	9.3 (**25**)	84.1 (**130**)	1159

	3-7 km	220.8 (**65**)	16.5 (**20**)	221.4 (**70**)	996
	> 7 km	319.6 (**30**)	23.2 (**13**)	320.4 (**30**)	595
	All	184.3 (NA)	14.9 (NA)	184.9 (NA)	2750
CTT (K):					
	0-3 km	4.1 (NA)	0.50 (NA)	4.2 (NA)	1159
	3-7 km	14.8 (NA)	0.95 (NA)	14.8 (NA)	996
	> 7 km	26.1 (NA)	1.52 (NA)	26.1 (NA)	595
	All	12.7 (**6.0**)	0.88 (**1.5**)	12.8 (**3.0**)	2750
CTH (km):					
	0-3 km	0.80 (NA)	0.10 (NA)	0.80 (NA)	1159
	3-7 km	2.65 (NA)	0.18 (NA)	2.66 (NA)	996
	> 7 km	4.55 (NA)	0.27 (NA)	4.56 (NA)	595
	All	2.28 (**2.0**)	0.16 (**0.3**)	2.29 (**2.0**)	2750

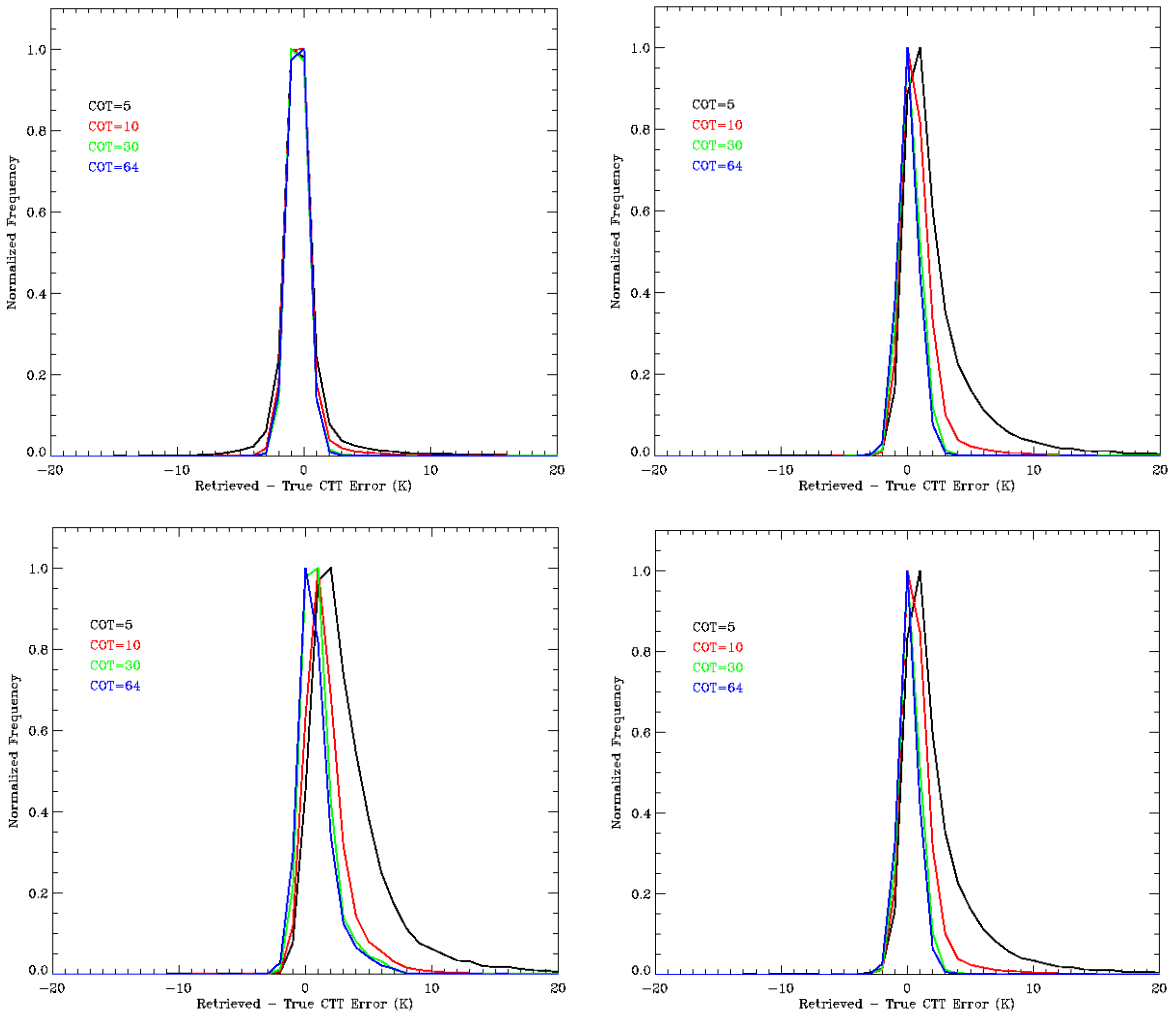

Figure 32. Histogram of CTT retrieval errors as a function of COT for COT>1. Top left: Window IR algorithm. Top right: BackUp WindowIR algorithm. Bottom left: BackUp PW Regression algorithm. Bottom right: Brightness temperatures

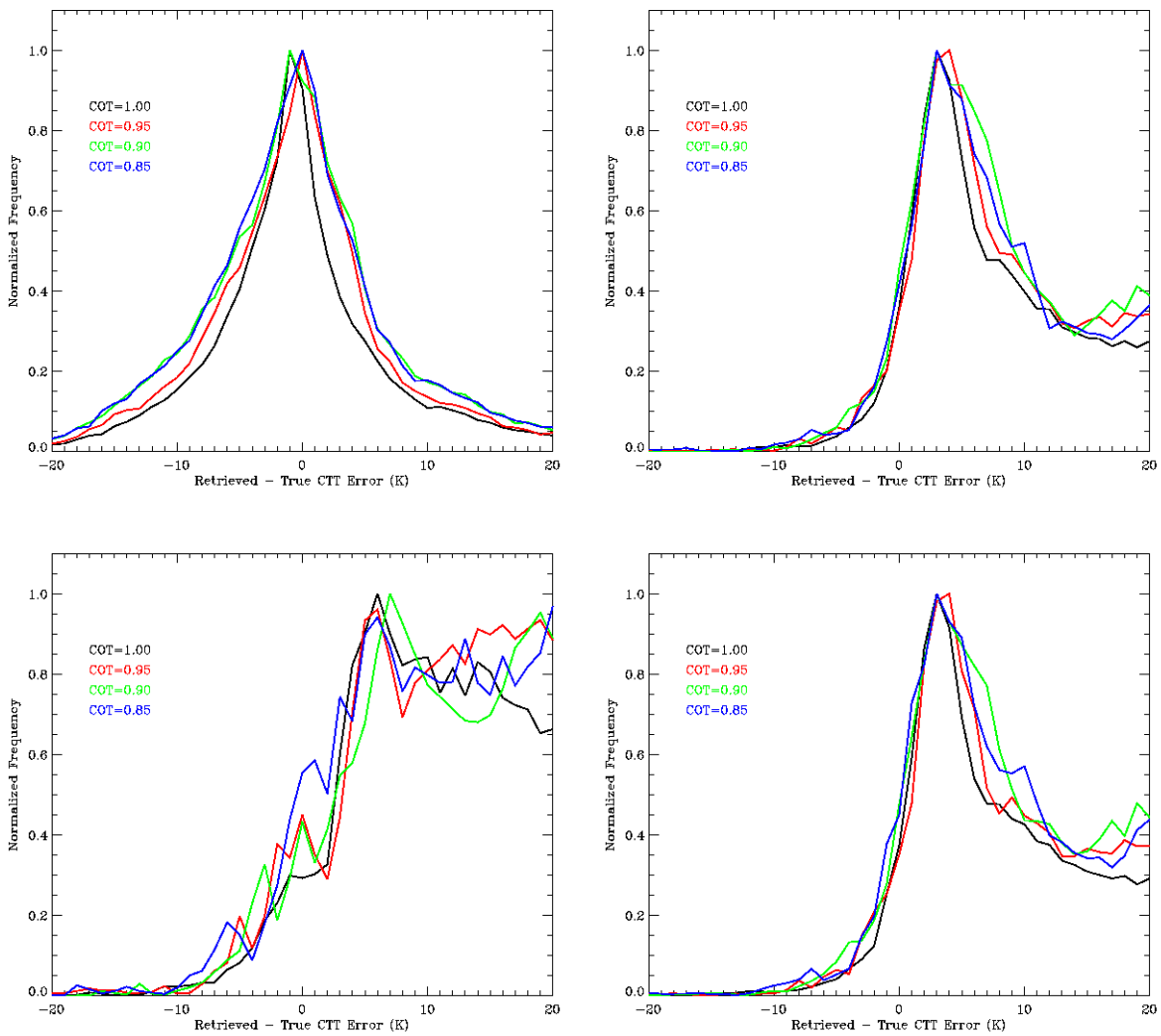

Figure 33. Histogram of CTT retrieval errors as a function of COT for COT≤1. Top left: Window IR algorithm. Top right: BackUp WindowIR algorithm. Bottom left: BackUp PW Regression algorithm. Bottom right: Brightness temperatures

Figure 34 presents the performance of CTP for the primary and the three alternate back-up algorithms with high optical thickness on the left and low optical thickness on the right. Similarly, Figure 35 presents performance for CTT and Figure 36 for CTH.

For high optical thickness (COT>1), the baseline algorithm provides better than required performance in all cases. The fallback algorithms also meet or exceed the minimum performance requriements in most cases. The Precipitable water black body correction algorithm (BB-Reg) is noticebly worse than the other fall-back algorithms and has slightly worse than required performance in a number of cases. We believe that the problems with the BB-Reg algorithm are associated with the specific regression coefficients and model are not appropriate for the bandpass used here. Another exception is CTT accuracy where all the backup algorithms perform slightly worse than required for > 7 km. Since the backup algorithms are only used a small fraction of time (<<1%), we expect overall performance to meet requirements for COT>1.

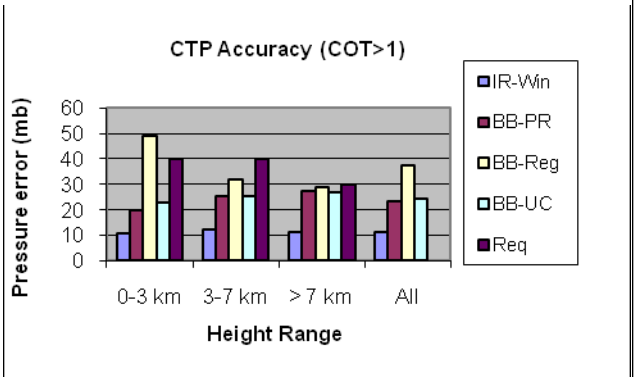
CTP Accuracy (COT>1)
Pressure error (mb)
60
50
40
30
20
10
0
0-3 km
3-7 km
> 7 km
All
Height Range
IR-Win
BB-PR
BB-Reg
BB-UC
Req

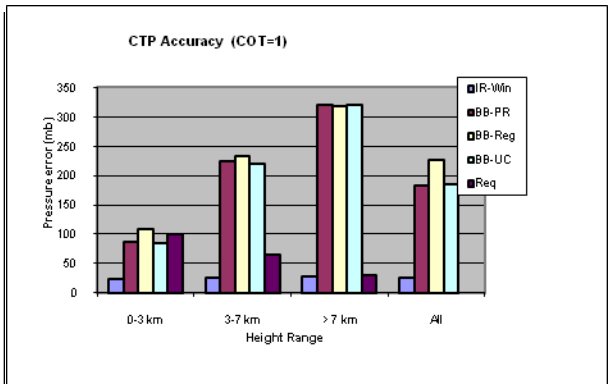
CTP Accuracy (COT=1)
Pressure error (mb)
350
300
250
200
150
100
50
0
0-3 km
3-7 km
> 7 km
All
Height Range
IR-Win
BB-PR
BB-Reg
BB-UC
Req

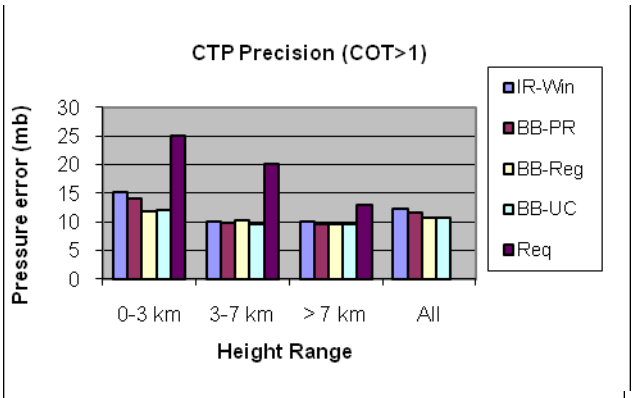
CTP Precision (COT>1)
Pressure error (mb)
30
25
20
15
10
5
0
0-3 km
3-7 km
> 7 km
All
Height Range
IR-Win
BB-PR
BB-Reg
BB-UC
Req

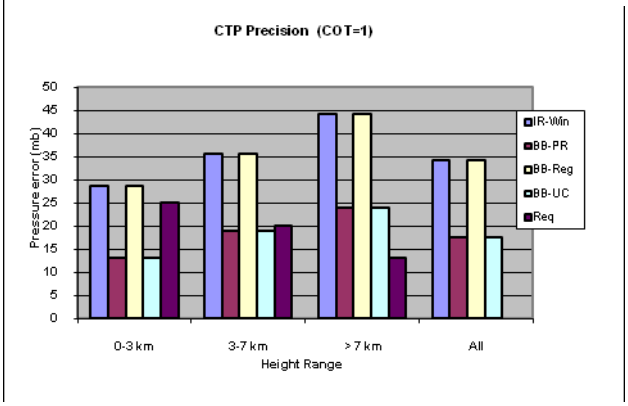
CTP Precision (COT=1)
Pressure error (mb)
50
45
40
35
30
25
20
15
10
5
0
0-3 km
3-7 km
> 7 km
All
Height Range
IR-Win
BB-PR
BB-Reg
BB-UC
Req

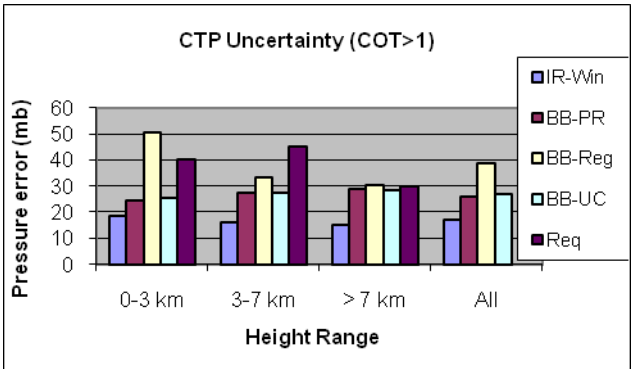
CTP Uncertainty (COT>1)
Pressure error (mb)
60
50
40
30
20
10
0
0-3 km
3-7 km
> 7 km
All
Height Range
IR-Win
BB-PR
BB-Reg
BB-UC
Req

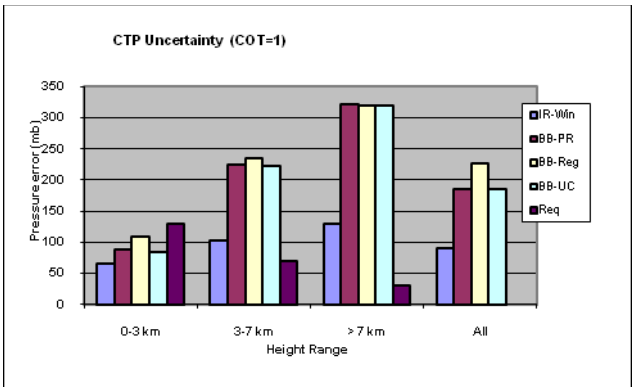

Figure 34. CTP accuracy, precision, uncertainty performance comparison for COT > 1 (left) and COT=1 (right). Shown are results for IR-Win: Window IR algorithm, BB-PR: Window-IR Phylsical Retireval BackUp Algorithm, BB-Reg: Precipitable Water Regression BackUp algorithm, BB-UC: BackUp with no atmospheric correction, and Req: the requirements.

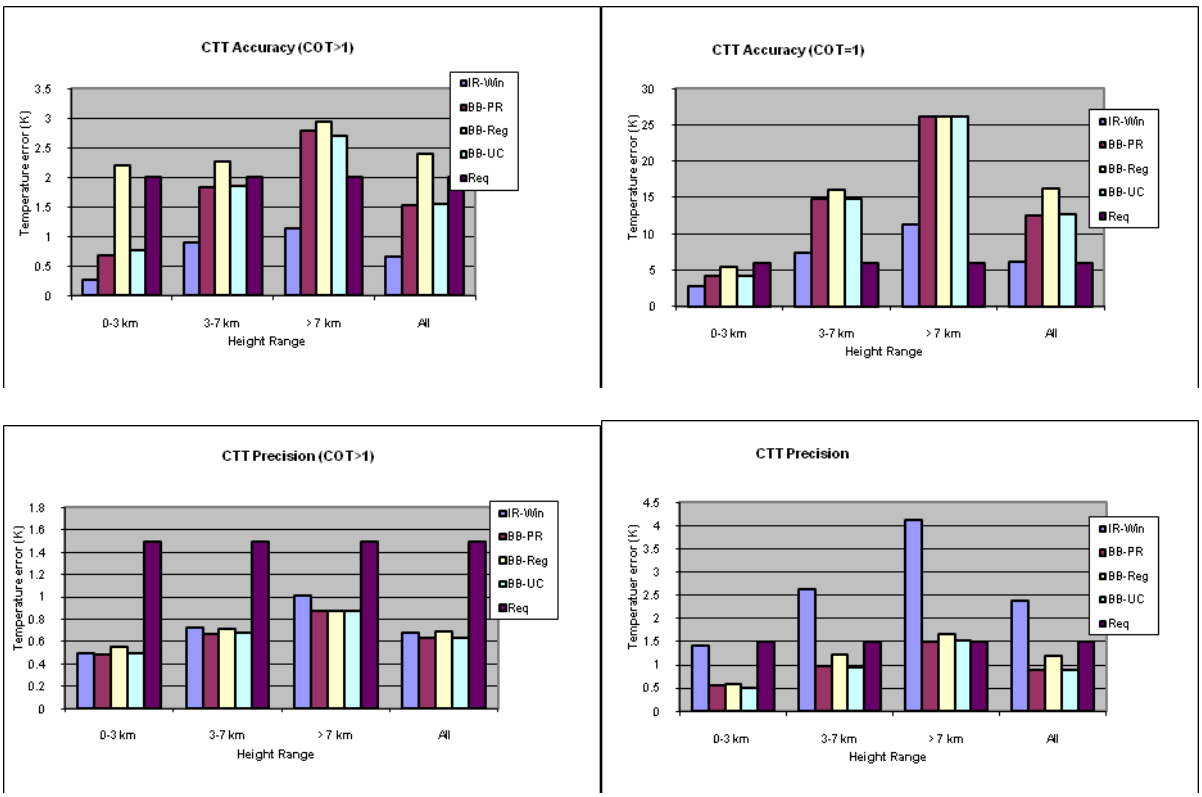

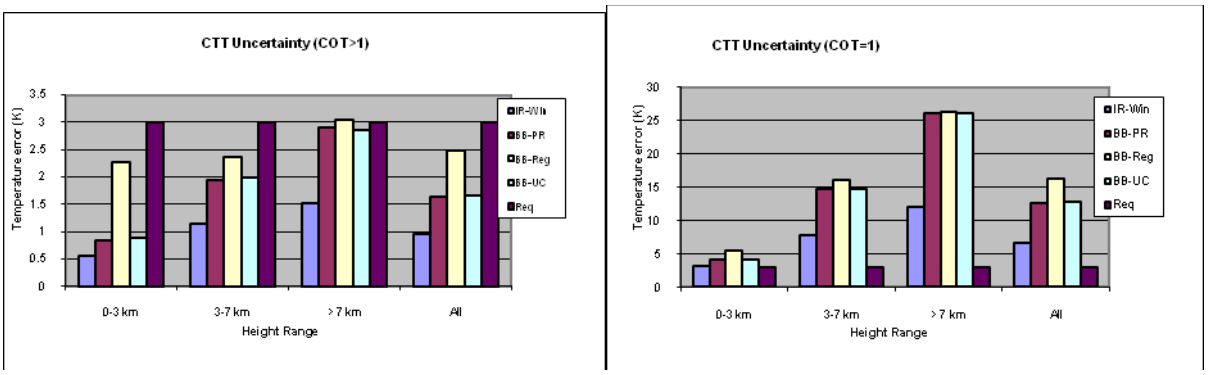

Figure 35. CTT accuracy, precision, uncertainty performance comparison for COT > 1 (left) and COT=1 (right). Shown are results for IR-Win: Window IR algorithm, BB-PR: Window-IR BackUp Algorithm, BB-Reg: Precipitable Water Regression BackUp algorithm, BB-UC: BackUp with no atmospheric correction, and Req: the requirements.

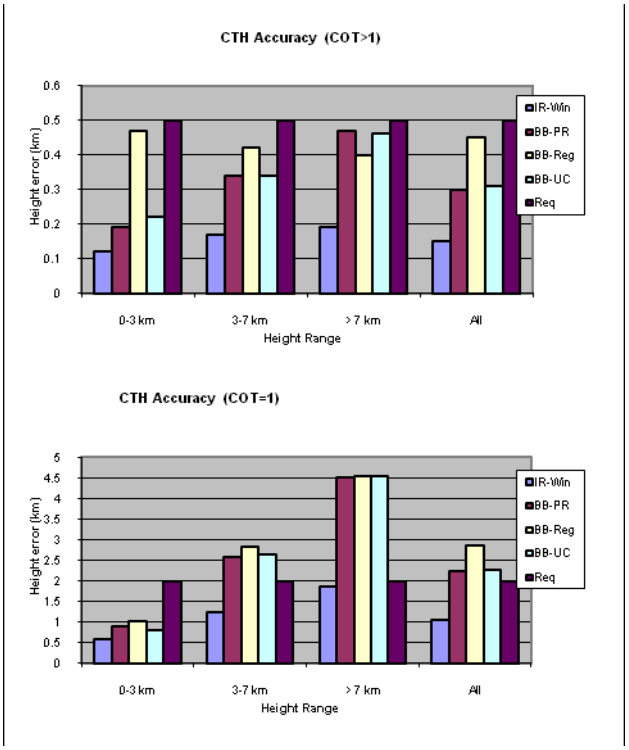

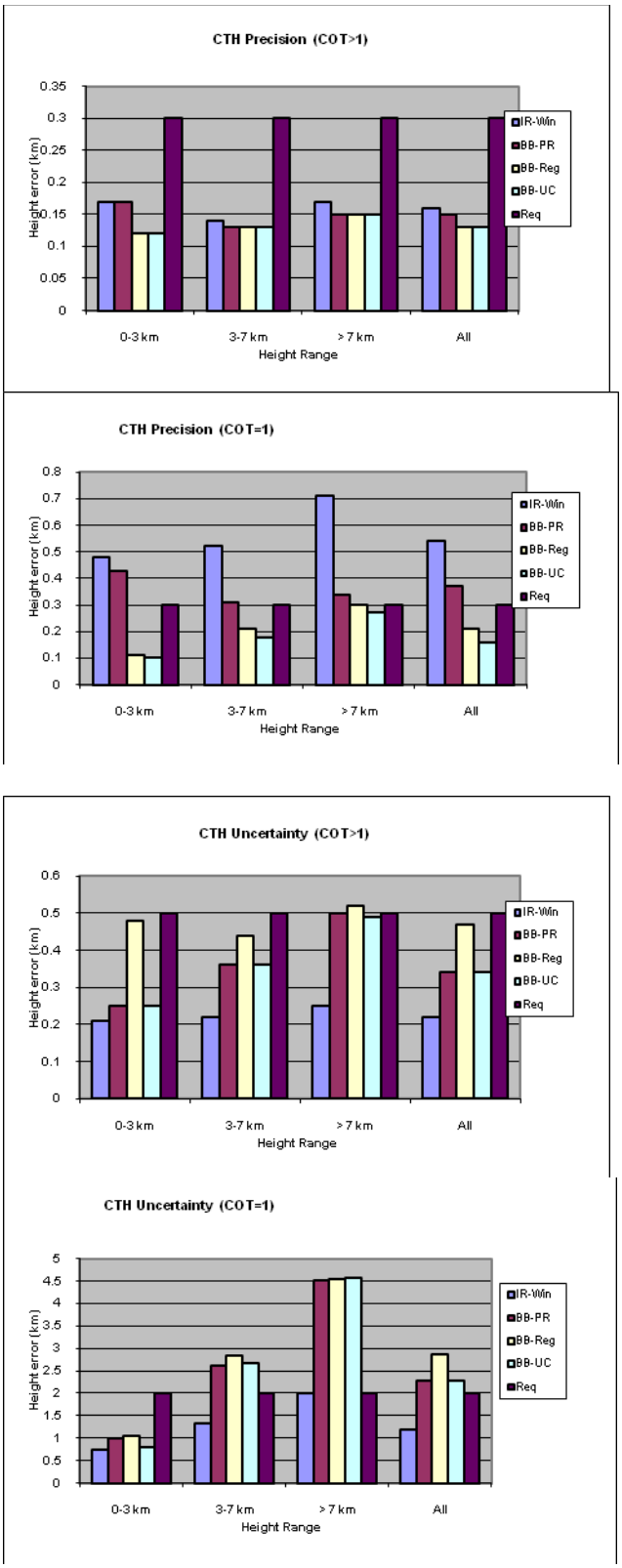

Figure 36. CTH accuracy, precision, uncertainty performance comparison for COT > 1 (left) and COT=1 (right). Shown are results for IR-Win: Window IR algorithm, BB-PR:

Window-IR BackUp Algorithm, BB-Reg: Precipitable Water Regression BackUp algorithm, BB-UC: BackUp with no atmospheric correction, and Req: the requirements.

Next we discuss low optical thickness clouds with COT=1. The general behavior observed is:

- Baseline algorithm has better performance than back-ups for accuracy and precision
- Baseline algorithm has worse performance than the backup for precision
- Performance degrades for higher layers

Ignoring the BB-Reg back-up algoritm (which has the problems noted in the discussion of the COT >1), the reason that the precision is better for the back-up compared to the baseline algorithms is that for low COT, the back-up algorithm is sensitive to random errors in many of the inputs. The overall baseline algorithm performance is clearly better than the back-ups as can be seen from the uncertainty plots.

The worsening performance with altitude is a characteric of the one channel cloud top retrieval approach and varies in the opposite direction as the requriements (which become more stringent with increase in altitude).

A summary of performance against requirements for the non-day/ water conditions is given in Table 18. For COT>1 requirements are always met. For COT=1, the most significant problems arise with precision and uncertainty. These cases are driven primarily by sensitivity to the following inputs: COT, surface temperature, surface emissivity and not the algorithm itself.

Table 18. Sumary of performance of non-day/ water algorithm against Cloud Top Parameter EDR performance requirements. Key: yes [green] = meets or exceed requriements; no [red] = does not meet; nearly [yellow] = within ~30% of meeting requirements; N/S = not specified.

Measurement Quality	Altitude range	COT > 1			COT = 1		
		CTP	CTT	CTH	CTP	CTT	CTH
Accuracy	0-3 km	yes	yes	yes	yes	yes	yes
	3-7 km	yes	yes	yes	yes	nearly	yes
	>7 km	yes	yes	yes	yes	no	yes
	All	N/S	yes	yes	N/S	yes	yes
Precision	0-3 km	yes	yes	yes	nearly	yes	no
	3-7 km	yes	yes	yes	no	no	no
	>7 km	yes	yes	yes	no	no	no
	All	N/S	yes	yes	N/S	no	no
Uncertainty	0-3 km	yes	yes	yes	yes	yes	yes
	3-7 km	yes	yes	yes	no	no	yes
	>7 km	yes	yes	yes	no	no	yes
	All	N/S	yes	yes	N/S	no	yes

The results indicate that the uncorrected brightness temperature algorithm (BB-UC) performs about equally with the black body physical retireval (BB-PR). We expect that the BB-Reg would also perform on par with these two with a new regression model/ coefficients. The majority of the time there is only very small absorption above the cloud and so the magnitude of the

atmsopheric correction is small. We expect that in the small number of cases with low clouds, high water vapor and high scan angle, the BB-Reg is preferred, but these are not frequent enough in the sample data to influence the results significantly.

3.5 PRACTICAL CONSIDERATIONS

The discussions in this section apply mainly to the Window IR and cloud top parameter interpolation algorithms. See Ou *et al.* (2004) for a discussion of the IR Cirrus and Water Cloud Parameter Retrieval Algorithms, which estimate CTT for ice clouds and water clouds at night.

3.5.1 Numerical Computation Considerations

Paragraph SRDV3.2.1.5.4-1 of the VIIRS SRD states the following:

> "The scientific SDR and EDR algorithms delivered by the VIIRS contractor shall be convertible into operational code that is compatible with a 20 minute maximum processing time at either the DoD Centrals or DoD field terminals for the conversion of all pertinent RDRs into all required EDRs for the site or terminal, including those based wholly or in part on data from other sensor suites."

RDR here stands for Raw Data Record. This essentially means that any and all EDRs must be completely processed from VIIRS raw data, including calibration and geo-referencing within 20 minutes from the time the raw data are available. This requirement is a strong reminder that VIIRS is an operational instrument.

Several provisions have been implemented to optimize the speed and efficiency of the infrared window algorithm, the most computationally expensive part of the algorithm. The OSS model LUTs were design for a minimal number of vertical levels (24 compared with 100 for the CrIS version) and a limited number of spectral "nodes" (6 compared with several thousand for the CrIS version). Since the RT model computational cost is close to linear in each of these values, the result is a model orders of magnitude faster than that used for the more demanding CrIS application. The other feature concerns the choice of the first guess. The method employed here (using a retrieved value of CTP from nearby point with similar M15 radiance) has been shown to dramatically reduce the number of iterations required for convergence compared with one based on assuming the cloud top temperature is the same as the brightness temperature of band M15.

3.5.2 Configuration of Retrievals

The retrieval of cloud top parameters will follow execution of the VIIRs Cloud Mask/Phase algorithm, which provides cloud mask and phase for each pixel and the Cloud Optical Properties algorithm, which provides CTT for all but daytime water clouds. For water clouds during daytime, the Window IR algorithm is executed to determine CTT. CTH is computed via linear interpolation from an ancillary atmospheric profile. CTP is calculated from CTT, CTH and the atmospheric profile via the hypsometric equation. All UCLA IR algorithms are contained within the Cloud Optical Properties Unit. The Window IR algorithm and interpolation functions are within the Cloud Top Parameters Unit.

3.5.3 Quality Assessment and Diagnostics

The assessment of the quality of retrievals will fall into four categories: Sensor Parameters; Environmental Scenario; Cloud Scenario; and Ancillary Data. Experience gained through simulations, and eventually by validation, will be captured and used to assess the quality of retrievals and provide guidance to the users of these products in the form of data quality flags. A list of parameters or situations that may influence data quality follows.

- *Sensor Parameters.* The qualities of sensor data include:
  - Sensor noise.
  - Radiance calibration.
  - Geolocation.
  - MTF
  - Band-to-Band registration.
- *Environmental Scenario.* Particulars of the environmental scenario that may affect retrieval accuracy include:
  - Values of Environmental Parameters. Sensitivity studies and flowdown indicate that retrieval accuracy is a function of the particular values of some environmental parameters (e.g, surface temperature, surface emissivity, sounding data).
  - Atmospheric inversion/isothermal identified in sounding.
  - Atmospheric water vapor absorption
- *Cloud Scenario.* The qualities or values of other cloud parameters that may affect retrieval accuracy include:
  - Cloud optical depth. Flowdown results show that retrieval accuracy can be a function of optical depth.
  - Cloud effective particle size. Flowdown results show that retrieval accuracy can be a function of effective particle size.
  - Existence of multilayer clouds. Multilayer clouds are difficult to identify and have an impact on radiance measurements. The primary problem is when a thin cloud overlays a lower cloud layer. Therefore, multi-layer clouds will affect retrievals when a single layer cloud is assumed in the radiative transfer analysis or retrieval algorithm and a multi-layer cloud actually exists within the field-of-view.
  - Satellite viewing geometry. Flowdown results show some sensitivity to satellite view geometry.
  - Solar position. Solar position influences UCLA IR cirrus parameter retrievals during daytime.
  - Non-overcast cloudy pixel. Sub-pixel cloud fractions less than one result in under-

estimation of CTH.

- *Ancillary Data*
  - In general, the quality of ancillary data affects the quality of retrievals. This has been explored in the Error Budget studies.

3.5.4 Exception Handling

We define "exception handling" as the procedure for handling missing or degraded data or a degraded processing environment. Table 19 lists VIIRS and ancillary data and their potential sources.

Table 19. Data used by Retrieval Algorithms.

Data Type	Description	Essential/ Nonessential	Potential Source*
VIIRS CTT IP	Cloud top temperature as determined by the COP unit	Essential for all ice clouds and for nighttime water clouds	1: VIIRS COP IP 2: Other NPOESS CTT
VIIRS COP IP	Cloud optical thickness and effective particle size	Essential for day/ water clouds	1: VIIRS COP IP 2: Use default value for water clouds
VIIRS Radiances	10.763μm brightness temperatures	Essential for daytime water clouds	1: VIIRS SDRs 2: None
Cloud Mask	Cloud/no cloud for each pixel	Essential	1: VIIRS Cloud Mask algorithm 2: Cloud/no cloud based on simple thresholding
Cloud Phase	Ice cloud or water cloud flag	Essential	1: VIIRS Cloud Mask algorithm 2: CMIS IWC and CLW data
Atmospheric Sounding	Atmospheric temperature and moisture as functions of pressure and height	Essential	1: NCEP analysis/forecast 2: CMIS sounding data 3: CrIS sounding data
*1 = Primary Potential Source	*2 = Secondary Potential Source		*3 = Tertiary Potential Source

3.6 ALGORITHM VALIDATION

Potential Cloud Top Parameter validation data sources include the following:

- Radiance data collected by the MODIS Airborne Simulator (MAS), with cloud tops determined from the on-board lidar data.

- MODIS data when available, together with the use of data from associated retrieval algorithm validation campaigns.

The validation effort should be able to take advantage of past and planned cloud field campaigns (such as FIRE-I, FIRE-II, ARM Spring 2000, FIRE Tropical 2002/2003, and the Terra validation studies). Regardless of the data used, it is essential that the data sets include reliable radiance

data at or very near the proposed VIIRS wave bands, all required ancillary data, and an accurate description of the associated cloud parameters (type, base, height, optical properties, etc.) for ground truth. The required validation data and procedures that can be used for validating algorithm performance can be briefly summarized as:

- Collect statistically significant samples of co-located in-situ cloud parameter measurements and VIIRS-like measurements.
- Modify/create VIIRS-like measurements with VIIRS instrument specification noise.
- Perform EDR retrieval using ATBD described algorithms.
- Co-register in-situs and EDR retrievals by taking into account spatial, temporal, and viewing discrepancy.
- Compute statistical accuracy, precision and uncertainty EDR estimates using retrievals and in-situ data.

4.0 ASSUMPTIONS AND LIMITATIONS

4.1 ASSUMPTIONS

The major assumptions listed below relate to the Window IR and Cloud Top Parameter Interpolation Algorithms. See Ou *et al.* (2004) for a description of the assumptions made in the Cloud Optical Properties Retrieval Algorithm.

- The retrieval algorithm is based on plane-parallel radiative transfer theory. Horizontal inhomogeneities in cloud and environmental parameters and their effects on radiative transfer are not modeled.
- At this time, multilayer cloud conditions are not modeled in the radiative transfer solution. Degraded performance is expected when multilayer clouds are present within the same pixel.
- It is assumed that the atmosphere is in thermodynamic equilibrium and that hydrostatic equilibrium applies.
- It is assumed that the optical properties of water droplet clouds are not sensitive to the exact shape of the particle size distribution.
- It is assumed that no sub-pixel clouds exist.
- It is assumed that the 10.763 μm micron channel is not affected by aerosol absorption.

4.2 LIMITATIONS

No major limitations have yet been identified for the Window IR and Cloud Top Parameter Interpolation Algorithms. The algorithms are applicable both day and night, and results indicate accurate retrievals are possible over the full range of viewing geometries. See Ou, *et al.* (2004)

for a description of the limitations of the Cloud Optical Properties Retrieval Algorithm. We do expect degraded performance when multilayer and sub-pixel clouds are present within pixels and when a temperature inversion/isothermal is present in the atmosphere. The impacts of these conditions on retrieval accuracy have not yet been quantified.

5.0 REFERENCES

Atmospheric and Environmental Research (AER), Inc. 2004: *Algorithm Theoretical Basis Document for the Cross-Track Infrared Sounder (CrIS), Volume II, Environmental Data Records*, Version 4.1, May 19, 2004.

Chylek, P, P. Damiano, and E.P. Shettle, 1992: Infrared emittance of water clouds. *Journal of the Atmospheric Sciences,* Vol. 49, No. 16, 15 August 1992.

Liou, K.N., 1992: *Radiation and Cloud Processes in the Atmosphere: Theory, observation, and modeling*. New York: Oxford University Press.

Menzel, P. and K. Strabala, 1997: *Cloud Top Properties and Cloud Phase Algorithm Theoretical Basis Document.* MODIS Algorithm Theoretical Basis Document No. ATBD-MOD-04, October 1997 (version 5).

Moncet, J., Uymin, G, Snell, H. E., 2004: *Atmospheric radiance modeling using the Optimal Spectral Sampling method,* SPIE Defense and Security Symposium, 13 April 2004, Orlando Florida – Conference 5425: Algorithms and Technologies for Hyperspectral and Ultraspectral Imagery X, pp. 5525-5537.

Ou, S.C., K.N. Liou, Y. Takano, G.J. Higgins, A. George and R.L. Slonaker, 2004: *VIIRS Cloud Effective Particle Size and Cloud Optical Thickness Algorithm Theoretical Basis Document.* Y2393, Version 5, Revision 2. Raytheon ITSS.

Planet, W.G. (ed.), 1988: *Data extraction and calibration of TIROS-N/NOAA radiometers.* NOAA Technical Memorandum NESS 107 – Rev. 1, Oct. 1988. 130 pp.

Raytheon VIIRS Error Budget, Version 3 (Y3249)

SRD. *Visible/Infrared Imager/Radiometer Suite (VIIRS) Sensor Requirements Document (SRD) for National Polar-orbiting Operational Environmental Satellite System (NPOESS) spacecraft and sensors.* Associate Directorate for Acquisition NPOESS Integrated Program Office. Version 2, Revision a, 4 November 1999. F04701-97-C-0028.

Rossow, W.B., L.C. Garder, P.J. Lu, and A.W. Walker, 1991: *International Satellite Cloud Climatology Project (ISCCP) Documentation of Cloud Data.* WMO/TD-No. 266, World Meteorological Organization, 76 pp.

Stewart, R.H., 1985: *Methods of Satellite Oceanography*, University of California Press, Berkeley, 360 pp.

Wallace, J.M. and P.V. Hobbs, 1977: *Atmospheric Science An Introductory Survey*, Academic Press, San Diego, 467 pp.